Geological Survey of Finland

Bulletin 286

Petrography and geochemistry of the Eurajoki stock, a rapakivi-granite complex with greisen-type mineralization in southwestern Finland

by Ilmari Haapala

Geologinen tutkimuslaitos . Espoo 1977

The Geological Survey of Finland, Bulletin 286

PETROGRAPHY AND GEOCHEMISTRY OF THE EURAJOKI STOCK, A RAPAKIVI-GRANITE COMPLEX WITH GREISEN-TYPE MINERALIZATION IN SOUTHWESTERN FINLAND

BY
ILMARI HAAPALA

WITH 101 FIGURES AND 13 TABLES IN TEXT AND ONE APPENDED MAP

GEOLOGINEN TUTKIMUSLAITOS
ESPOO 1977

Haapala, I. 1977: Petrography and geochemistry of the Eurajoki stock, a rapakivi-granite complex with greisen-type mineralization in southwestern Finland. *Geological Survey of Finland, Bulletin 286.* 128 pages, 101 figures, 13 tables, one appended map.

The composite Eurajoki stock is a satellite of the Laitila rapakivi massif, age about 1 570 Ma. The main rock units of the stock are: Tarkki granite, Väkkärä granite and porphyry dikes. Greisen-type Sn, Be, W and sulphide mineralizations occur in various parts of the stock.

The Tarkki granite is a fayalite-bearing biotite-hornblende granite, which represents the most basic members of the Fennoscandian rapakivi granites. This granite originally crystallized from H_2O-undersaturated magma, but later activity of volatiles is proved by various mineral alterations.

The Väkkärä granite forms a younger, complex, shallow-level intrusive body in the central parts of the stock. It is composed of several types of acidic supersolvus granite, which are often characterized by marked mineral alterations. The crystallization of the complex was probably completed from residual magma saturated with volatiles. The late-stage types are peraluminous topaz-bearing microcline-albite granites, in which the dark mica is lithian siderophyllite (protolithionite). Accessory constituents include monazite, Nb- and Ta-rich cassiterite, bastnaesite, xenotime, columbite and thorite. Geochemically, the late-stage types are characterized by anomalously high contents of F, Li, Ga, Rb, Sn and Nb and by unusually low contents of Mg, Fe, Ti, Ba, Sr and Zr. These mineralogical and geochemical peculiarities are interpreted to be due to magmatic evolution (extreme fractionation) and superimposed autometamorphic — autometasomatic alterations.

Most of the porphyry dikes are quartz porphyry, which shows much the same mineralogical and geochemical characteristics as the topaz-bearing Väkkärä granite; some of the dikes have a mineral composition corresponding to dacite.

The secondary processes are manifested in the greisenization, which has locally affected all the rock units of the Eurajoki stock. The presumably most intensively greisenized and mineralized apical parts of the Väkkärä granite have been removed by erosion.

ISBN 951-690-068-2

Helsinki 1977. Valtion painatuskeskus

CONTENTS

INTRODUCTION

The petrology and geochemistry of the rapakivi granites of Finland have been studied intensively since the end of the 19th century, but in general very little attention has been paid to the rapakivis as possible ore-bearing granites. Yet, the Sn-Zn-Cu skarn ore field in Pitkäranta, Soviet Karelia, has been interpreted by several researchers to be genetically related to the nearby Salmi rapakivi massif (e.g., Trüdstedt 1907), and some small galena veins have long been known to occur in rapakivi areas (Vaasjoki 1956).

Exploration of Finnish rapakivi granites in search for tin and related mineralizations has been conducted since 1967 by the Exploration Department of the Geological Surveyof Finland. The investigations were started in the Eurajoki area of SW Finland, from where the Geological Survey had received an erratic boulder sample containing sphalerite, chalcopyrite and a little cassiterite as long ago as 1956. At that time, however, the Outokumpu Co. was at work in the area, and therefore no further work was initiated by the Exploration Department. In 1966 the Geological Survey took some granite and gneiss samples from the area, and when it was noted that the samples of the so-called »Väkkärä granite» were highly anomalous in tin (80 and 90 ppm), systematic geological, geochemical and geophysical studies were begun there in the spring of 1967. Very soon greisen bodies containing cassiterite, Be-minerals, wolframite and sulphides were found in different parts of the Eurajoki granite complex. It also become known that the first findings of sulphides and tin in the Eurajoki area had actually been made back in 1956 by Outokumpu prospectors (Outokumpu Co. had established two zinc claims in the Eurajoki area in 1957—59). The Geological Survey continued its investigation in the Laitila, Wiborg (Viipuri) and Vehmaa rapakivi areas, and interesting Sn, Be, W and sulphide mineralizations were found also in Kymi, contained in the Wiborg rapakivi massif. In addition, greisen veins with very poor or no ore mineralization were found in association with younger biotite granites in many other localities, in the rapakivi areas studies. Unfortunately, no one of the occurrences so far found has proved to be of economic significance.

Short reports containing some petrographic and geochemical data obtained on the granites during the exploration work have been published by Haapala (1973, 1974, 1976), and descriptions of the greisens and their specific minerals have been written by Haapala and Ojanperä (1969, 1972) and by Haapala and Laajoki (1969). The present study will give a more detailed description of the petrography and geochemistry of the Eurajoki granite stock. A short description of the greisens is also included. It is hoped that this study will shed some new light on the late-stage varieties of the rapakivi granites and be of some use to possible later rare-metal prospectors in the rapakivi granite areas. It is intended to produce a corresponding study later from the Kymi area.

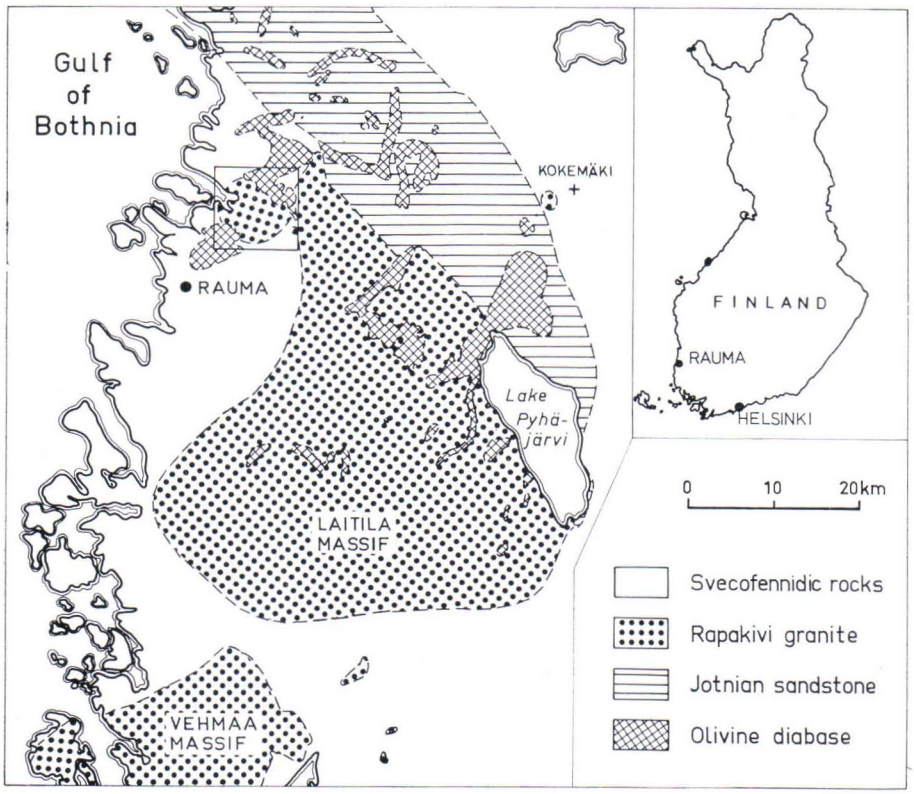

Fig. 1. Geological sketch map of the Satakunta region showing the location of the Eurajoki stock (outlined area). The map is based on the maps of Laitakari (1928), Kahma (1951) and Härme (1958) and on the author's observations.

THE GEOLOGICAL OUTLINE OF THE SATAKUNTA REGION

The Precambrian bedrock of Satakunta consists of four major formations (Fig. 1), which differ from each other in age and petrogenesis (Sederholm 1911, Laitakari 1925, Kahma 1951). According to current views, the formations are as follows:

	Approximate age
— olivine diabase	1 250—1 270 Ma
— Jotnian sandstone	1 300—1 400 Ma
— rapakivi granite	1 550—1 600 Ma
— Svecofennidic metamorphic and igneous rocks	1 850—1 900 Ma

The Svecofennidic schists and gneisses were metamorphosed and migmatitized, and different types of igneous rocks were emplaced during the Svecokarelian orogeny about 1850—1900 Ma ago. The postorogenic (possibly anorogenic) rapakivi granites

were intruded in several phases into the overlying metamorphosed rocks during an advanced stage of stabilization about 1 550—1 600 Ma ago. The main part of the rapakivi mass is contained inside the pear-shaped Laitila massif (batholith); but around it there are some smaller satellites, of which the Eurajoki stock (Fig. 1) is the largest. After a long period of denudation, the Jotnian sedimentary formation, consisting of arkosic sandstone and thin shale intercalations, was deposited on the deeply eroded platform. This unmetamorphosed formation fills a NW-striking graben about 20 km wide; in this downfaulted block, part of the sandstone formation has resisted erosion. Radiometric age determinations (K-Ar method) of the shale layers indicate an age of about 1 300 Ma (Simonen 1960). An interpretation of recently measured gravity profile across the formation gave a mean depth of about 1.3 km and a maximum depth of about 1.8 km (Elo 1976), which is in agreement with previous seismic and indirect magnetic investigations (see Puranen 1963). There are no sure observations that the sandstone contains rapakivi material, although this would be expected on the basis of the age relations. The youngest rocks of the region, the olivine diabases, occur as steeply-dipping or subhorizontal dikes traversing the Jotnian sandstone, rapakivi granites and Svecofennidic metamorphic rocks. They represent hypabyssal injections of basaltic magma into a stable platform characterized by faulting tectonics. The recent Rb-Sr and zircon determinations (Veli Suominen, oral communication in 1976) indicate an age of 1 250—1 270 for the olivine diabases of Satakunta.

THE EURAJOKI STOCK

The Eurajoki granite stock intrudes Svecofennidic migmatitic rocks and contacts the Laitila rapakivi massif, into which it can be included as a satellite. The diameter of this rounded stock is 8—8.5 km. The contact between the Laitila massif and the hornblende-bearing granite (Tarkki granite) of the Eurajoki stock is visible on a small outcrop about 1.5 km north of the Eurajoki church (outcrop 215/IH/67; coordinates x = 6789.40, y = 539.28 on the appended map [1]). The contact is sharp and at the contact there are some migmatite xenoliths, but it has not been possible to determine with certainty the age relations between the granites on the basis of the field observations. The contact between the Eurajoki stock and the surrounding migmatitic rocks is visible in several places. The contact is usually seen to be sharply cutting (Fig. 3), and where the dip has been observed it has been nearly vertical. Breccia is visible in some contact outcrops. In some places there also occur more indistinct, migmatitic contacts (e.g., outcrop 138/IH/67; coordinates x = 6788.0, y = 531.2; see also Sederholm 1911, p. 101). On the northwestern margin of the stock, the foliation of the migmatitic mica gneiss closely follows the strike direction

[1]) In the following description, the locations of important outcrops and samples of the Eurajoki area are given by using the Finnish map coordinates, which are marked also on the appended geologic map. In addition, the outcrops (and samples) to which reference is made in the text are marked on a separate index map (Fig. 2).

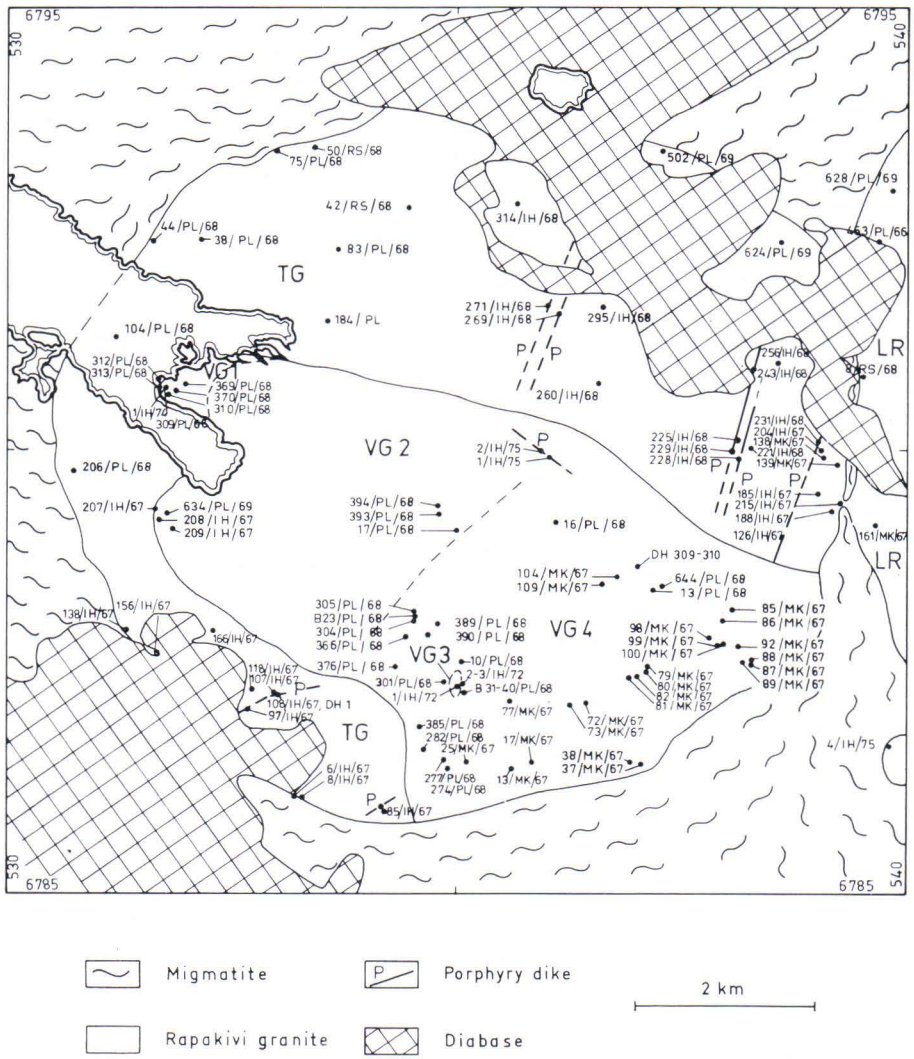

Fig. 2. Lithologic map of the Eurajoki area showing the locations of the outcrops (and samples(to which reference is made in the text. The different rapakivi types are differentiated with letter symbols: LR, Laitila rapakivi granite; TG, Tarkki granite; VG, Väkkärä granite (VG 1, contact type; VG 2, even-grained type; VG 3, coarse-grained type; VG 4, porphyritic type). In most cases, the code of the sample is the same as that of the corresponding outcrop, but the sample code may also contain certain additional letter signs (e.g., outcrop 17/PL/68, sample 17/PL/68/IH).

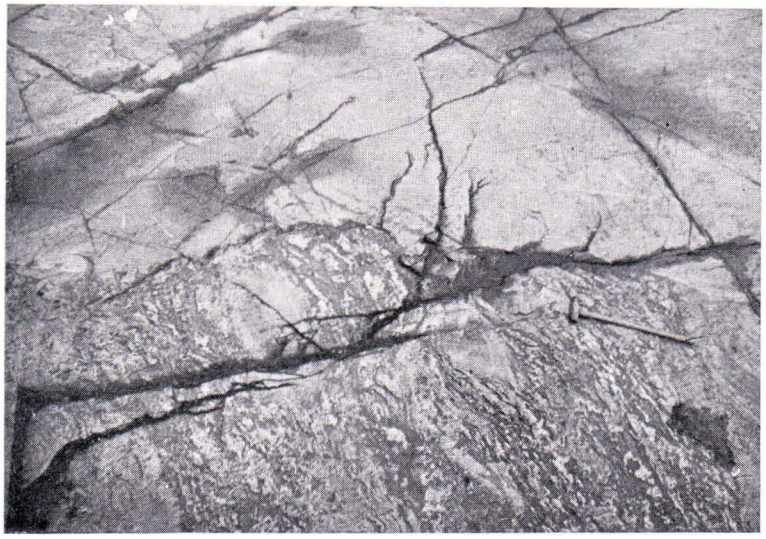

Fig. 3. Contact between the Tarkki granite of the Eurajoki stock and migmatite. The dark areas in the granite (upper part of the photograph) are due to moisture. Outcrop 6/IH/67, map coordinates x = 6 786.10, y = 533.21.

Fig. 4. Contact between the Tarkki granite (dark gray) and the contact type of the Väkkärä granite (light gray). An obvious inclusion of the Tarkki granite in the Väkkärä granite. Outcrop 313/PL/68; x = 6 790.70, y = 531.70.

of the contact within a zone a few hundred meters wide. The dip of the foliation is 65—80°SE, which is possibly also the dip of the contact.

The Eurajoki stock is polyphasic. Except for the southeastern part, the marginal parts of the stock are composed of a reddish gray, even-grained hornblende-bearing

granite known in the literature (Laitakari 1928, Eskola 1928, Kahma 1951, etc.) as Tarkki granite. The central part of the stock consists of a light red granite formation called Väkkärä granite by Laitakari (1928) and others. These names are used in this paper, although the present studies show that the Väkkärä granite itself is composed of several different granite types.

The contact between the Tarkki granite and the rocks of the Väkkärä granite complex is visible in several places in the western and southwestern parts of the stock. It has been also intersected by two drill holes. The contact relations show that the Väkkärä granite is younger than the Tarkki granite. The contact is sharp and usually rectilinear or angular; in some places the Väkkärä granite sends apophyses into the Tarkki granite, inclusions of which it also contains (Fig. 4). The rocks of the Väkkärä granite tend also to be more fine-grained at the contact. The contact dips gently (10—45°) outwards. Obviously the Väkkärä granite forms a younger, cupola-shaped complex intrusive body within the Eurajoki stock.

The granites of the Eurajoki stock are cut by porphyry dikes 1—15 m in width. Seven of the eight known dikes occur in the Tarkki granite in a subparallel setting; only one has been found in the Väkkärä granite. Aplite and pegmatite dikes are relatively rare. Greisen and quartz veins occur in different parts of the stock; in the Väkkärä granite, also more irregular greisen bodies occur.

The Eurajoki stock possesses features typical of the centred complexes (*cf.*, Kaitaro 1956, Pitcher and Berger 1972, p. 186), the mechanisms of emplacement having presumably been magmatic stoping and cauldron subsidence. Among several analogous complexes, reference will be made here only to the Ahvenisto massif in Finland (Savolahti 1956, Buddington 1959) and the Rosses complex in Donegal, Northern Ireland (Pitcher and Berger, *op. cit.*).

In both the northern and southern parts of the stock, the Tarkki granite is intersected by diabase dikes. The dip of the dikes varies, but many of them (e.g., the big ones marked on the map and those intersected by deep drillings) are subhorizontal. The contact phenomena between the Tarkki granite and the olivine diabase dikes were the main objects of the studies of Laitakari (1928) and Kahma (1951).

RADIOMETRIC AGES

Isotopic zircon ages were determined by O. Kouvo (Geological Survey of Finland, Annual report 1968) and M. Vaasjoki for two samples of the Tarkki granite (together five zircon fractions) and one sample of the Väkkärä granite (contact type) by using the lead-uranium method. In addition, lead isotope ratios were determined and the ages calculated for galena fractions of three greisen veins intersecting the Tarkki and Väkkärä granites. The results of the analyses will be presented and the problems of the radiometric ages of the granites and associated veins will be discussed in detail by M. Vaasjoki in the near future, and here the matter will be treated only briefly.

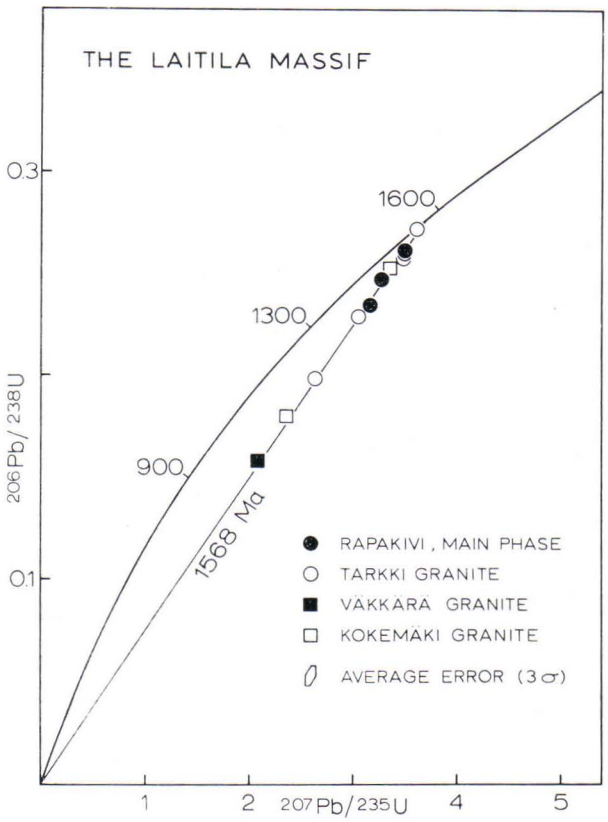

Fig. 5. A concordia diagram of granites of the Laitila rapakivi massif. By courtesy of M. Vaasjoki.

All the available zircon isotope determinations of the Tarkki and Väkkärä granites and other granites of the Laitila massif fall in the concordia diagram on or very near a straight line running through the origin and intersecting the concordia graph at the point 1 570 Ma (Fig. 5). This line deviates slightly from the corresponding diffusion isochron calculated on the basis of the radition damage model of Wasserburg (1963). The zircon of the Väkkärä granite shows a much more discordant age than the zircon fractions of the Tarkki granite. Calculations based on the Wasserburg model would indicate a somewhat higher age for the Väkkärä granite than for the Tarkki granite, which is in contradiction to field observations. Possibly some later geological event has slightly affected the isotope composition of the zircon of the Eurajoki granites, causing deviation from the simple radiation damage model. The preliminary results of the radiometric age determinations from the topaz-bearing types of Väkkärä granite suggest slightly younger ages.

The available isotopic data do not indicate any marked age difference between the granites of the Eurajoki stock and the main phase of the Laitila massif. The age 1 570

Ma should be considered as a minimum age, which is evidently not far from the true age. This conclusion is supported by the lead isotope ratios of the three greisen galenas from the Eurajoki stock, which, using the two-stage model of Stacey and Kramers (1975), indicate the ages 1 575—1 608 Ma.

THE TARKKI GRANITE

General petrography

The Tarkki granite is a homogeneous, reddish-gray, equigranular, medium-grained massive rock, which contains sparsely distributed ovoids (Ø 3—6 cm) of plagioclase-mantled alkali feldspar. The distance between neighboring ovoids in the outcrops is often several meters. The average grain size is 2—4 mm. Some inclusion-like, very coarse-grained feldspar accumulations, some tens of cm in diameter, have been noticed in the granite. Against the migmatitic country rock, the Tarkki granite sometimes has a fine-grained granophyric seam a couple of cm in width, but ordinary fine-grained contact varieties are lacking. This suggests that during the crystallization of the Tarkki granite the country rock was hot, presumably owing either to a relatively deep intrusion level (in comparison with the intrusion level of the Väkkärä granite) or to the heating effect of the Laitila rapakivi intrusion.

The major constituents are alkali feldspar, quartz, more or less sericitized plagioclase as well as partly chloritized biotite and hornblende. Common accessories are fayalite and its alteration products iddingsite and grunerite, ilmenite, apatite, zircon, fluorite and fine-grained magnetite; there also occur in very small amounts danalite, perrierite or chevkinite and pyrite. The results of the point-counting analyses of 26

Table 1

Modal composition (vol. %) of the Tarkki granite, based on point-counting analyses of 26 thin sections.

	Minimum	Maximum	Mean	Standard deviat.
Alkali feldspar	25.5	45.9	35.7	6.2
Quartz	22.7	39.4	26.9	3.3
Plagioclase	13.6	31.8	20.2	4.6
Biotite	1.5	14.8	8.3	2.1
Chlorite	0.4	12.9	3.8	3.0
(Biotite + chlorite)	5.6	20.6	12.1	3.4
Hornblende	0.0	0.9	2.2	2.5
Fayalite + iddingsite	0.0	6.3	0.9	0.8
Apatite	0.2	2.3	0.8	0.5
Fluorite	0.0	0.5	0.1	0.1
Zircon	0.0	0.5	0.2	0.1
Opaques	0.1	6.8	1.2	1.2
			100.3	

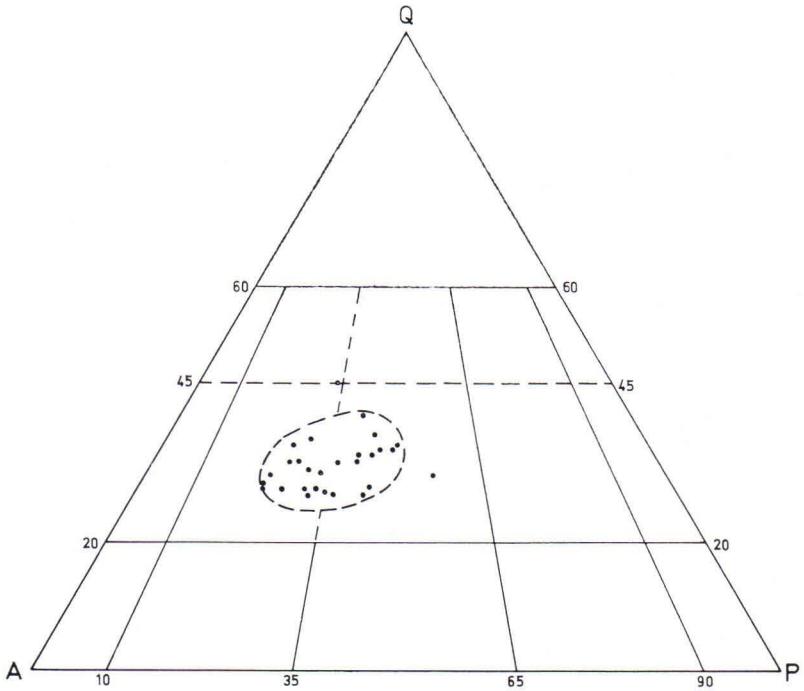

Fig. 6. Alkali feldspar—plagioclase—quartz diagram, after Streckeisen (1967), of the Tarkki granite.

samples (1 000—2 000 points from each) are summarized in Table 1, and the alkali feldspar—plagioclase—quartz relations are presented in a Streckeisen diagram in Fig. 6. In this diagram, the points of the Tarkki granite fall into the central parts of the granite field. Two chemical analyses of the Tarkki granite are presented in Table 10 (p. 98).

The texture is hypidiomorphic—granular. The grain boundaries between the feldspar minerals are usually sutured; the quartz—feldspar boundaries are usually smoother. The quartz grains usually show an undulatory extinction; in some instances, they are granulated. The plagioclase nearly always shows a euhedral form against the other major constituents, but sometimes it follows anhedrally the crystal faces of the quartz, and occasionally it is corroded and partly replaced by alkali feldspar. Quartz occurs partly as euhedral or subhedral grains, but in many cases it is anhedral and fills the interstices between other minerals. A small percentage of the quartz occurs as concave or drop-like inclusions in alkali feldspar, as a micrographic intergrowth with alkali feldspar and, rarely, plagioclase, and as a myrmekitic intergrowth with plagioclase. The alkali feldspar usually occurs as subhedral or anhedral grains. Some of the grains show crystal faces against other alkali feldspar grains, and others show faces against hornblende, biotite and late quartz (Fig. 8), and very rarely also against plagioclase. In a few cases, hornblende and biotite show crystal faces against alkali feldspar and quartz. Not unfrequently, alkali feldspar fills the interstices between

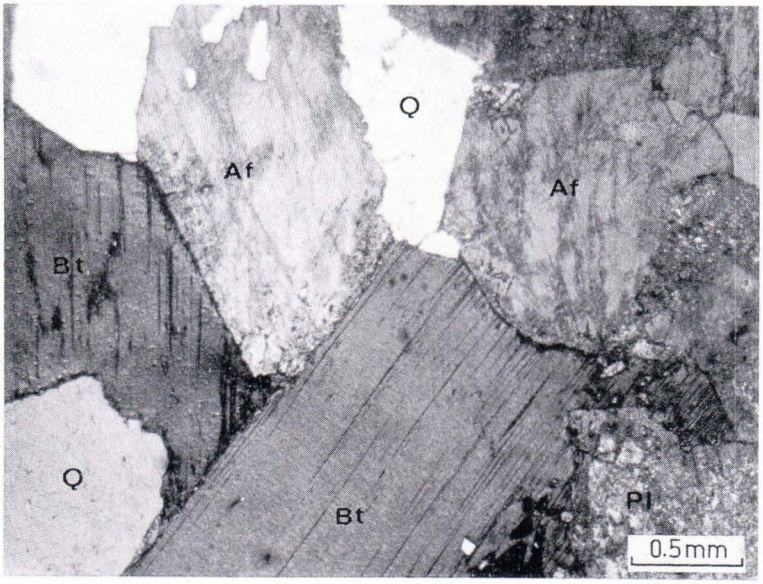

Fig. 7. Anhedral biotite (Bt) flakes between plagioclase, alkali feldspar (Af) and quartz (Q) grains in the Tarkki granite. Sample 138/MK/67.

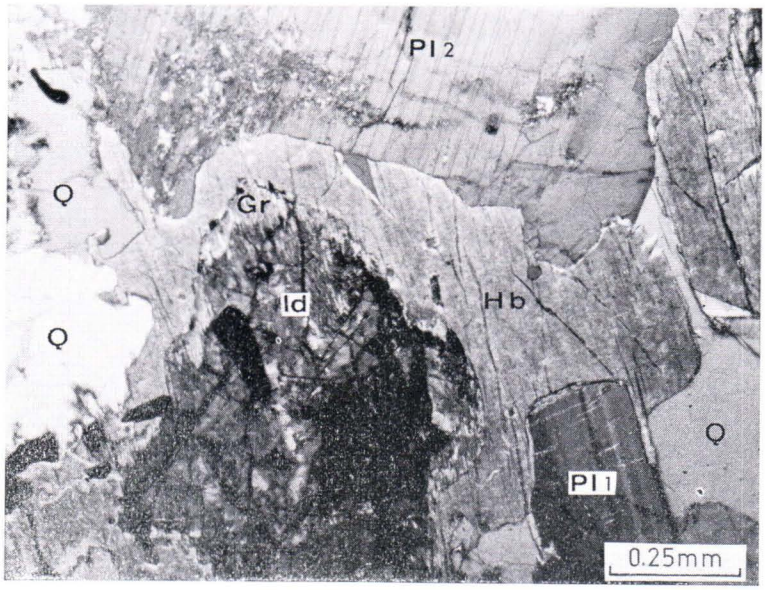

Fig. 8. Photomicrograph of the Tarkki granite showing iddingsite (Id), hornblende (Hb), plagioclase (Pl) and quartz (Q). Between the iddingsite and surrounding hornblende, a light grunerite seam (Gr). Plagioclase Pl 1 is euhedral against hornblende, whereas Pl 2 and hornblende show mutual boundaries. Iddingsite contains opaque inclusions. Sample 75/PL/68.

plagioclase laths and subhedral—euhedral quartz grains. The biotite and the hornblende are typically anhedral against plagioclase and early quartz (*cf.*, Figs. 7 and 8). Rarely, biotite, bluish-green hornblende and chlorite intersect other minerals as thin veinlets. The biotite and chlorite are sometimes also seen to occur as small flakes in feldspar minerals, obviously replacing them. The accessories fayalite, ilmenite, apatite and zircon occur as euhedral or subhedral grains. The ilmenite is usually present as inclusions in hornblende and biotite. Apatite and zircon commonly appear as inclusions in biotite, sometimes also as zone-controlled inclusions in plagioclase. Apatite has been found also as euhedral inclusions in fayalite, and it may also show a crystal form against zircon.

Mineralogy

The alkali feldspar of the Tarkki granite generally shows a faint perthite texture, but some grains or parts of grains appear homogeneous under the microscope. The obliquity (triclinicity) is 0.0—0.2. A more detailed description of the alkali feldspar is given on pp. 73—89.

The plagioclase is commonly heavily sericitized. In less altered plagioclase, the zonal structure is clearly visible. Electron microprobe determinations from two samples and numerous optical determinations (refractive indices α and γ, extinction angle) show the anorthite content of central parts of fresh grains to be 38—49 mole %. Against alkali feldspar, the plagioclase often has an albitic margin (see p. 19). Commonly the plagioclase contains small, uniformly oriented inclusions of alkali feldspar, which often tend to be rectangular in shape (Fig. 9). The diameter of the inclusions is about 0.1 mm or less. A fine perthite texture is occasionally visible in the inclusions. In some cases the alkali feldspar inclusions are rimmed by albitic plagioclase, but usually no such zones are visible. Similar »antiperthitic» alkali feldspar plebs in plagioclase have been described by, e.g., Gates and Scheerer (1963), Czamanske (1965) and Vogel *et al.* (1968). In a few cases, the plagioclase is partly replaced along fractures by K-feldspar with the same optical orientation as the inclusions.

The prevailing amphibole of the Tarkki granite is a calcic amphibole (hornblende) with X light buff, Y greenish brown, Z brownish green to greenish brown, $2V\alpha$ 74°; α' 1.690—1.692, γ' 1.707—1.712, cΛZ 14—15°. Electron microprobe analyses (Table 2, anal. 2 and 3) indicate that this amphibole is a ferro-edenitic hornblende. Amphiboles highly similar in composition have been described from an amphibole—alkali feldspar granite in Massachusetts, U.S.A. (Toulmin 1964), and from the Younger Granites of Nigeria (e.g., analyses A.19 and A.21 in Borley and Frost 1963). The rapakivi ferrohastingsite analyses published by Simonen and Vorma (1969) have all higher Al_2O_3 contents, but the composition of the amphibole from the tirilite (dark-colored, even-grained rapakivi granite) is not far from that of the amphibole of the Tarkki granite.

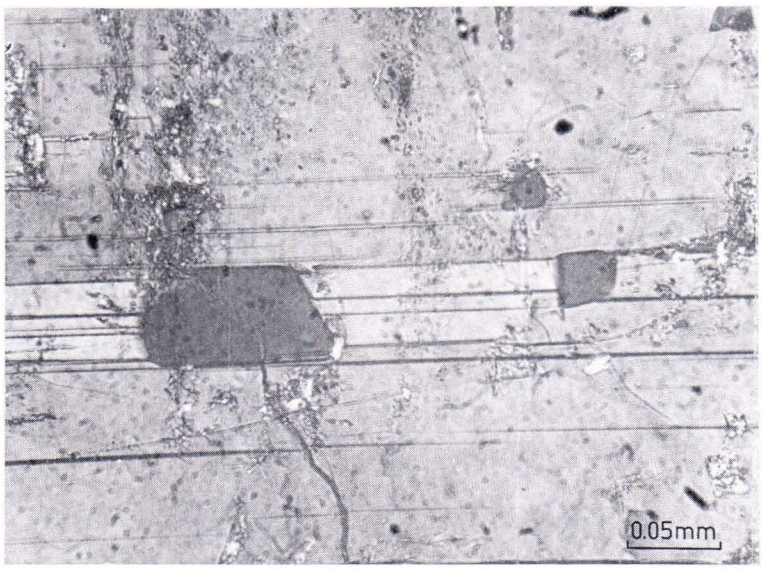

Fig. 9. Alkali feldspar inclusions in plagioclase. Tarkki granite, sample 44/PL/68.

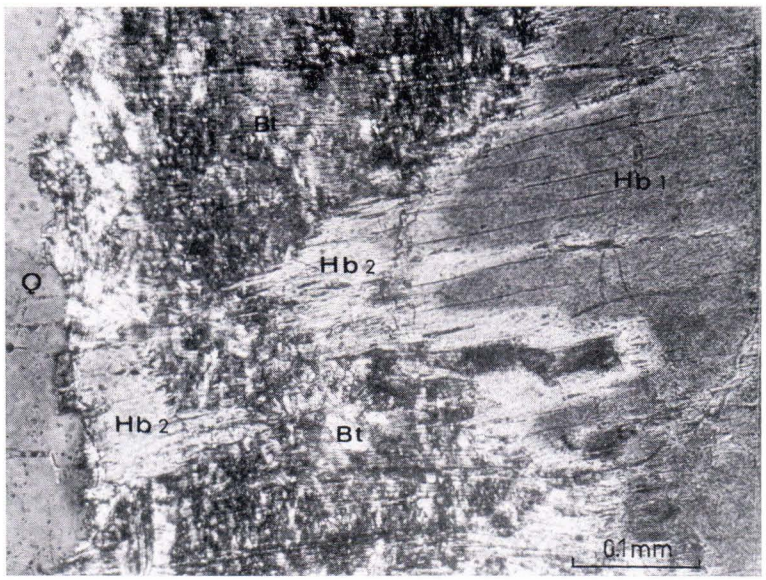

Fig. 10. Seam of bluish-green hornblende (Hb 2) between brownish-green hornblende (Hb 1) and secondary brownish-green biotite (Bt). Sample 188/IH/67.

Table 2

Electron-microprobe analyses of fayalite and amphiboles from the Tarkki granite. Raw data processing after the method of Bence and Albee (1968). Anal. Tuula Paasivirta.

	1	2	3	4	5
SiO_2	29.1	41.4	42.1	41.4	47.9
TiO_2	0.0	1.9	2.0	0.0	0.0
Al_2O_3	0.1	6.2	6.0	6.5	0.6
FeO (total iron)	68.3	31.8	29.0	35.6	47.7
MnO	0.8	0.2	0.2	0.4	0.5
MgO	1.2	3.4	5.4	0.9	1.4
CaO	0.1	10.6	11.2	10.9	1.2
Na_2O	0.7	1.9	2.0	2.2	0.4
K_2O	0.2	1.6	1.6	1.1	0.0
Σ	100.5	99.0	99.5	99.0	99.7
α'			1.691	1.690	
γ'			1.707	1.706	
$2V\alpha(°)$		74	74	68	
$c\Lambda Z(°)$		14	15	25	
X		Buff	Buff	Buff	
Y		Greenish brown	Greenish brown	Green	
Z		Brownish green	Brownish green	Blue green	

1. Fayalite, sample 44/PL/68 (x = 6 792.35, y = 531.64)
2. Hornblende, sample 44/PL/68
3. Hornblende, sample 188/IH/67 (x = 6 789.34, y = 539.18)
4. Hornblende (secondary), sample 188/IH/67
5. Grunerite, sample 44/PL/68

The brownish-green amphibole has commonly altered along the margins of grains and irregular cutting zones (fractures) to green hornblende, and in many cases further to bluish-green hornblende (X light buff, Y dull green, Z deep blue-green, α' 1.690—1.692, γ' 1.706—1.711, $c\Lambda Z$ 24—25°), which has either retained the orientation of the host amphibole or occurs as fine-grained aggregates. In some cases, the bluish-green hornblende occurs as a seam between the brownish-green hornblende and secondary brownish-green biotite (Fig. 10). Electron microprobe analysis (Table 2, anal. 4) indicates that also this secondary amphibole belongs to calcic amphiboles having a simplified formula $(Na, K)_{0\cdot9}\ Ca_{1\cdot9}\ (Fe, Mg, Mn, Al)_{5\cdot1}\ Al_{1\cdot2}\ Si_{7\cdot8}O_{22}(OH)_2$, and thus corresponds closely to the ferroedenite. During the alteration, the TiO_2 has been leached out, the MgO and K_2O contents have decreased and the iron content increased. The complete alteration series of hornblende in the Tarkki granite is as follows: brownish-green hornblende → green hornblende → bluish-green hornblende → biotite → chlorite.

The biotite occurs usually either as independent flakes or as an intergrowth with hornblende obviously replacing it along fractures and grain margins. The biotite is usually of a dark reddish-brown color, but occasionally green or brownish-green biotite occurs as an alteration product of hornblende and brown biotite. The biotite

itself has commonly been partly replaced by a green chlorite. Two electron microprobe analyses of biotite are presented in Table 7, and a wet-chemical analysis in Table 8. These biotite analyses fall into the same compositional field as the previously published Finnish rapakivi biotite analyses, which are all of hornblende-bearing granites (see Simonen and Vorma 1969). The slightly higher TiO_2 and MgO contents in the biotite of the Tarkki granite are in agreement with the more basic nature of this rock.

The fayalite has commonly been replaced partly or totally by iddingsite. Between the fayalite or iddingsite and brownish-green hornblende, there often occurs a thin seam of colorless grunerite, homoaxially intergrown with the hornblende. Partial microprobe analyses of fayalite and grunerite are presented in Table 2.

The alteration phenomena observed in the Tarkki granite (alteration of fayalite, hornblende, biotite and plagioclase, development of microscopic chlorite—biotite—hornblende, etc., veins, greisenization, etc.) have been caused partly by fluids related to the Tarkki granite itself, partly (especially greisenization) by fluids emanating from the younger Väkkärä granite.

Micrographic feldspar—quartz intergrowths

In the Tarkki granite, feldspar and quartz form two types of intimate intergrowth: micrographic (granophyric) intergrowth and myrmekite. Because these intergrowths may provide important information on the reaction sequences in the granite, they are described here in detail.

A micrographic (granophyric) texture is visible in some of the 26 thin sections of Tarkki granite studied. The texture is usually of the radiating fringe or insular type, but also vermicular and cuneiform types occur (the names are from Smith 1974, p. 584). In the case of the radiating fringe type, the core is usually alkali feldspar (Fig. 11), rarely plagioclase (Fig. 12). Occasionally, different types of micrographic texture occur in the same thin section (Fig. 13). In the same alkali feldspar grain, there are commonly several domains that differ from each other in the orientation of the quartz individuals. Usually the orientation of the quartz units change abruptly at the grain boundaries, but sometimes they continue with the same optical orientation (verified with the gypsum plate) from one alkali feldspar grain into another, sometimes also from alkali feldspar to plagioclase (Fig. 14). Analogous textures have been described by Drescher-Kaaden (1969) and Augustithis (1974) from different granitoids, by Augustithis also from Finnish rapakivi granites. These authors interpreted the texture (quartz individuals intersecting the grain boundaries) to be due to later infiltration of quartz, but such evidence may be regarded equivocal (e.g., Smith 1974, p. 586). Very rarely, the micrographic or concave quartz continues as vein-like bodies between two feldspar grains, or the intergranular quartz enters an alkali feldspar grain along cleavage fractures, thus suggesting that in these cases the quartz is younger than the feldspar. In many other cases, however, the micrographic texture of the Tarkki granite may well be produced by a simultaneous crystallization of quartz and feldspar.

A very pronounced micrographic texture occurs in the Tarkki granite at the contact against the younger diabase. Here the heat flowing from the crystallizing diabase magma has often caused partial remelting of the granite components (Laitakari 1928, Kahma 1951). Quartz forms different types (often radiating fringe and cuneiform types) of intergrowth with both alkali feldspar and plagioclase. An example of a peculiar, breccia-like plagioclase—quartz intergrowth is shown in Fig. 15. The newly formed minerals (quartz and feldspars) may intersect the older minerals as monomineralic veins or as vein-like bodies of quartz—feldspar intergrowth. Obviously some of the micrographic textures observed in the Eurajoki granites, although far from diabase outcrops, are produced by subhorizontal diabase dikes located just over or below the present erosion niveau.

Myrmekite

Rims or grain rows of myrmekite and sodic plagioclase occur in most of the sections of Tarkki granite studied. Myrmekite and sodic plagioclase usually form thin rims between plagioclase and alkali feldspar (microperthite) grains or thin double rims or grain rows between two alkali feldspar grains. Very rarely, sodic plagioclase with or without vermicular or drop-like quartz occur as vein-like bodies in alkali feldspar. The width of the rims and rows is usually about 50 μm or less.

Myrmekite and sodic plagioclase rims occurring between plagioclase and alkali feldspar grains show generally the following characteristics:

1) The boundary between plagioclase and the myrmekite (or sodic plagioclase) rim is commonly smooth (rectlinear or angular), whereas the boundary between the rim and alkali feldspar tends to be irregular (Fig. 16). Often the myrmekite forms wart-like projections into the alkali feldspar. Sometimes, however, myrmekite and sodic plagioclase rims cut the primary zonal plagioclase (Fig. 17). Besides the common appearance of vermicular quartz, the rim—plagioclase boundary is often marked by a sharp change in the plagioclase composition and/or by a difference (sometimes very slight) in the amount and nature of alteration and pigmentation (Fig. 18). The rims are typically less and/or more finely pigmented than the core plagioclase.

2) When plagioclase is in contact with both alkali feldspar and late quartz or biotite (all typically anhedral against plagioclase), the plagioclase—quartz or plagioclase—biotite boundary often continues uniformly as a plagioclase—myrmekite or plagioclase—sodic plagioclase boundary between plagioclase and alkali feldspar, and the myrmekite or sodic plagioclase projects irregularly into the alkali feldspar (Figs. 18—20). In the cases depicted, the quartz and the biotite are anhedral against alkali feldspar or show mutual boundaries with it.

3) The rim material in some cases contains inclusions (relicts) of alkali feldspar with the same orientation as the host alkali feldspar.

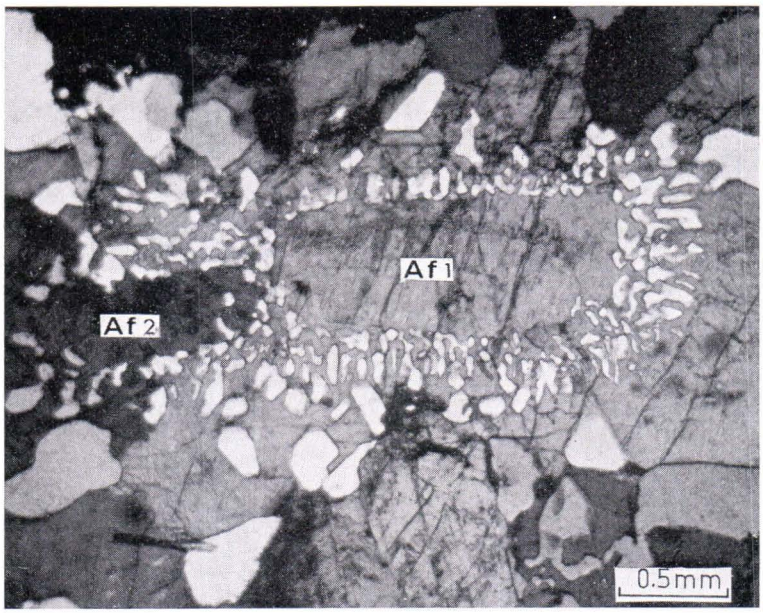

Fig. 11. Micrographic alkali feldspar—quartz intergrowth of the radiating fringe type. The quartz individuals enclosed in alkali feldspar Af 2 extinguish simultaneously but have an opposite optical orientation compared with the quartz individuals in Af 1. Sample 502/PL/69.

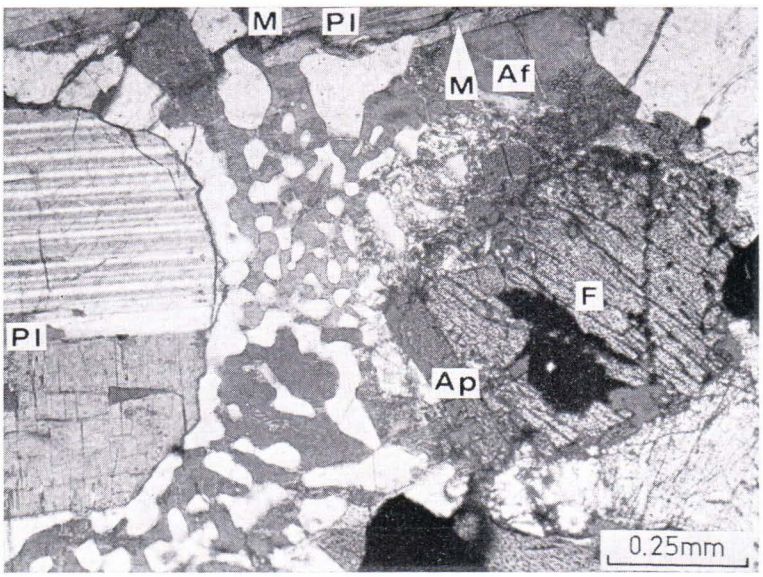

Fig. 12. Micrographic alkali feldspar—quartz intergrowth surrounding a euhedral plagioclase grain. Myrmekite is not present where quartz is between plagioclase (Pl) and alkali feldspar (Af), but occurs where these minerals are in direct contact (M). F fayalite, Ap apatite. Sample 75/PL/68.

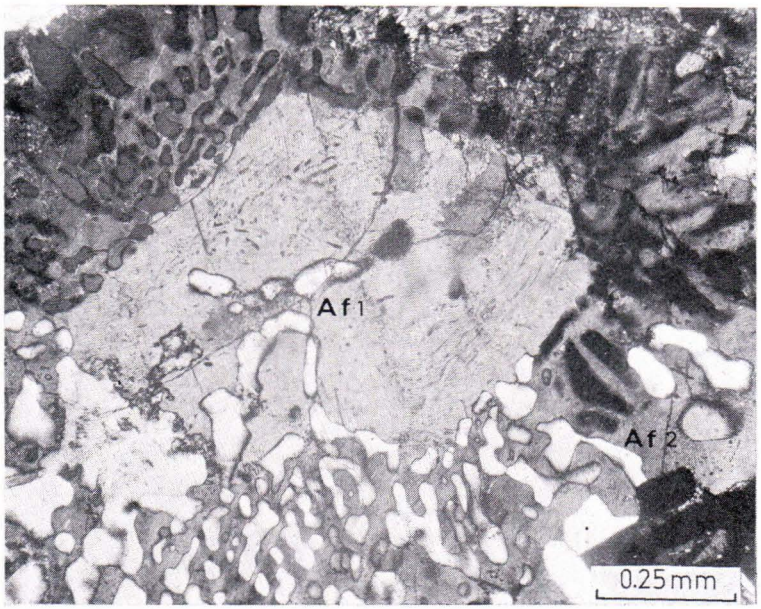

Fig. 13. Two types of micrographic alkali feldspar—quartz intergrowth. The inner alkali feldspar grain (Af 1) contains fine vermicular quartz and coarser quartz rods, all in uniform optical orientation. In the surrounding alkali feldspar grain (Af 2), there are coarser quartz rods in two different orientations, one of them being the same as in the quartz of Af 1. The coarse quartz individuals form with Af 2 a radiating fringe type intergrowth around Af 1. Sample 502/PL/69.

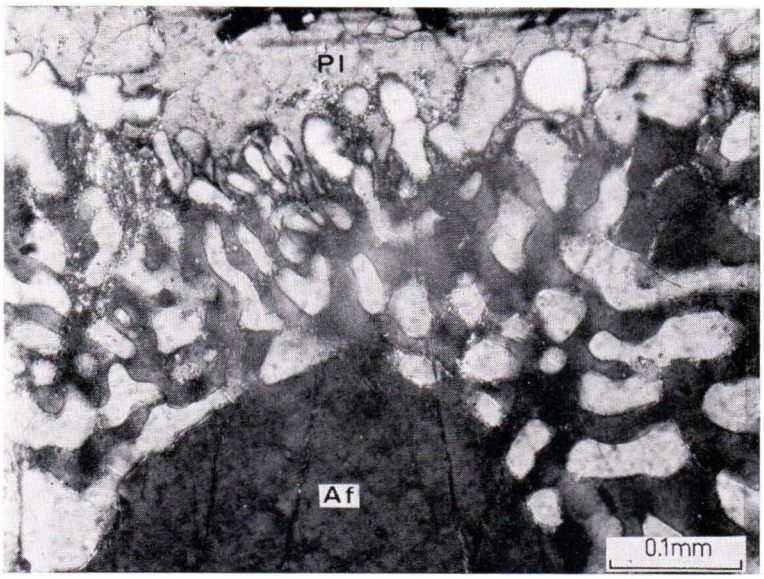

Fig. 14. Micrographic alkali feldspar—quartz intergrowth of the radiating fringe type. The quartz units continue a short distance into the adjacent plagioclase (Pl) grain, mostly with uniform orientation. At the grain contact, the plagioclase also contains fine myrmekitic quartz vermicules between the coarser quartz units. The myrmekite quartz shows the same optical orientation as the coarser micrographic quartz. Sample 75/PL/68.

Fig. 15. Micrographic texture in Tarkki granite at the contact against a large diabase sheet. The alkali feldspar grain is surrounded by plagioclase. The quartz forms a breccia-like intergrowth with plagioclase and enters the alkali feldspar as thin veins (white). The dark blebs in the alkali feldspar are plagioclase. Sample 156/IH/67.

4) The rim plagioclase is nearly always in crystallographic continuity with the host plagioclase. The twinning of the host plagioclase either continues to the rim or ends at the rim boundary. In rare instances, the extinction of the twins in the rims is reversed in relation to the twins of the host plagioclase.

5) The rim plagioclase is commonly zoned, the anorthite content decreasing against alkali feldspar. Two zones differing in composition (oligoclase and albite) are often seen.

6) Microscopic quartz vermicules may be present in the whole rim; they may be confined only to a certain zone approximately similar in composition or to part of it; or they may be lacking. If quartz units are present in two zones, they are thicker in the zone adjacent to the host plagioclase. Commonly there is a very thin water-clear albite seam without quartz vermicules against the alkali feldspar (Fig. 20).

7) The quartz vermicules tend to be oriented perpendicular to the rim boundaries. In wart-like bodies they form irregular fans, whose wide end points to alkali feldspar. When the quartz units form V-, Y- or U-shaped bodies, they open into the direction of alkali feldspar.

The myrmekite—sodic plagioclase formations between two adjacent alkali feldspar grains tend to be more poorly developed than the rims between plagioclase and alkali feldspar. These intergranular precipitates are typically composed of a double rim or double row of single blebs usually elongated parallel to the grain boundary. Each

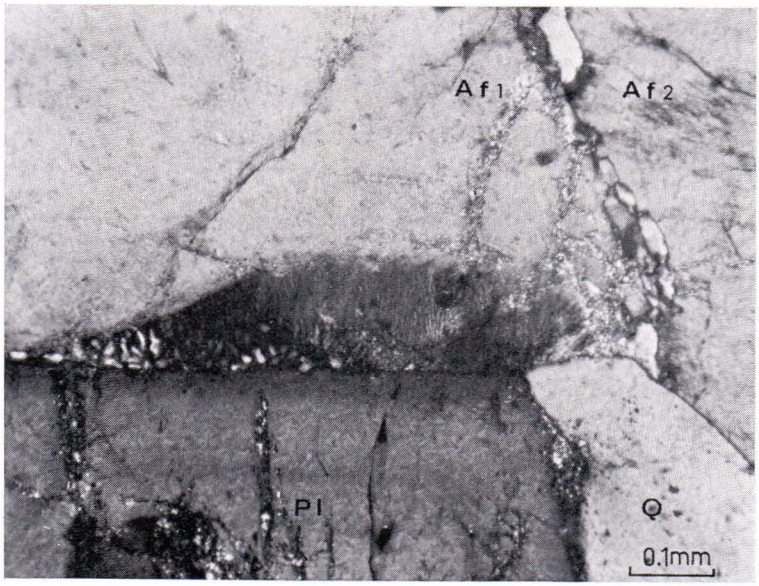

Fig. 16. Myrmekite on zoned plagioclase (Pl) crystal against alkali feldspar. Also a thin double myrmekite rim between two alkali feldspar (Af 1 and Af 2) grains. Q quartz. Sample 44/PL/68.

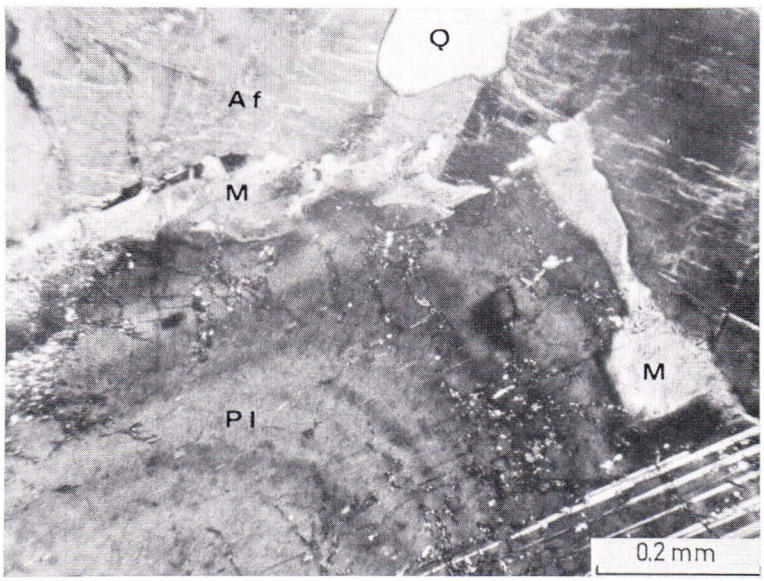

Fig. 17. Myrmekite rim (M) cuts the zoned structure of a plagioclase (Pl) grain. Af alkali feldspar, Q quartz. Sample 44/PL/68.

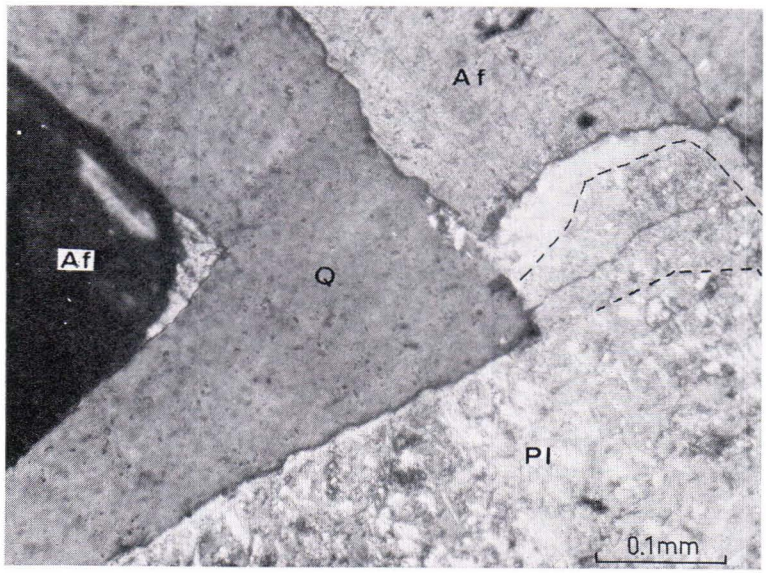

Fig. 18. Contact area between plagioclase (Pl), alkali feldspar (Af) and interstitial quartz (Q). Against alkali feldspar, the plagioclase shows a wart-like projection. The plagioclase—quartz boundary can be followed in plagioclase as a boundary between coarsely sericitic plagioclase and finely pigmented plagioclase. The outer zone against the alkali feldspar is free of inclusions. The zone boundaries are accentuated with a broken line. Sample 225/IH/68.

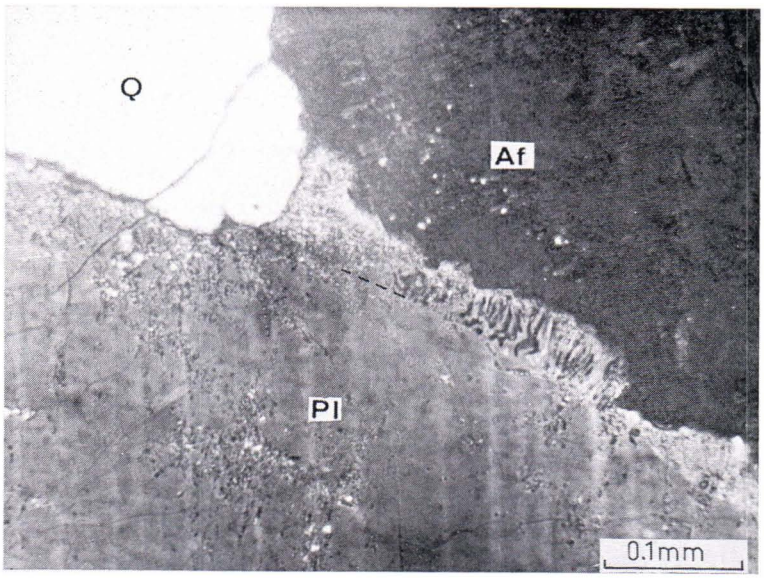

Fig. 19. Contact area between plagioclase (Pl), alkali feldspar (Af) and interstitial quartz (Q). A myrmekite rim between plagioclase and alkali feldspar. The quartz—plagioclase boundary continues uniformly as a plagioclase—myrmekite boundary between plagioclase and alkali feldspar. Sample 83/PL/68.

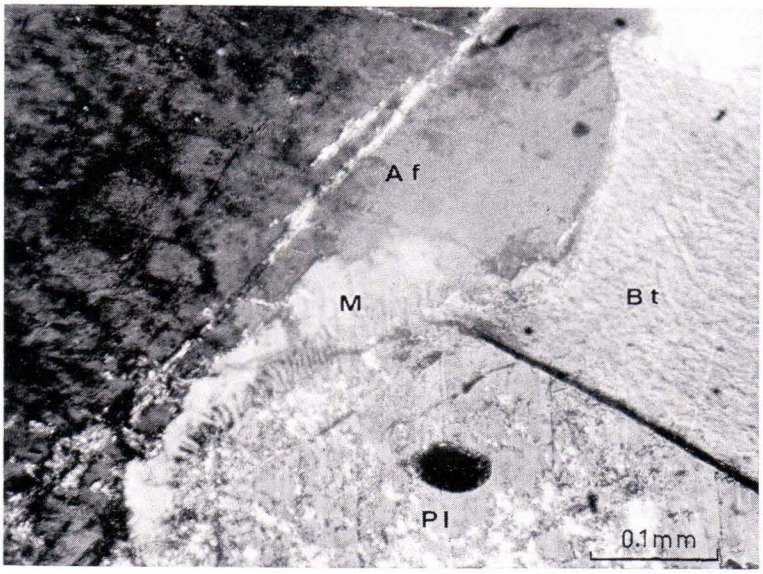

Fig. 20. Contact area between plagioclase (Pl), alkali feldspar (Af) and anhedral biotite (Bt). Myrmekite (M) between plagioclase and alkali feldspar. Plagioclase—biotite boundary continues as plagioclase—myrmekite boundary between plagioclase and alkali feldspar. An apatite inclusion (black) in plagioclase. Sample 104/PL/68.

Fig. 21. Double myrmekite rim between two alkali feldspar grains. The plagioclase units of the rim have the same optical orientation as the perthite albite on the opposite side of the rim. The perthite texture of the albite grains is a combination of very faint film perthite (not visible in the photomicrograph) and irregular vein and string perthite. Sample 44/PL/68.

plagioclase grain has become oriented according to the alkali feldspar on the opposite side of the rim, and projects into the alkali feldspar with which it shows no common orientation (Fig. 21). These »swapped rims» often form wart-like or mushroom-shaped projections into the host alkali feldspar. The rims follow the points 3, 5, 6 and 7 as listed for the plagioclase—alkali feldspar boundary precipitates (with the exeption that the alkali feldspar substitutes for the plagioclase substratum), except that the zoning is not so clear and common as at the plagioclase—alkali feldspar boundaries.

The literature dealing with myrmekite is voluminous, and many different hypotheses have been advanced to explain its origin. Phillips (1974) grouped the hypotheses into five main categories:

1) Simultaneous or direct crystallization of plagioclase and quartz from a melt or solution.

2) Replacement of potash feldspar by plagioclase, by the action of Na- and Ca-rich solutions or emanations ($KAlSi_3O_8 + Na^+ \rightarrow NaAlSi_3O_8 + K^+$, $2KAlSi_3O_8 + Ca^{++} \rightarrow CaAl_2Si_2O_8 + 4SiO_2 + 2K^+$).

3) Reactions associated with the replacement of plagioclase by potash feldspar.

4) Solid-state exsolution of the myrmekite components from the alkali feldspar. With the unmixing, the hypothetical high-temperature Schwantke's molecule reverts to anorthite and silica ($CaAl_2Si_6O_{16} \rightarrow CaAl_2Si_2O_8 + 4SiO_2$), which together with the exsolved albite form myrmekite.

5) Recrystallizing quartz involved with blastic plagioclase.

In the present textural description, points 1, 2 and 3 (p. 19) indicate that in the Tarkki granite the myrmekite plagioclase (and sodic plagioclase rims) between plagioclase and alkali feldspar have nucleated on pre-existing plagioclase and grown into alkali feldspar. Such complex features as those in Fig. 17 can be ascribed to the following events: 1. alkali feldspar corroded earlier plagioclase; 2. sodic plagioclase with or without quartz vermicules nucleated on plagioclase and grew into alkali feldspar. Between two adjacent alkali feldspar grains, the sodic plagioclase has nucleated on one of the feldspar grains, adopting its crystallographic orientation, and grown into another. The nucleation and growth mechanism of the plagioclase rims has been explained by Ramberg (1962) on the basis of energetic and crystallochemical data as the migration of the incoherent grain boundaries. Thus the textural and mineralogical relations associated with myrmekite in the Tarkki granite are consistent with both the exsolution hypothesis (4) and the replacement hypothesis (2). The exsolution hypothesis is supported by the observation that in microscopically homogeneous or nearly homogeneous alkali feldspar, the albite (possibly also anorthite) contents tend to be slightly higher than in clearly perthitic grains or perthitic parts of grains in the same thin section (see p. 86), and that myrmekite is associated with perthitic alkali feldspar. Also the normal zoning of the myrmekite plagioclase is in agreement with the exsolution hypothesis. On the other hand, the rare occurrence of myrmekite as veins in alkali feldspar (Fig. 22) suggests a replacement origin (see

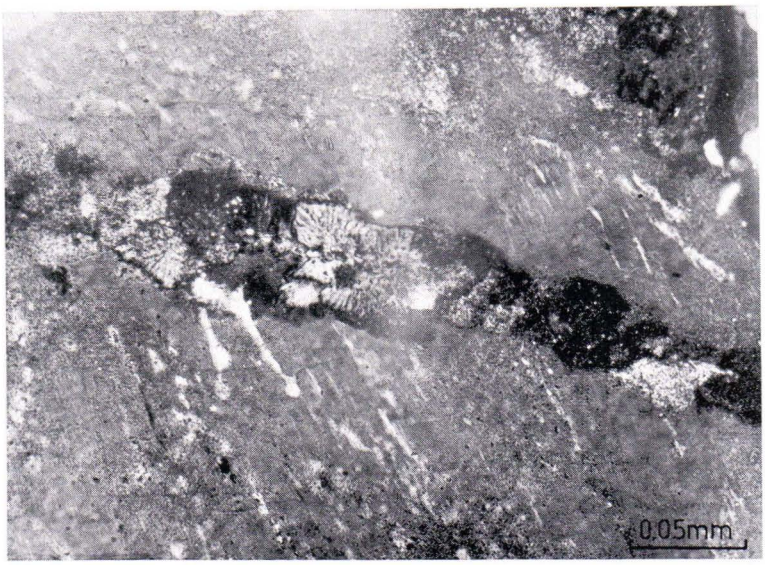

Fig. 22. Myrmekite vein in perthitic alkali feldspar. The vein contains differently oriented plagioclase grains with myrmekite quartz. Sample 185/IH/67.

Smith 1974, p. 560), although it can also be thought that the vein material is leached out from the alkali feldspar into the fracture. It appears to the writer that it is not possible at present to distinguish completely between myrmekitization caused by exsolution and metasomatic replacement. The relations may still be complicated by the possible solution, migration and redeposition of the exsolved material by interstitial fluids. Probably exsolution was the most important factor in the genesis of the myrmekite and sodic plagioclase rims in the Tarkki granite, but even the possibility of a metasomatic origin cannot be ruled out, and recrystallization may still have modified the textures.

THE VÄKKÄRÄ GRANITE

Since Laitakari's study (1928), the so-called Väkkärä granite has been known as a topaz-bearing rapakivi granite. During the remapping in 1967—70, it became clear that the Väkkärä granite is not homogeneous but consists of several varieties, which differ from each other in texture and/or mineral composition. The writer (1974) has differentiated the following main types of Väkkärä granite: contact type, even-grained type, porphyritic type and coarse-grained type. Photographs showing the macroscopic texture of the most important types are presented in Figs. 23—26, and the results of point-counting (modal) analyses are summarized in Table 3 and in Fig. 27. The distinction between these types is not always easily apparent, and because in addition there are wide areas without any outcrops, the marking of the

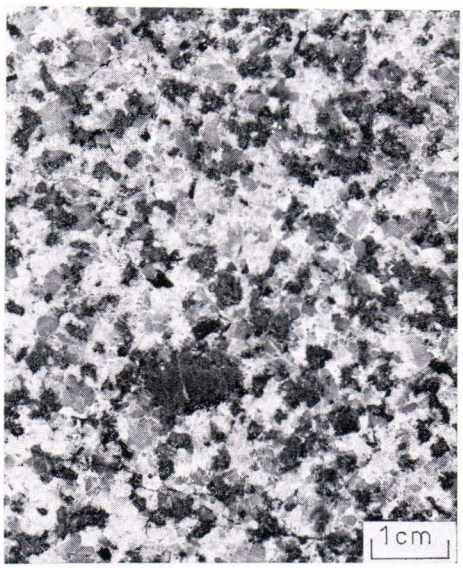

Fig. 23. Polished sample of the Tarkki granite. Sample 85/IH/67. Photo E. Halme.

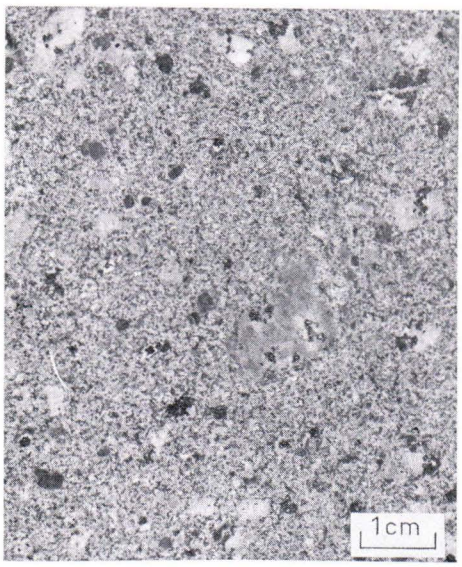

Fig. 24. Polished sample of the contact type of Väkkärä granite. Sample 309/PL/68/IH. Photo E. Halme.

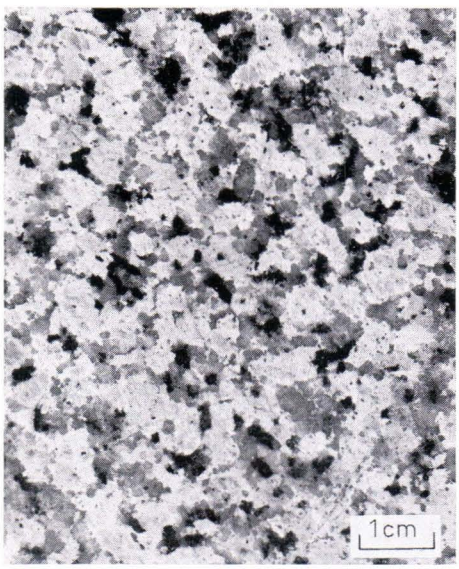

Fig. 25. Polished sample of the even-grained type of Väkkärä granite. Sample 17/PL/6/IIH. Photo E. Halme.

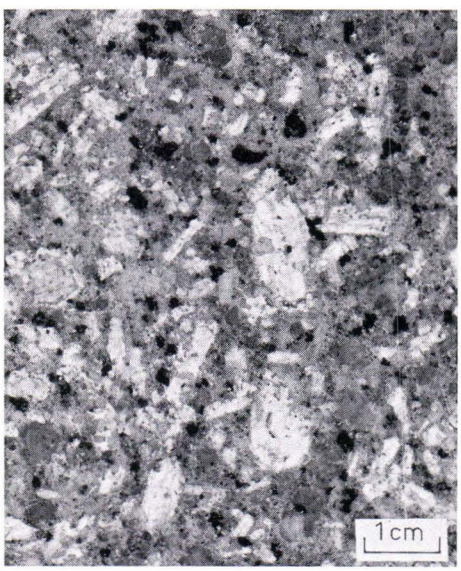

Fig. 26. Polished sample of the porphyritic type of Väkkärä granite. Sample 98/MK/687/H. Photo E. Halme.

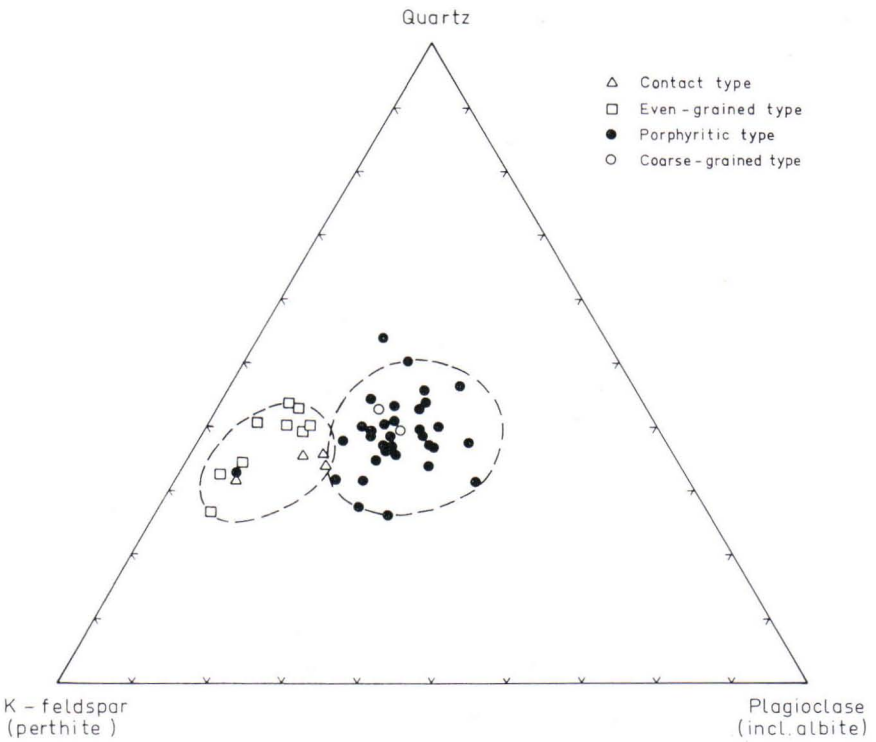

Fig. 27. Modal plagioclase (incl. albite), potassic alkali feldspar and quartz in Väkkärä granite.

Table 3

Modal composition (vol %) of the different types of Väkkärä granite. The number of thin sections is given in brackets after the name of the granite type.

	Contact type (4)			Even-grained type (9)			Coarse-grained type (2)			Porphyritic type (32)			
	min.	max.	mean	min.	max.	mean	min.	max.	mean	min.	max.	mean	stand. deviat.
K-feldspar	40.7	56.5	45.7	41.9	60.1	49.0	32.0	34.3	33.2	25.1	44.4	31.9	4.0
Quartz	29.8	31.1	30.6	24.4	39.5	35.3	34.7	40.7	37.7	24.0	47.2	35.3	5.4
Plagiocl. (+ seric.)	7.6	18.3	14.2	5.5	12.7	8.8	20.3	27.0	23.7	16.6	36.8	23.9	4.9
Biotite, Chlorite	5.4	10.2	7.8	2.0	7.6	4.8	1.9	3.6	2.8	2.2	8.2	4.8	1.8
Muscovite	0.0	0.5	0.1	0.0	0.6	0.1	0.0	0.0	0.0	0.0	3.5	0.3	0.8
Topaz	0.0	0.0	0.0	0.0	0.3	0.0	0.6	2.1	1.4	0.0	4.3	2.1	1.5
Fluorite	0.2	1.2	0.5	0.7	1.3	0.9	0.6	1.5	1.1	0.0	3.0	1.4	0.7
Others	0.4	1.5	1.1	0.2	4.5	1.1	0.1	1.1	0.1	0.1	1.6	0.4	0.4
			100.0			100.0			100.0			100.1	

Fig. 28. Contact between the Tarkki granite (lower part of the photograph) and the contact type of the Väkkärä granite. Outcrop 312/PL/68; x = 6 790.80, y = 531.72.

areal distribution of the granite types on the appended map is only approximate. In all the types, the plagioclase is characteristically albite (An usually 0—5 %), and in the classification scheme recommended by the International Union of Geological Sciences (Geotimes, October 1973, pp. 26—30), they thus fall into field 2 (alkali feldspar granite). Because, in addition, the content of dark constituents is steadily less than 10 per cent, the name alaskite can be used to designate these rocks. Secondary alterations are common. The contacts between the different types are not exposed, except the contact between the porphyritic and coarse-grained types in one outcrop; and thus it is not known if the contacts are gradational or sharp. The different types probably represent more or less different stages of emplacement. If it is assumed that the types are genetically closely related to each other, then the petrographic and geochemical data obtained suggest the following order of formation: contact type → even-grained type → coarse-grained and porphyritic (topaz-bearing) types.

Contact type

The contact type is visible on the northwestern margin of the Väkkärä granite complex. A sharp contact against the Tarkki granite can be seen in several places on the shore cliffs (Fig. 28). The contact type contains some fragments of Tarkki granite and it also sends apophyses into the Tarkki granite.

The contact type is a reddish-gray or gray porphyritic rock, which contains in a fine-grained ground mass (average grain size 0.3—0.5 mm) angular or corroded

megacrysts of alkali feldspar, plagioclase (albite and oligoclase—albite) and quartz, 1—10 mm in diameter (Fig. 29). The ground mass contains the same minerals and, in addition, dark reddish-brown biotite (electron microprobe analysis in Table 7, p. 90) which has partly altered to green biotite and chlorite. In some cases, biotite and chlorite form larger irregular aggregates. As accessories, the ground mass contains in relative abundance zircon, ilmenite, anatase, monazite, apatite, xenotime and magnetite. Secondary fluorite occurs as thin veins and patches in feldspar.

The feldspar megacrysts, especially alkali feldspar, commonly contain at their margins drop-like quartz inclusions. At the margins of alkali feldspar megacrysts, the quartz often forms micrographic intergrowths of the radiating fringe type. Very rarely, the core of such a megacryst is composed of plagioclase. A more irregular micrographic intergrowth occurs sometimes in the ground mass. In some cases, the quartz units continue from one grain to another without any change in crystallographic orientations. A very pronounced micrographic alkali feldspar—quartz intergrowth occurs in a thin seam at the immediate contact against the Tarkki granite. Concave quartz inclusions are present occasionally in the alkali feldspar megacrysts. Both the megacryst and the ground-mass alkali feldspar are typically perthitic (p. 73).

Fine-grained, slightly porphyritic, light-red granite, which may represent the contact type, has been found in a couple of very small isolated outcrops also in the northern part of the Väkkärä granite complex (e.g., the immediate country rock of the dark porphyry dike DP III in outcrop 1/IH/75).

Even-grained type

The even-grained type of Väkkärä granite is a light-red, medium-grained rock (prevailing grain size 3—6 mm), which contains as its main constituents alkali feldspar, quartz, plagioclase (An_{2-7}) and altered biotite. The content of plagioclase is notably low (Table 3). Zircon, ilmenite, anatase and monazite are typical accessories. Secondary topaz and cassiterite occur in very small amounts in the outcrops (17, 393 and 394/PL/68) around coordinates x = 7 789 and y = 535 in the central part of the granite stock.

The texture is hypidiomorphic—granular. The alkali feldspar grains are typically somewhat larger than the grains of other minerals. Quartz occurs in part as euhedral grains showing crystal faces against alkali feldspar and plagioclase, but commonly it forms anhedral grains and interstitial tongues between the feldspars. In the alkali feldspar, the quartz commonly occurs as euhedral or irregular, sometimes concave inclusions, or as a micrographic intergrowth. In the latter case, the intergrowth is often of the radiating fringe type; in some cases, it appears to be quite irregular. The boundaries between the feldspar grains are generally sutured. The plagioclase usually shows euhedral outlines against alkali feldspar, but in some cases the alkali feldspar is euhedral against plagioclase. The biotite shows two main modes of occurrence.

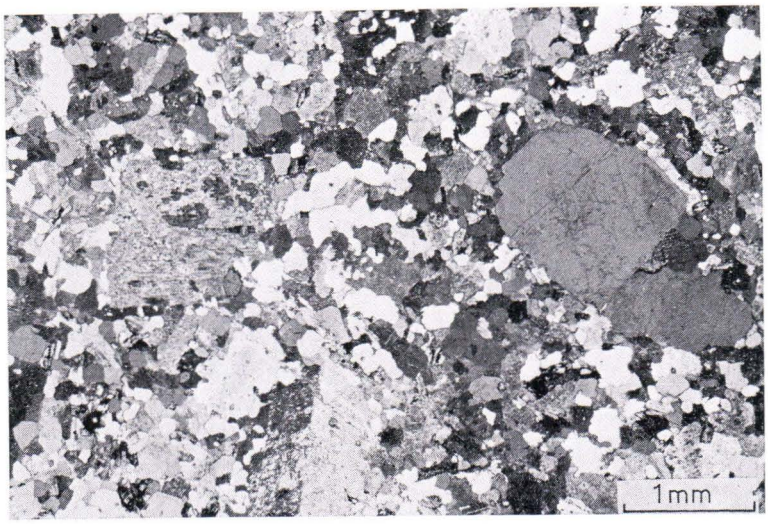

Fig. 29. Photomicrograph of the contact type of Väkkärä granite. The megacrysts are quartz, plagioclase and perthitic alkali feldspar. The plagioclase megacryst is partly replaced by fluorite. Photo E. Halme.

Fig. 30. Photomicrograph of the even-grained type of Väkkärä granite. An anhedral biotite aggregate between the quartz and feldspar grains. Photo E. Halme.

Flakes of dark red-brown biotite or its alteration products (green biotite, chlorite, muscovite, anatase and iron oxide) are in part euhedral against quartz and feldspars (1st generation); but in part more or less altered biotite occurs as anhedral aggregates between feldspar and quartz grains (2nd generation, Fig. 30). Microprobe analyses of both generations are shown in Table 7. It is possible that some of the euhedral

aggregates are pseudomorphs after hornblende (*cf.*, Laitakari 1928). In some places microscopic veins of sericite, chlorite and biotite intersect the quartz and feldspars.

The alkali feldspar is perthitic and conspicuously pigmented by minute inclusions. Its structural state varies greatly (p. 75). The plagioclase is usually markedly sericitized and to a small extent fluoritized. Numerous optical determinations and electron microprobe analyses show that its composition varies from An_2 to An_7. Often the plagioclase is seen to contain small irregular or rectangular inclusions (Ø 0.02—0.15 mm) of uniformly oriented K-feldspar. Some of these inclusions tend to be concentrated near the grain boundaries. Usually the inclusions have nearly the same optical orientation as the host plagioclase, but in some cases they have become orientated according to the adjacent alkali feldspar grains.

Porphyritic and coarse-grained (topaz-bearing) types

The porphyritic and the coarse-grained types of Väkkärä granite differ from each other only slightly in texture, and therefore they are described here together as topaz-bearing types. The porphyritic type occupies most of the southeastern part of the Eurajoki stock, an area of more than 10 km². The contact between the porphyritic type and the Tarkki granite is visible in one outcrop on the southern margin of the Väkkärä granite complex, and it has been intersected also by two drill holes. At the contact, the porphyritic type is somewhat finer-grained than farther away from the contact. The coarse-grained type is met with only in a small area within the porphyritic Väkkärä granite. The contact between the coarse-grained and the porphyritic types is clearly visible in one outcrop; the contact is relatively sharp or the types grade into each other within a few centimeters. The porphyritic type is finer-grained at the contact than usually and nearly equigranular, thus making the distinction between these types easier in the field.

Both topaz-bearing types are light red in color. In the porphyritic type, the fine- to medium-grained ground mass (the average grain size varies from 0.1 to 2 mm) contains typically larger insets of perthite (length 1—3 cm) and quartz (Ø 0.5—1 cm), sometimes also albite (Figs. 31—35). The amount and the size of the megacrysts vary, and in places (near contacts?) the granite changes gradually to a nearly equigranular fine-grained rock. The coarse-grained type does not show any clear porphyritic texture, although the closely packed K-feldspar grains tend to be somewhat larger (commonly 0.7—1.5 cm in diameter) than the quartz and albite grains. It also disintegrates easier than the porphyritic type, and in some places it contains an abundance of hematite pigment as streaks in mica and feldspars. The topaz content of these granites is usually 1—3 %. Typical accessories include, besides topaz, monazite, cassiterite, bastnaesite, xenotime, ilmenite, columbite and thorite (see Table 10). The columbite occurs as very small tabular black crystals. An electron microprobe analysis of columbite from the heavy mineral fraction of sample 10/PL/68/IH gave the result FeO (total iron) 16, MnO 4, Nb_2O_5 16, TiO_2 1, Sc_2O_3 1 and WO_3 3 wt-%.

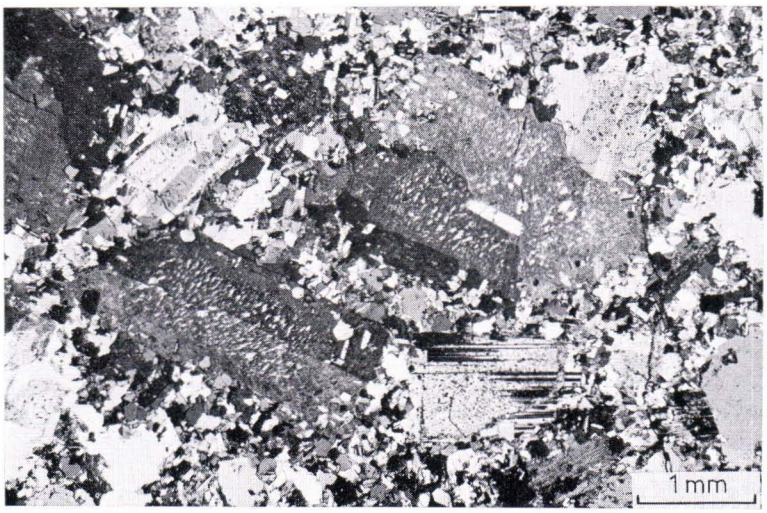

Fig. 31. Photomicrograph of the porphyritic type of Väkkärä granite. Megacrysts of perthitic alkali feldspar, quartz and albite in a fine-grained ground mass rich in albite. The central parts of the alkali feldspar megacrysts are markedly perthitic, the margins nearly homogeneous. Sample 98/MK/67/ER. Photo E. Halme.

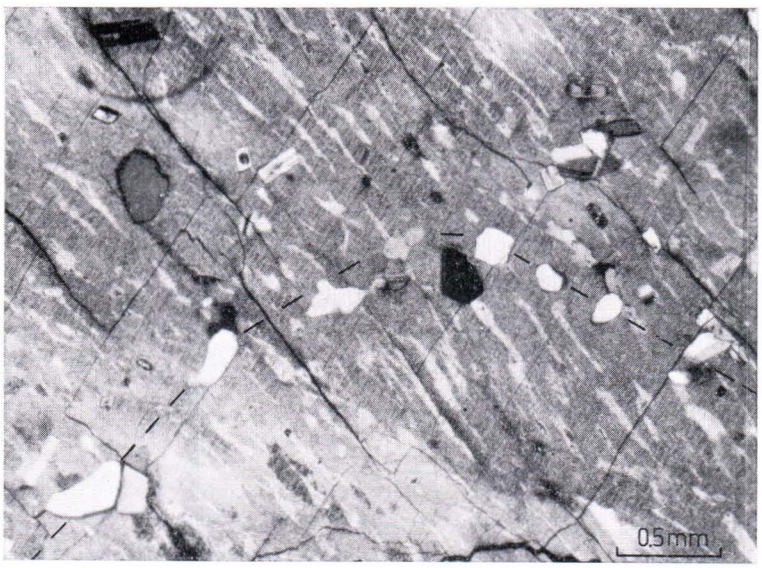

Fig. 32. Zonally arranged quartz and plagioclase inclusions in a perthitic alkali feldspar megacryst. The inclusion-rich zone is emphasized with a dotted line. Sample 37/MK/67.

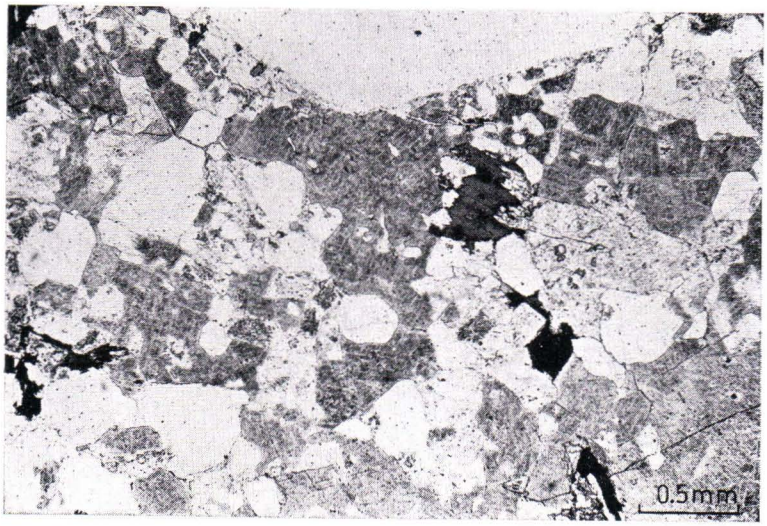

Fig. 33. Ground mass (microcline, quartz, albite, biotite, topaz) with a quartz megacryst at the upper part of the photograph. Sample 109/MK/67. One nicol. Photo E. Halme.

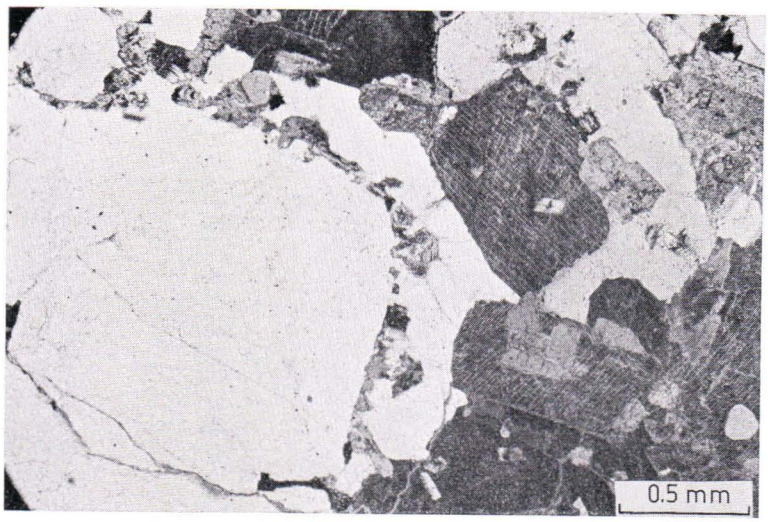

Fig. 34. Part of a quartz megacryst. Mineral inclusions border the euhedral core; the marginal quartz zone has grown anhedrally against the ground-mass feldspar. Sample 109/MK/67. One nicol. Photo E. Halme.

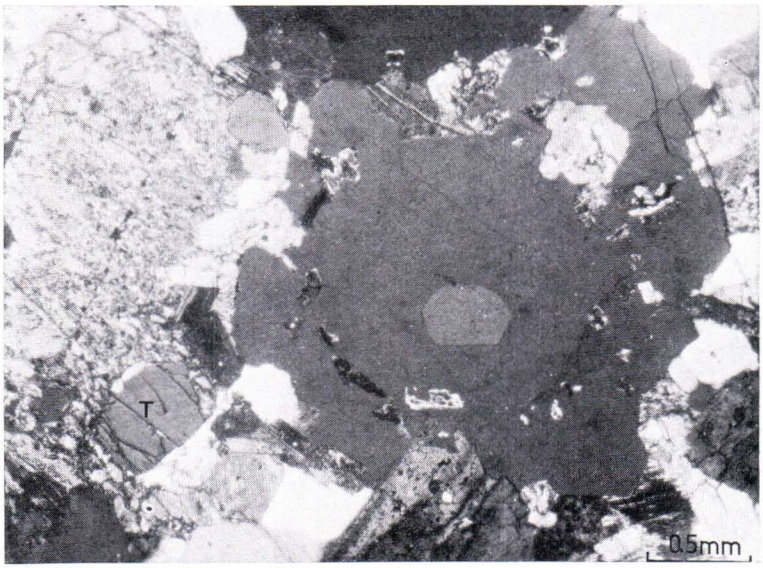

Fig. 35. Quartz megacryst showing three growth stages: 1) a euhedral center with optical orientation slightly differing from that of the surrounding quartz, 2) a euhedral crystal bordered by mineral (feldspars, biotite) inclusions and 3) an irregular (anhedral) marginal zone. T topaz. Sample 282/PL/68.

In the porphyritic type, the megacrysts of coarsely perthitic alkali feldspar have often been observed to contain in the marginal parts zonally arranged mineral inclusions (Fig. 32). The inclusions are mainly small quartz grains, but differently oriented plagioclase and biotite grains may likewise be present. Also in the central parts of the megacrysts, discrete, differently oriented plagioclase laths often appear as inclusions. Occasionally, there are micrographic quartz—microcline intergrowths of the radiating-fringe type around the euhedral perthitic microcline core. Outwards from the inclusion-rich zone, the alkali feldspar has in many cases grown anhedrally against the minerals of the ground mass. The amount of perthite albite is typically lower at the margins of the megacrysts than at the central parts (Fig. 31), obviously owing either to the lower crystallization temperature (subsolvus conditions) or to the exsolution of albite across the grain boundaries. In many cases, the larger quartz grains also contain zonally arranged mineral inclusions (alkali feldspar, plagioclase, dark brown mica, zircon, topaz, fluorite). Usually there is only one inclusion zone (Figs. 34 and 35), but sometimes two or even three inclusion zones are present. The association of the inclusion minerals usually differs in different zones. Sometimes an inner zone is met with containing only a few zircon inclusions. At the margins, anhedral quartz fills the spaces between feldspar grains (Figs. 34 and 35). In the ground mass, turbid (inclusion-rich) plagioclase and some quartz occur as the most euhedral minerals. The alkali feldspar may show euhedral outlines against other alkali feldspar grains, mica, chlorite and topaz (Figs. 36 and 39). In some places, however, biotite and topaz are euhedral

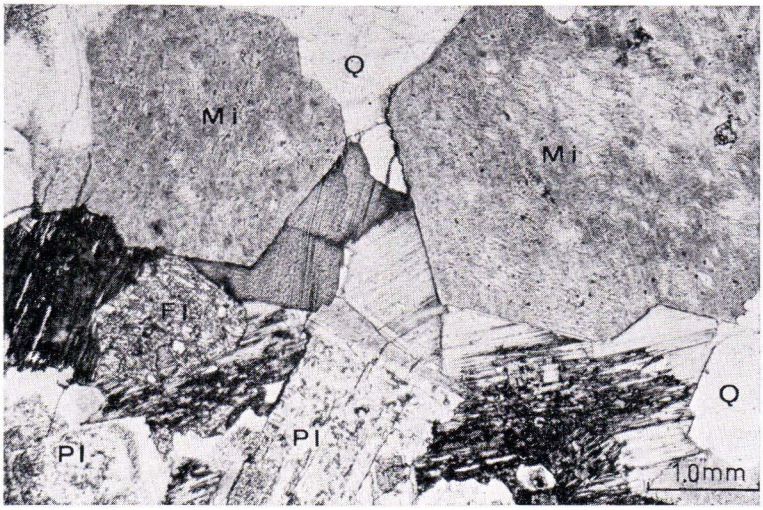

Fig. 36. Anhedral biotite flakes between microcline (Mi), plagioclase (Pl) and quartz (Q) grains. A euhedral fluorite grain (Fl) embedded in biotite. Sample 25/MK/67. Oblique nicols. Photo E. Halme.

against alkali feldspar and quartz. Albitic plagioclase occurs partly as euhedral or subhedral turbid grains, and partly as water-clear albite rims or grain rows or single grains located usually between turbid plagioclase and K-feldspar or between two adjacent K-feldspar grains (p. 77). According to the optical and electron microprobe determinations, the anorthite content of the plagioclase is constantly less than 5 mole-%. Mica minerals and chlorite occur in some places also as small flakes or vein-like bodies replacing feldspar.

Topaz occurs in various associations and it has obviously formed at different stages, being in part a primary constituent of the rock and in part a replacement product.

A small percentage of the topaz occurs as small, euhedral, single or zone-controlled inclusions in quartz crystals, sometimes also in feldspar. An example of such a topaz inclusion is presented in Fig. 37. In this case, rows of secondary fluid inclusions radiate from the edges of the topaz crystal into the surrounding quartz. The order of events seems to have been as follow: 1) topaz crystal was enclosed in a growing quartz crystal; 2) during cooling, the much higher thermal contraction of quartz compared to that of topaz caused the development of roughly radial cracks in the quartz around the topaz inclusion, the tension being strongest at the edges of the topaz crystal; 3) fluids filled the cracks, and during the rehealing rows of secondary fluid inclusions were formed. The thermal volume expansions (in per cent) of quartz and topaz from 20°C to the temperatures indicated are as follows (Skinner 1966):

	100°	200°	400°	500°	550°	570°	580°	600°	800°
Quartz	0.36	0.78	1.89	2.70	3.33	3.76	4.55	4.52	4.42
Topaz	0.10	0.27	0.65					1.08	1.56

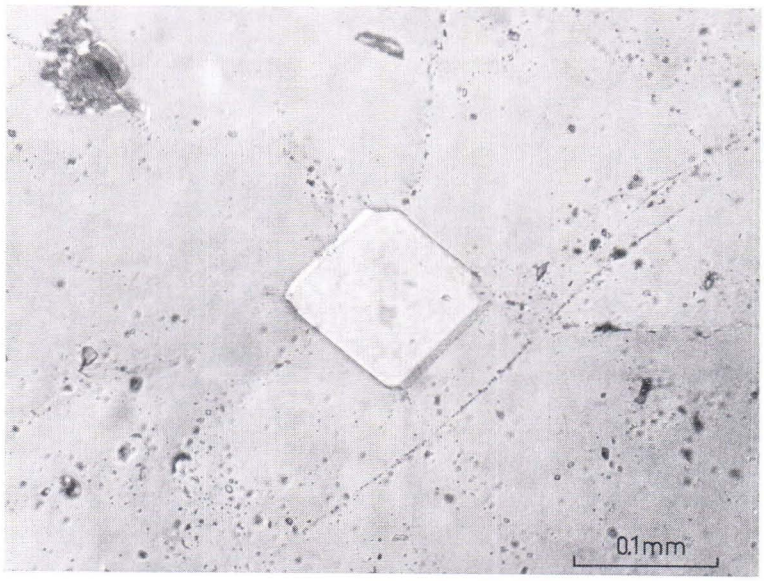

Fig. 37. Euhedral single topaz inclusion in a quartz megacryst. Rows of secondary fluid inclusions (healed fractures) radiate from the edges of the topaz crystal into the surrounding quartz. Sample 87/MK/67.

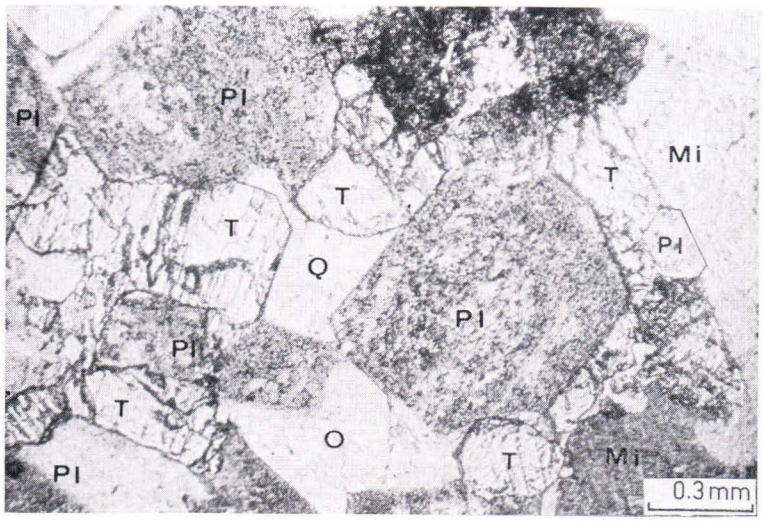

Fig. 38. Relations between albitic plagioclase (Pl), microcline (Mi), topaz (T) and late quartz (Q). Plagioclase and microcline show faces against topaz, whereas topaz is euhedral against quartz. Recrystallization has markedly affected the grain borders, especially those between microcline and topaz. Sample 25/MK/67. One nicol. Photo E. Halme.

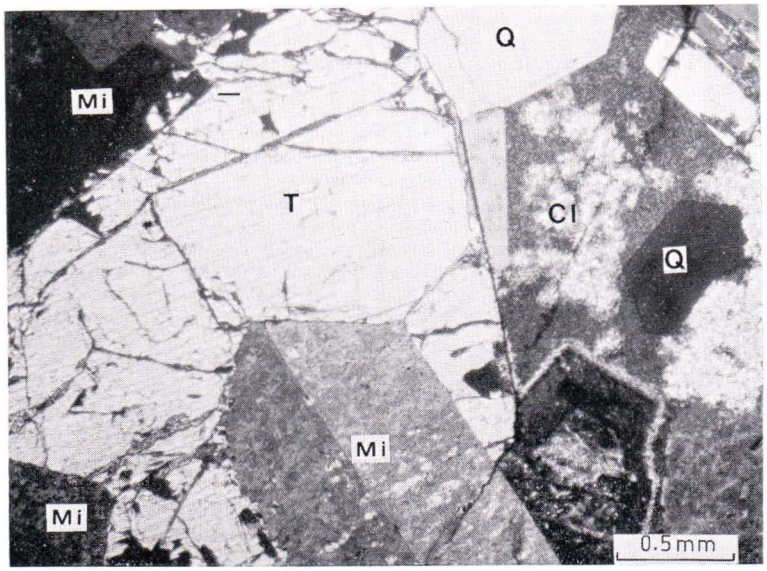

Fig. 39. Anhedral topaz (T) grain between microcline (Mi) grains. Recrystallization has to some degree affected the grain borders. In the right part of the photograph, there is an intergranular cavity filled by clay minerals (Cl). Q quartz. The topaz grain was partly fractured and broken during preparation of the thin section. Sample 25/MK/67.

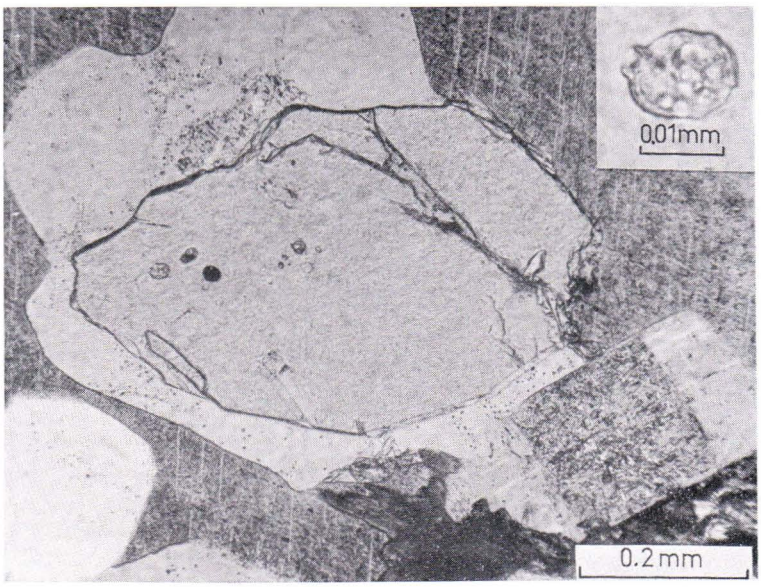

Fig. 40. Topaz grain surrounded by quartz and microcline and containing a group of very fine-grained, crystalline inclusions. The inset shows enlargement of one of the inclusions. The inclusion consists mainly of crystalline phases, but it appears to contain also some liquid (or glass) and irregular gas bubbles (dark gray). Sample 301/PL/68. One nicol.

A rapid change in volume (about 0.8 %) takes place in the quartz at the $\alpha - \beta$ inversion point (573°C at 1 atm., 599°C at 1 000 bar), and it is possible that the cracks originated at the inversion from high to low quartz. An opposite mode of origin, with topaz having crystallized (replacing quartz) from fluids circulating in fractures of quartz, does not appear probable. Small topaz crystals have been found in quartz also without any surrounding cracks. The occurrence of early topaz in mineralized granites in Spain has been reported recently by Saavedra (1976).

Commonly topaz occurs as subhedral or anhedral grains (Ø 1—2 mm or less) between early quartz and feldspar crystals. The alkali feldspar usually is euhedral against topaz, whereas the topaz shows crystal faces against late quartz (Figs. 38 and 39). Obviously, also this topaz should be ragarded as a primary constituent of the rock rather than metasomatic.

In the turbid plagioclase, topaz occurs ubiquitously as very small inclusions together with fluorite ± sericite ± quartz, and is then presumably produced by the reaction between plagioclase and fluorine-rich fluids. In some cases, topaz replaces feldspar as larger grains. In greisenized granite, the topaz replaces potash feldspar, producing a perthite-like texture (Fig. 62). Secondary topaz occurs also as fracture fillings (irregular, flattened grains) in quartz. This type of occurrence differs plainly from the euhedral topaz inclusions in quartz described earlier.

In some cases, the presumably primary topaz contains extremely fine-grained crystalline inclusions (Fig. 40), which possibly represent crystallized melt inclusions. Similar very small inclusions consisting mainly of glassy or very fine-grained crystalline material have sometimes been found also in quartz. In some cases these inclusions clearly follow the growth zones of quartz.

A characteristic feature of the porphyritic type of Väkkärä granite is the occurrence in it of small miarolitic cavities, which are usually filled with kaolinite, sericite and chlorite. The size of the cavities varies from microscopic interstitial vugs (Fig. 41) to pegmatite-lined druses with a volume of several cubic centimeters. Many of the cavities are lined with water-clear crystals of quartz, topaz and albite, in some cases also by microcline, fluorite and brown mica. The abundant occurrence of miarolitic cavities provides strong evidence of the occurrence of a separate fluid phase during the formation of this topaz-bearing granite (see Roedder and Coombs 1967, p. 421). The apparently primary fluid inclusions sometimes visible in the quartz and topaz crystals lining the cavities probably represent this fluid. During subsequent history of the rock, the »fluid inclusions» represented by the interstitial cavities leaked and postmagmatic fluids migrating in microfractures may have dissolved some daughter minerals and deposited clay minerals. This is indicated by the fact that in some cases microscopic veins of clay minerals enter the cavities, and that the topaz, quartz and feldspar crystals projecting into the cavities are occasionally partly replaced by the clay minerals. Thus the form of these »fluid inclusions» is primary but the content largely secondary.

Small pegmatitic veinlets and pockets are relatively common in the porphyritic

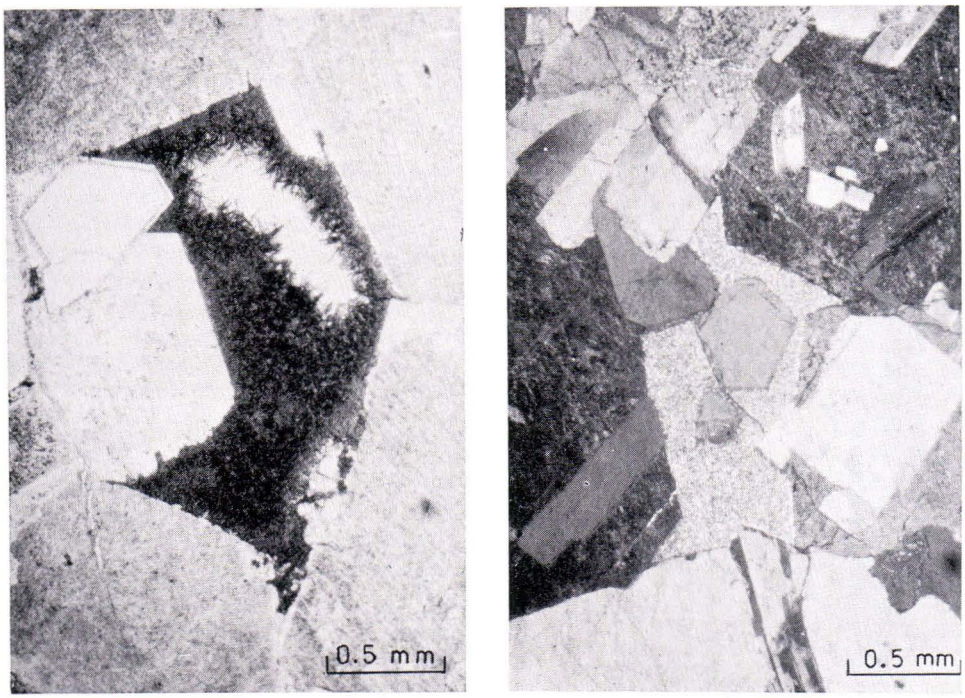

a b

Fig. 41. Interstitial cavities filled by clay minerals in the porphyritic type of Väkkärä granite. In *a* (sample 277/PL/68/IH), the cavity is partly filled with small chlorite crystals projecting into the open central part. In *b* (sample 85/MK/67), the cavity is filled with sericite. Note the inclusion zones in the quartz crystals in the cavities. Oblique nicols.

Väkkärä granite. They contain feldspar, quartz, dark mica and topaz as the main constituents. The topaz is often transparent with a bluish tint. Cassiterite and columbite also occur commonly in small amounts. The cassiterite forms rounded crystals about 1 cm or less in diameter. Columbite occurs in quartz as dark brown, thin, flattened, tapering needles, which are usually only a few mm in length. A microprobe analysis of one such crystal (sample 104/MK/67/IH) gave FeO 19.7, MnO 1.6, Nb_2O_5 69.0 and Ta_2O_5 6.2 wt-%.

Greisenized granite

Metasomatic (autometasomatic) alteration of the minerals, especially the chloritization and muscovitization of biotite, is common in all types of the Väkkärä granite and also in the Tarkki granite. In some places, the Väkkärä granite has been altered so extensively that the rock may be called greisenized granite, a rock intermediate between unaltered granite and greisen. Greisenized granite occurs usually around the ordinary greisen bodies and in areas where greisen bodies are common.

Marked recrystallization has affected both the texture and the mineral composition of the greisenized granite. The texture is granular, with only slight remnants of the hypidiomorphic texture. The modes show typically enhanced amounts of quartz, topaz, chlorite and white or pale brown mica (protolithionite). Topaz and quartz often replace alkali feldspar as vein-like bodies (Figs. 62 and 63). Also chlorite and mica minerals replace feldspar as irregular vein-like or tongue-shaped bodies (Fig. 60) or as single flakes. Dark brown biotite is not present. The alkali feldspar is in general not perthitic, but in some places the K-feldspar contains single irregular albite patches. The patchy extinction texture (patchy twinning, see p. 77) of the K-feldspar is very pronounced.

THE PORPHYRY DIKES

The granites of the Eurajoki stock are cut by porphyry dikes. On the basis of their appearance and mineral composition, the dikes can be divided into two distinct groups, 1) quartz porphyry (QP) dikes and 2) dark porphyry (DP) dikes. The dikes are marked QP I—V and DP I—III on the appended map.

Quartz porphyry dikes

Quartz porphyry dikes have only been found in the Tarkki granite in the southern and northeastern parts of the Eurajoki stock. The strikes of the dikes (QP I and II) on the southern side of the stock are N40°E—N75°E, and of those (QP III—V) in the northeastern part N-S — N30°E; the dip is vertical or nearly so. The widths of the dikes QP I—V are 1, 1, 10, 3 and 15 m, respectively.

The dikes are light red in color. Against the country rock, they typically have a darker chilled margin (average grain size $\sim$ 0.01 mm), in which an indistinct flow banding and mineral parallelism is often visible (Fig. 42). In some places, there is a vague contact between the chilled margin and the center, suggesting that the magma had moved on and passed its concealed contact phase. The grain size of the ground mass as well as the amount and size of the megacrysts increase towards the central parts of the dikes. In the central parts of the widest dikes, the average grain size of the ground mass is about 0.2 mm, and the alkali feldspar megacrysts are up to 2—3 cm in length. Sometimes a flow texture is visible also in the central parts of the dikes as a statistical orientation of the feldspar and quartz megacrysts.

The contact areas between the three rocks (Tarkki granite, Väkkärä granite and porphyry dikes) are not exposed. Only dike QP III (a topaz-bearing quartz porphyry — granite porphyry dike) is visible on an outcrop (126/IH/67; x = 6 789.00, y = 538.63) quite near the Tarkki granite — Väkkärä granite contact. In this case, no distinct chilled margins are visible in the dike, but the rock is relatively coarse-

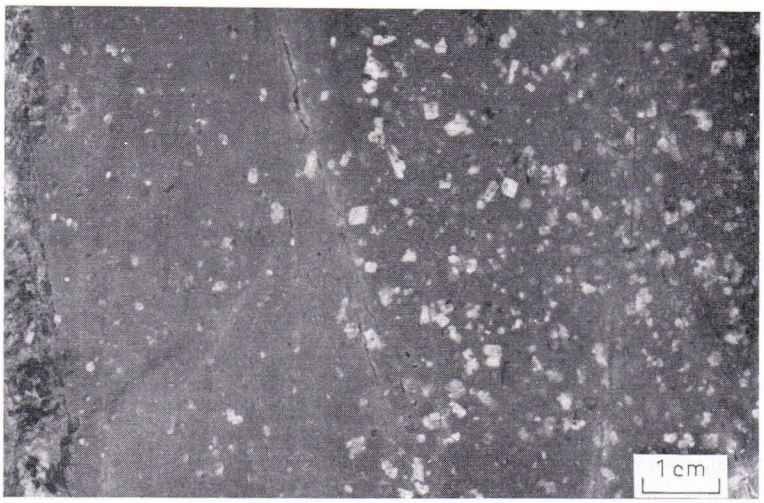

Fig. 42. Contact zone of a quartz porphyry dike against the Tarkki granite (on the left). At the central part of this dike the alkali feldspar megacrysts are up to 2—3 cm in length. Dike QP V, sample 228/IH/68. Polished specimen. Photo E. Halme.

grained (the average grain size in the ground mass being about 0.2 mm) throughout the dike. Obviously the same dike is exposed on another outcrop (231/IH/67; x = 6 790.13, y = 539.06) about 1.5 km in a horizontal direction from the contact mentioned, and now the dike has clear chilled margins. An obvious explanation of this phenomenon is that the porphyry dike in question and the topaz-bearing Väkkärä granite were formed approximately simultaneously and that the crystallizing Väkkärä granite heated the Tarkki granite near the contact, thus preventing the formation of chilled margins in the quartz porphyry dike. A close association of the Väkkärä granite and the quartz porphyry dikes in time is indicated also by the fact that in some places (e.g., the greisen vein swarm between the villages of Lapijoki and Hankkila at x = 6 787.30, y = 533.0) the greisenization has affected also the quartz porphyry dikes.

The dikes consist essentially of megacrysts of perthitic microcline, albite and quartz embedded into an aphanitic ground mass of the same constituents. Dark or white mica, chlorite and topaz are met with as megacrysts in some samples, but they are more common in the ground mass. Fluorite occurs commonly in small amounts in the ground mass, and rarely also bigger fluorite insets may be detected. Part of fluorite is clearly secondary. The high content of Sn (up to 125 ppm) in the dikes indicates the presence of accessory cassiterite, and apatite has been identified as an accessory mineral. The relative amounts of the different megacryst species vary from the contact to the central parts of the dikes (Table 4), and certain differences exist also between the mineral relations of the different dikes.

Table 4

Modal analyses (vol. %) of the quartz porphyry dikes of the Eurajoki stock.

Dike Sample	QP I 97B/IH/67	QP II 85B/IH/67	QP III 126B/IH/67	QP III 126B/IH/67*	QP IV (contact) 228A/IH/68	QP V (contact) 229A/IH/68	QP V (center) 229B/IH/68
K-feldspar	26.1	10.7	20.7	35.6	2.3	3.8	10.1
Plagioclase		2.1	13.8	24.1	2.4	1.8	0.9
Quartz	6.1	4.6	14.7	30.9	0.6	0.3	31.2
Biotite (Muscovite) ..	0.4	0.8	0.6	4.8	—	—	0.7
Chlorite	0.3	0.5	—		—	—	
Topaz	0.2	—	0.8	2.9	—	—	—
Fluorite	—	—	—	1.3	—	—	—
Others	—	—	—	0.4	—	—	—
Ground mass ...	66.9	81.3	49.4		94.7	94.1	57.1
	100.0	100.0	100.0	100.0	100.0	100.0	100.0

* Minerals of the ground mass included

The albite megacrysts show in part a continuous, uniform albite lamellation, in part the twinning is less regular (twin units end by tapering) and a shadowy extinction is typical. Slight sericitization is commonly present, particularly in the regularly twinned megacrysts. In the unusually coarse-grained dike QP III, the plagioclase also contains very small secondary inclusions of fluorite, topaz and quartz (see p. 58 and Fig. 58). Chessboard albite replacing K-feldspar may occasionally be present (see Fig. 58), but it is not typical. Not infrequently, the albite megacrysts are mantled by K-feldspar, which in many instances is perthitic. The poorly developed twinning and shadowy extinction or incipient mosaic texture are common, particularly in the albite of these zoned megacrysts.

Dike QP I is of especial interest because it contains more topaz than the other dikes. A chemical analysis made from this dike is presented in Table 10. The dike contains as megacrysts perthitic microcline (usually film perthite), albite, quartz and topaz. The aphanitic ground mass (average grain size about 0.01—0.02 mm) contains, in addition to these minerals, also some mica (usually medium brown or light), chlorite and fluorite. The albite megacrysts are commonly mantled by potassic alkali feldspar (Figs. 43 and 44). In some samples of the contact zone, the megacrysts consist nearly totally of such zoned feldspar intergrowths. The albite is often completely surrounded by K-feldspar, but in some cases the rim is incomplete. The albite core has euhedral outlines in certain places, but in other instances the boundary between albite and K-feldspar is irregular, suggesting replacement. In rare cases, the K-feldspar mantle is still surrounded by a thin albite rim. The albite megacrysts commonly show a dense, somewhat uncontinuous twinning; and in some grains of the analyzed sample, a clear cross-hatching is visible, indicating transformation. These albite megacrysts quite commonly contain patches of K-feldspar. Sometimes no twinning is visible in the albitic cores of the zoned megacrysts. A shadowy extinction or a poor mosaic texture is then typical (Fig. 44). Both albite and perthite commonly

occur as euhedral inclusions in the quartz megacrysts, albite also in the perthite megacrysts. The topaz megacrysts (Fig. 45) are often euhedral, but they may be also irregular and veined by a fine-grained micaceous material. Topaz has been found also as euhedral inclusions in quartz and perthite megacrysts (Fig. 46). Occasionally also the topaz megacrysts are seen to contain zonally arranged mineral inclusions at their margins. In the ground mass, topaz occurs as small needle-like prisms, which are often unevenly distributed but under the microscope do not show any textures indicating fracture-controlled replacement. Although many of the topaz grains in the quartz porphyry dikes can be explained to be of a metasomatic origin, a primary nature is often obvious (*cf.*, Fig. 46).

The topaz-bearing quartz porphyry dikes are quite similar to the topaz-bearing quartz keratofyres (ongonites) described recently by Kovalenko *et al.* (1971 and 1975) from Mongolia and Transbaikalia in the USSR. Kovalenko and his coworkers explained these rocks to be of magmatic origin, and they showed also experimentally that topaz and albite (An_{0-3}) can crystallize from a fluorine-rich ongonite melt (Kovalenko *et al.* 1974).

The similarities in mineralogical composition and geochemical properties (p. 103) between the quartz porphyry dikes and the Väkkärä granite indicate a close genetic connection between these rocks. It is possible that some of the quartz porphyry dikes are actually apophyses of the porphyritic Väkkärä granite. This is supported also by the lack of distinct chilled margins in dike QP III near the contact between the Tarkki and Väkkärä granites.

Dark porphyry dikes

In the northern part of the Eurajoki stock, there are three dark-colored porphyritic dikes, two of which run parallel with the nearby quartz porphyry dikes and one (dike DP III, the only porphyry dike found in the Väkkärä granite) approximately perpendicular to them. The widths of the dikes DP I—III are 3, 7 and 7 m, respectively. The dark porphyry dikes differ markedly from the quartz porphyry dikes in both their macroscopic and microscopic properties. The aphanitic ground mass is on a fresh surface dark grey or nearly black; on a weathered surface, it is dark grey or brown. The grain size of the ground mass and the megacrysts generally increases towards the central parts of the dikes (*cf.*, Figs. 47 and 48), although occasionally large feldspar insets occur at the contact.

The megacrysts consist mainly of markedly corroded and altered calcic plagioclase (An_{55-60}, zoning very weak or not visible), but also quartz, microperthitic alkali feldspar and ilmenite occur commonly in small amounts. The feldspar megacrysts are usually 1—3 cm in length, but occasionally alkali feldspar and plagioclase megacrysts up to 10 cm in length can be found. The plagioclase and quartz megacrysts occur commonly as conspicuously corroded crystals or as crystal fragments (Figs. 48 and 49); sometimes the quartz »megacrysts» are aggregates of several differently oriented

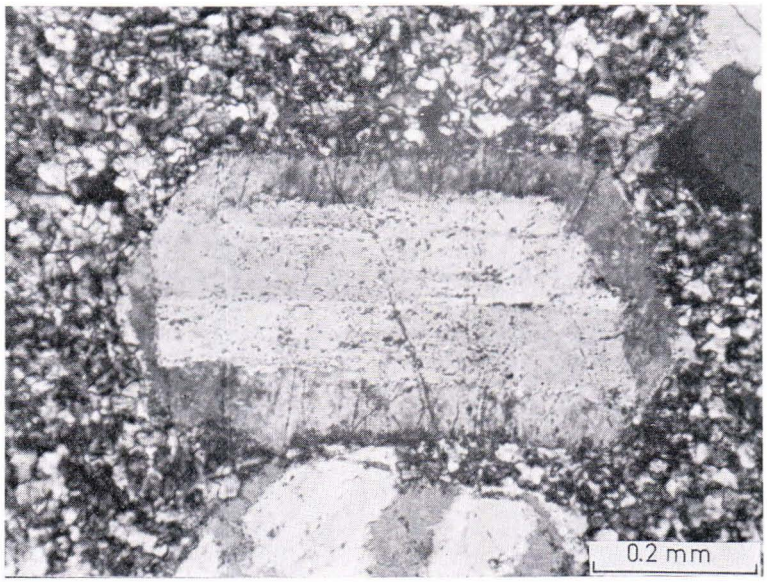

Fig. 43. Albite megacryst mantled and partly replaced by potassic alkali feldspar. The alkali feldspar in the lower part of the photograph shows irregular albite-K-feldspar intergrowth, suggesting replacement of albite by K-feldspar. Dike QP I, sample DH 1/21.9 m.

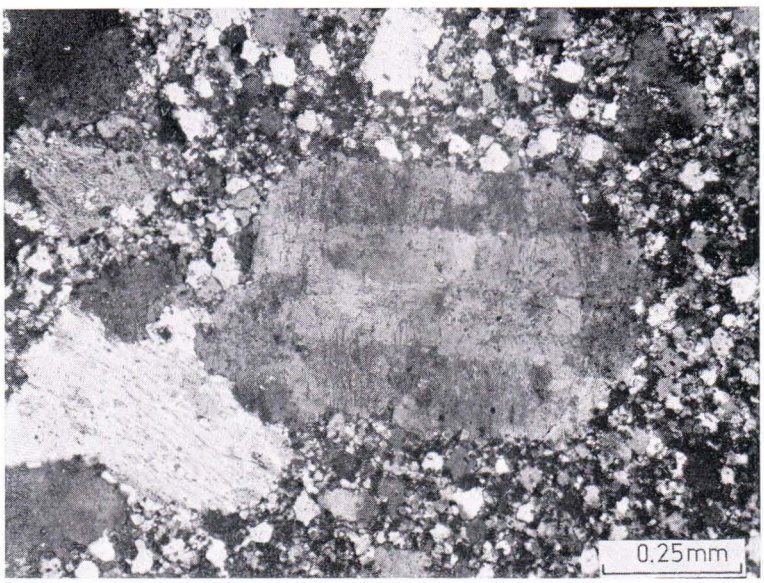

Fig. 44. Zoned alkali feldspar megacryst. Albite core surrounded and obviously partly replaced by potassic alkali feldspar. The core albite is not visibly twinned, but shows a prominently shadowy extinction. Dike QP I, sample 97 B/IH/67.

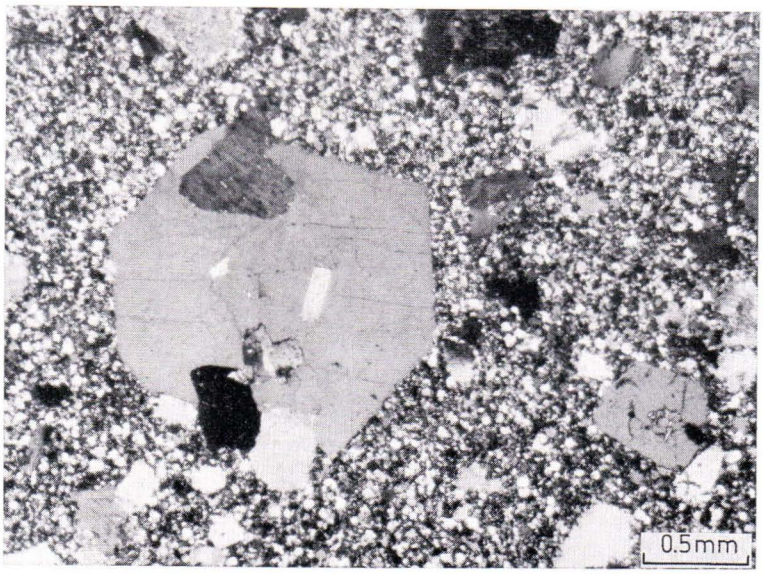

Fig. 45. Photomicrograph of the topaz-bearing quartz porphyry. The large quartz megacryst contains inclusions of potassic alkali feldspar and albite. A topaz megacryst (gray) on the right. Dike QP I, sample 97 B/IH/67. Oblique nicols.

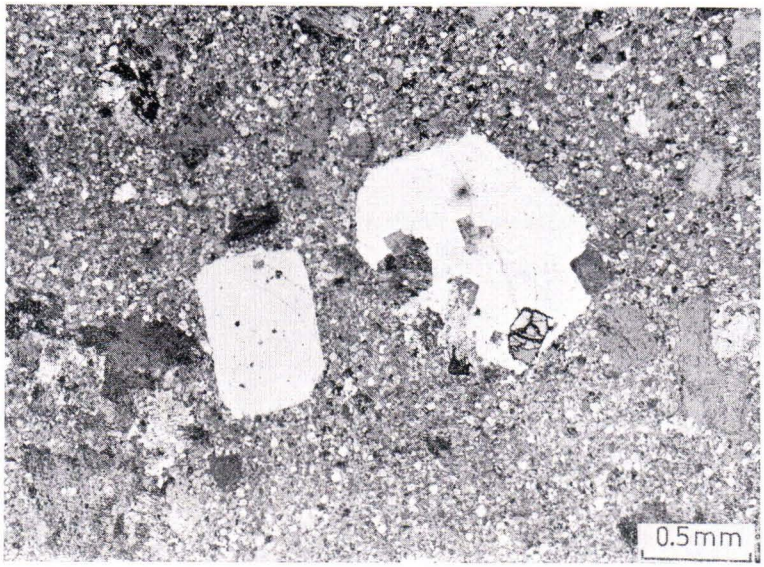

Fig. 46. Photomicrograph of the topaz-bearing quartz porphyry. The large quartz megacryst contains, besides the feldspar inclusions, also one euhedral topaz inclusion. The same sample as in Fig. 45. Oblique nicols. Photo E. Halme.

Fig. 47. Contact zone of a dark porphyry dike (DP III) against the Väkkärä granite. Polished specimen 1 A/IH/75. Photo E. Halme.

Fig. 48. Dark porphyry from the central part of dike DP III. The well-preserved large megacryst in the central part of the photograph is alkali feldspar, the corroded large megacrysts are plagioclase. Quartz megacrysts are only slightly lighter than the ground mass, and they are not easily distinguishable. One quartz megacryst is located about 1 cm below the lower end of the alkali feldspar megacryst, another triangular megacryst about 1.5 cm below the large corroded plagioclase megacryst. Specimen 1 C/IH/75. Photo E. Halme.

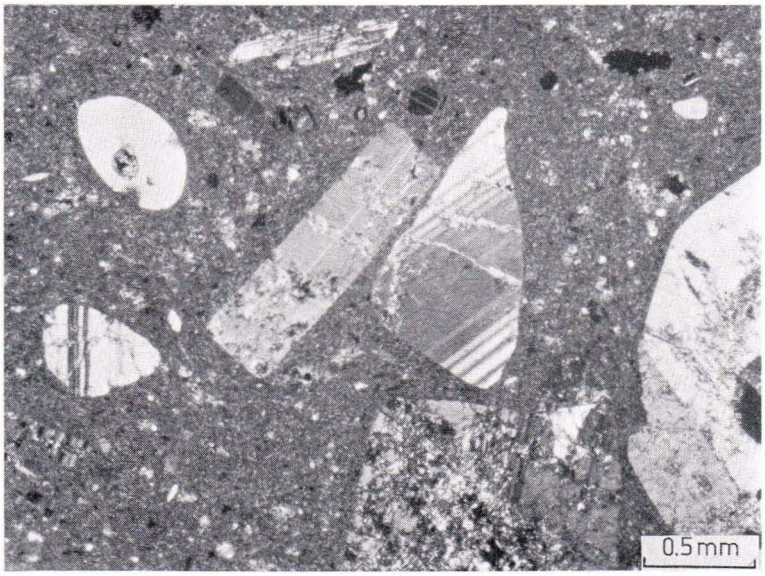

Fig. 49. Photomicrograph of the dark porphyry. Some of the plagioclase megacrysts are euhedral, some heavily corroded or broken into angular fragments, and may be considerably altered. The clear rounded megacryst is quartz. Dike DP III, sample 1 X/IH/75.

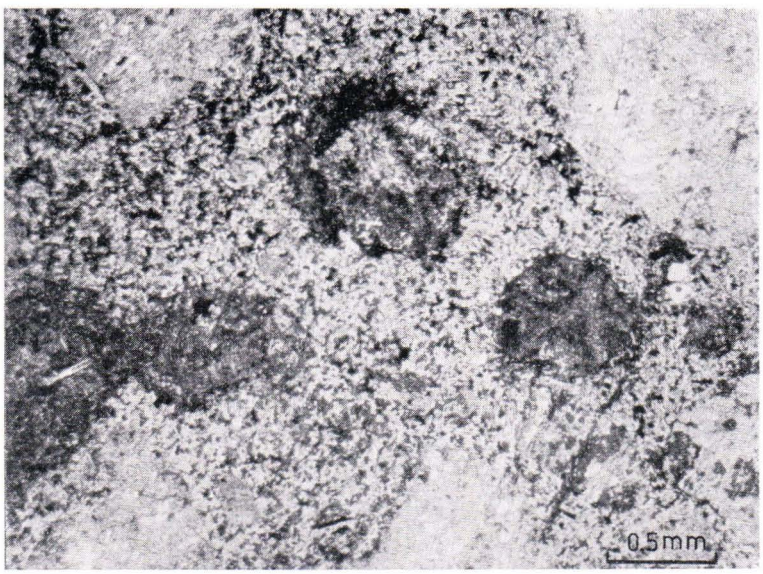

Fig. 50. Photomicrograph of the dark porphyry. Dark pseudomorphous megacrysts consisting of hornblende and chlorite, between larger plagioclase megacrysts. Dike DP I, sample 269 A/IH/68. One nicol.

grains. The alkali feldspar megacrysts are usually more idiomorphic and better preserved than the plagioclase. Bluish-green hornblende and biotite occur sometimes as single insets in the ground mass, but more commonly hornblende, biotite and chlorite separately or together form euhedral aggregates (Fig. 50), in which also carbonate may be present. Possibly these aggregates are pseudomorphs after pyroxene. Occasionally also apatite, sphene, anatase (dike DP I) and magnetite occur as megacrysts, but they are much more common in the ground mass.

The ground mass consists of varying amounts of plagioclase, brown or green biotite, bluish-green hornblende, alkali feldspar, quartz, apatite, sericite, epidote, sphene, anatase (dike DP I), Fe-Ti oxides, sulphides, prehnite, carbonate, fluorite (dike DP III) and zircon. In the contact zone of dike DP III, the extremely fine-grained ground mass consists essentially of brown biotite and tiny plagioclase laths with minor amounts of quartz and alkali feldspar, but in many instances the major dark minerals are chlorite, hornblende and green or brown biotite, and the amount of quartz and alkali feldspar may be notably high. In dike DP III, which intersects the fluorine-rich Väkkärä granite, also fluorite and sulphides (mainly pyrite and sphalerite, a little chalcopyrite and galena) occur in the ground mass, sometimes seen also as small insets. The sulphide minerals occur preferentially in the hornblende—chlorite—biotite—carbonate aggregates, obviously replacing these minerals.

Secondary alteration of minerals (propylitization) is notably prominent in the dark porphyry dikes, especially in dikes DP I and DP II. Plagioclase megacrysts are commonly largely replaced by sericite, epidote, prehnite, kaolinite and carbonate, sometimes along fractures also by K-feldspar. Sericite, epidote chlorite and carbonate are common secondary constituents in the ground mass. Sphene and anatase are probably formed at the expense of ilmenite.

It was not possible to determine by microscopic methods the mineral composition of the very fine-grained and usually highly altered ground mass of the dikes, but the relative amounts of the salic components were determined by using the X-ray powder diffraction method. Three samples from different parts of dike DP III gave the following result:

Sample	Plagioclase	K-feldspar	Quartz
1A/IH/75 (contact)	55	15	30
IC/IH/75 (center)	40	20	40
2/IH/75 (center)	50	20	30

In the classification scheme presented by Streckeisen (1967) for volcanic rocks, these composition points fall into the field of dacite.

Dike rocks corresponding to the dark porphyry dikes of the Eurajoki area have not been described from other rapakivi granite areas of Finland, but obviously very similar volcanics are to be found on the island of Hogland (Suursaari), in the center of the Gulf of Finland. The volcanics of Hogland represent lavas genetically related to the Wiborg rapakivi massif (Wahl 1947). The lavas are composed mainly of quartz

Table 5

Trace element contents of potassic alkali feldspar from the dark porphyry dike and the granites of the Eurajoki area. Emission spectrographic analyses (Ga) by Ringa Danielsson and X-ray fluorescence analyses (Bb, Sr, Ba) by Väinö Hoffrén. Contents in ppm.

Rock	Sample	Ga	Rb	Sr	Ba
Dark porphyry dike (DP III), megacrysts	1C/IH/75	49	500	130	1 700
Tarkki granite	85/IH/67	31	320	n.a.	n.a.
Porphyritic Laitila rapakivi, megacrysts ..	11A/IH/75	33	440	240	2 800
Väkkärä granite, porphyritic type	98/MK/67/ER	70	1 660	< 40	n.a.
Väkkärä granite, porphyritic type	301/PL/68	82	1 580	< 40	100
Väkkärä granite, coarse-grained type ...	1/IH/72	80	1 650	n.a.	n.a.

n.a. not analyzed

porphyries, but there are also some dark, more basic porphyry beds or patches. This dark porphyry (»Labradoritführender Porphyr» by Lemberg 1868; »labrador-quartzsyenitporphyry» by Wahl 1947) contains as megacrysts an abundance of labradorite, and in addition also some quartz and orthoclase. The ground mass contains as dark constituents bluish-green hornblende and greenish-brown biotite. Ilmenite and apatite are typical accessories. It is interesting that the old chemical analyses presented by Lemberg (1868) for the plagioclase and orthoclase megacrysts of the dark porphyry of Hogland correspond nearly exactly to the microprobe analyses (Table 6) of the feldspar megacrysts of dike DP III from Eurajoki.*)

In their microscopic characteristics, the dikes resemble also the lamprophyre dikes described by Sainsbury (1969) from the Lost River area in Alaska, which are associated with rhyolite dikes and Sn-Be deposits. According to Sainsbury, the oligoclase, orthoclase and quartz megacrysts of these dikes are xenocrysts derived from the adjacent granite. It is possible that also in the Eurajoki area, the dark porphyry dikes have received material by assimilation from the acidic country rocks; in dike DP III, there are irregular, weakly assimilated fragments of Väkkärä granite. However, the feldspar megacrysts of the dikes cannot be derived directly from the Tarkki and Väkkärä granites, because many of them are much bigger (up to 10 cm in length) than the feldspar crystals of these granites. Also in chemical composition, the feldspar megacrysts deviate from the feldspars of these granites (Table 5).

MINERAL REPLACEMENTS IN THE VÄKKÄRÄ GRANITE

In addition to the common mineral inversions and exsolution of feldspar to perthite and possibly to antiperthite, many reactions affected the mineral relations and texture of the Väkkärä granite after crystallization of the bulk of the magma. Textures indicating subsolidus reactions are much more pronounced in the Väkkärä granite than in the Tarkki granite and other granites of the Laitila massif.

*) It is assumed that the »NaO» and »KO» of Lemberg correspond to the Na_2O and K_2O of present-day usage.

In the following, a more detailed description will be given of microscopic textures that are or may be interpreted to be of replacement origin. Two main types of replacement textures are differentiated: 1) the replacement textures not directly connected to fissures and 2) microscopic replacement veins. The replacement textures of the first category were formed either before or after complete solidification of the rock (late-magmatic and postmagmatic stages in the sense of Kühne *et. al.* 1969), the microscopic replacement veins were formed after solidification and fracturing of the rock (post-magmatic stage).

In interpreting the textures, it must be remembered that all the replacement textures do not inevitably denote metasomatism. Corrosion and replacement textures can be formed in feldspar during the magmatic (or late-magmatic) stage as a result of fractional crystallization (*cf.*, Tuttle and Bowen 1958, pp. 131—134, Stewart and Roseboom 1962, pp. 308—309). Exsolution and autometamorphic adjustment of minerals to lower temperature may produce replacement textures without any marked material exchange with the surroundings.

Replacement textures not directly connected to fissures

It has been noted in the foregoing that both in the Tarkki granite and in the Väkkärä granite the mineral boundaries, especially those between feldspar minerals, are often sutured, even when there are no myrmekite or interstitial albite rims. Such textures are usually explained as a result of solution and reprecipitation, or, in other words, recrystallization. Sometimes the boundary textures between two differently oriented grains of one and the same mineral species (alkali feldspar or plagioclase) suggest the replacement of one grain by another (Figs. 51 and 52). Different twin units of plagioclase may show different stabilities in these processes (Fig. 52). Savolahti (1962, p. 90) described textures indicating replacement of K-feldspar by another, differently oriented K-feldspar grain in rapakivi granite and regarded it as an example of autometamorphism. Such reaction relations between two grains of the same mineral with similar compositions do not involve any exchange of material with the surroundings, only recrystallization. But if one mineral corrodes another, which has a different chemical composition, and the question is not one of exsolution or simple autometamorphic recrystallization, then some material exchange outside the mineral grains must be assumed. The textural relations between minerals suggest that a number of metasomatic replacement reactions have occurred in the Väkkärä granite: K-feldspatization of plagioclase, albitization of K-feldspar, replacement of feldspar minerals by topaz, fluorite, dark and white mica, chlorite, kaolinite and quartz, replacement of biotite by chlorite, muscovite, lithium-iron mica, iron oxide and anatase, replacement of topaz by sericite, etc. The final nature of the replacement reactions is not always clear. Especially, the textural relations between plagioclase and K-feldspar often offer more than one possible explanation.

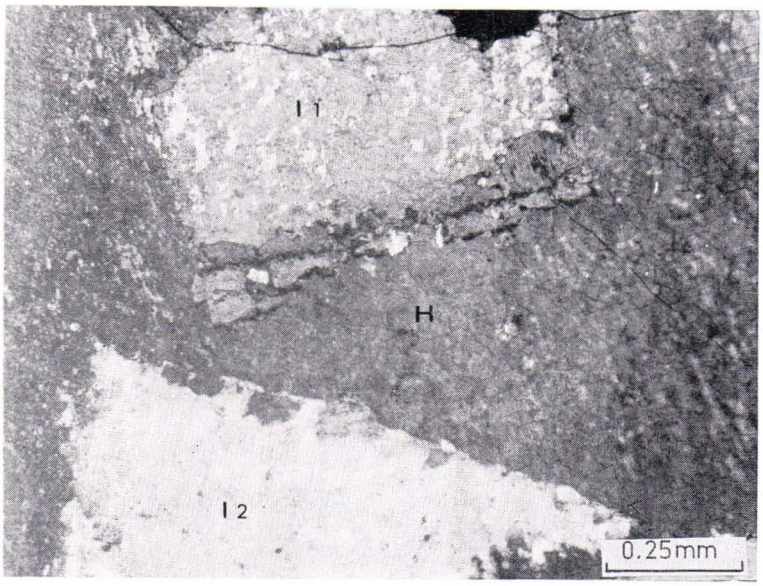

Fig. 51. Recrystallization phenomena at the boundary between differently oriented alkali feldspar grains. There are two differently oriented perthitic alkali feldspar inclusions (I 1 and I 2) in a large alkali feldspar host (H). The texture indicates that the host is replacing the inclusions. Even-grained type of Väkkärä granite, sample 634/PL/69.

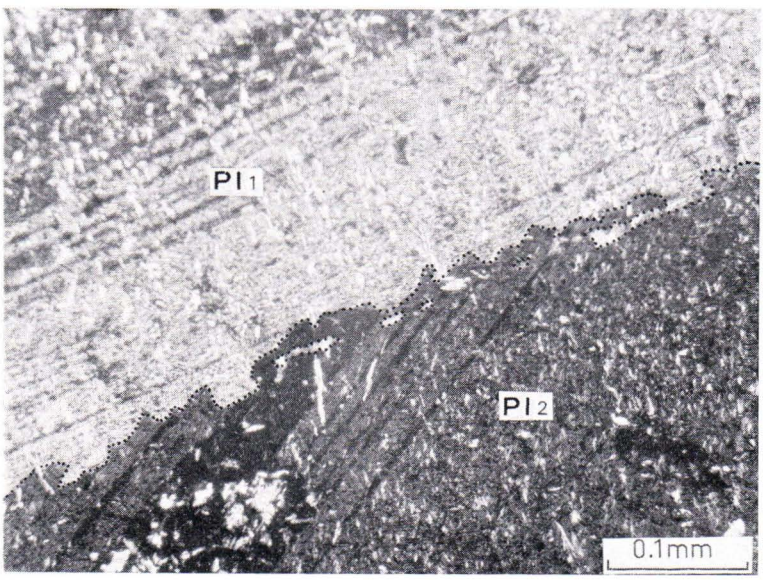

Fig. 52. Recrystallization at the boundary between two differently oriented, twinned plagioclase grains. The texture indicates that Pl 2 replaces Pl 1. Light lamellae of Pl 1 are partly left as relicts in Pl 2. The lighter twin lamellae of Pl 2 penetrate usually deeper into Pl 1 than the dark lamellae, but stop when they meet the darker lamellae of Pl 1. The optical orientation of the lighter lamellae of Pl 2 is nearly the same as that of the darker lamellae of Pl 1. The plagioclase grains are strongly sericitized. Even-grained type of Väkkärä granite, sample 209/IH/67.

Fig. 53. Replacement of plagioclase along margins by K-feldspar. The broken line shows the assumed border of the original plagioclase grain. The replacing K-feldspar is not perthitic. The small plagioclase inclusions (relicts) show the same optical orientation as the unreplaced plagioclase. Even-grained type of Väkkärä granite, sample 209/IH/67.

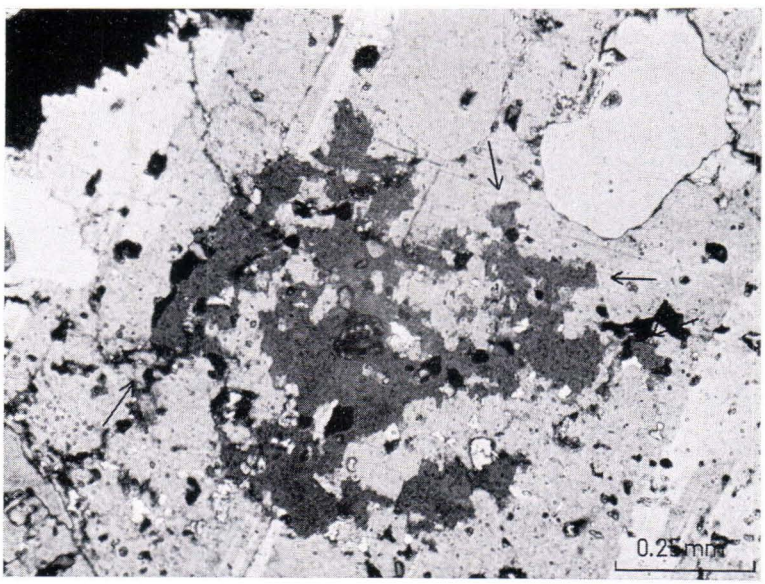

Fig. 54. Irregular fracture-controlled replacement of plagioclase grain. The most important fracture directions are marked with arrows in the photograph. The plagioclase inclusions in the replacing K-feldspar have the same optical orientation as the surrounding plagioclase. Porphyritic type of Väkkärä granite, sample 366/PL/68.

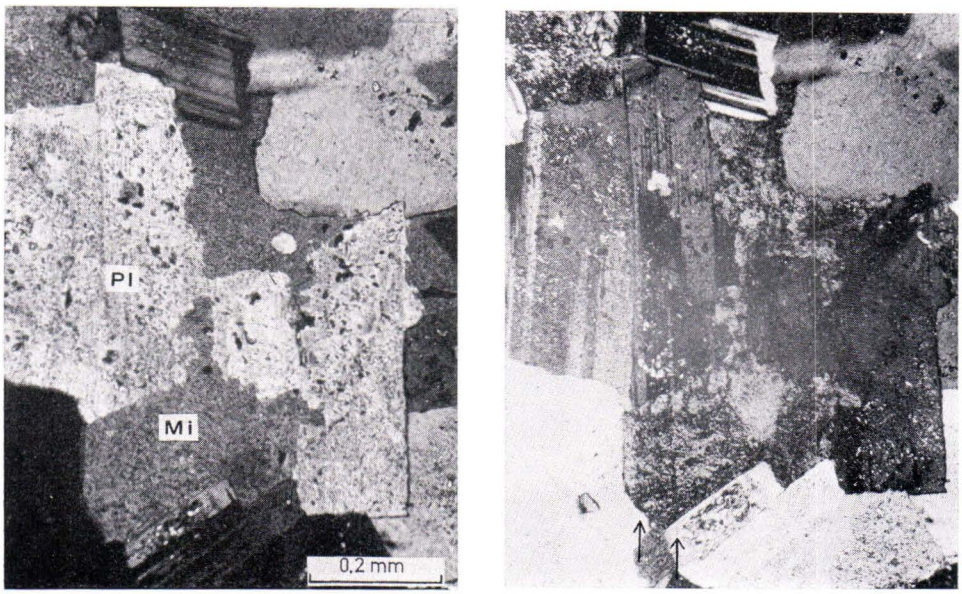

Fig. 55. Partial replacement of a subhedral plagioclase (Pl) grain by K-feldspar (Mi). In *a*, the nicols are in such a position that the microcline twinning is not visible. In *b*, a patchy twin texture (see p. 77) is visible in the microcline. Note the ghostly continuation in places of plagioclase twin texture in the replacing microcline as a statistical arrangement of the microcline twin patches in different associations along linear zones (see arrows in the left part of the photograph). Porphyritic type of Väkkärä granite, sample 301/PL/68.

Partial replacement of plagioclase by K-feldspar has been detected in many samples of the Eurajoki granites. Sometimes the replacing alkali feldspar has a perthite texture similar to the adjacent primary alkali feldspar, suggesting corrosion and replacement during an early (magmatic or late-magmatic) stage, but in many instances perthite texture is lacking in the replacing K-feldspar. The replacement is usually restricted to the marginal areas of the plagioclase grains (Fig. 53), or to some irregular fracture-controlled or zone-controlled replacement bodies in the inner parts of the plagioclase (Fig. 54). In some cases, also the crystallographic orientation of the plagioclase grains appears to control the replacement. Occasionally, textures suggesting more extensive replacement occur (Fig. 55). The water-clear albite rims are commonly absent or poorly developed at the contacts between turbid plagioclase and replacing K-feldspar. The replacement of plagioclase by K-feldspar has been described recently also in an even-grained biotite granite of the Wiborg massif by Vorma (1971).

In other instances, there are textures indicating an opposite reaction, replacement of potassic alkali feldspar by albite. In interpreting the textures, the main problem is now: Has the albite occurring as an intergrowth with K-feldspar formed by exsolution or by metasomatic replacement? The author is of the opinion that the perthite textures

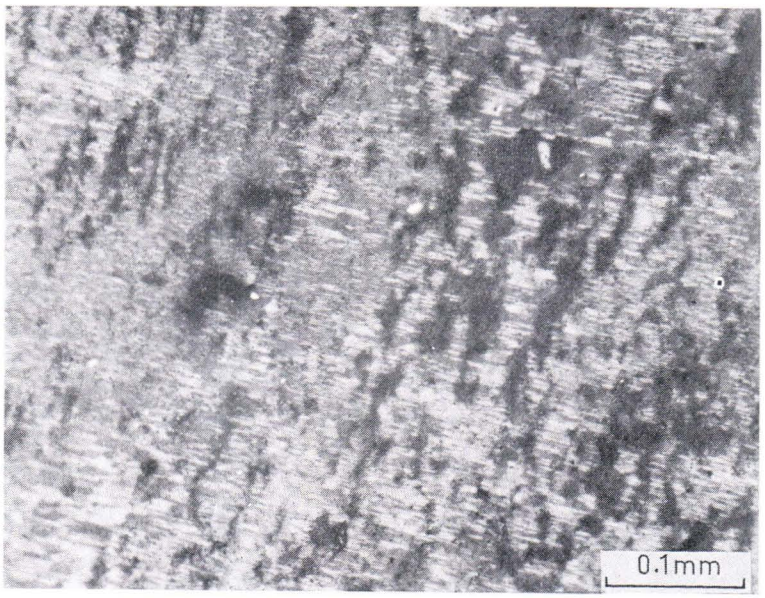

Fig. 56. Remnants of K-feldspar (dark grey patches and streaks) in replacing chessboard albite. Even-grained type of Väkkärä granite, sample 207/IH/67.

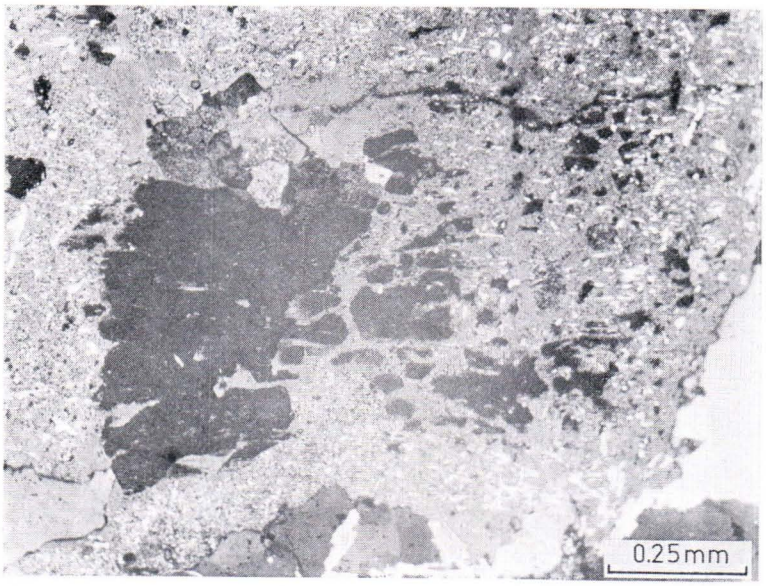

Fig. 57. Remnants of K-feldspar (dark grey) in replacing partly sericitized albite. Even-grained type of Väkkärä granite, sample 394/PL/68.

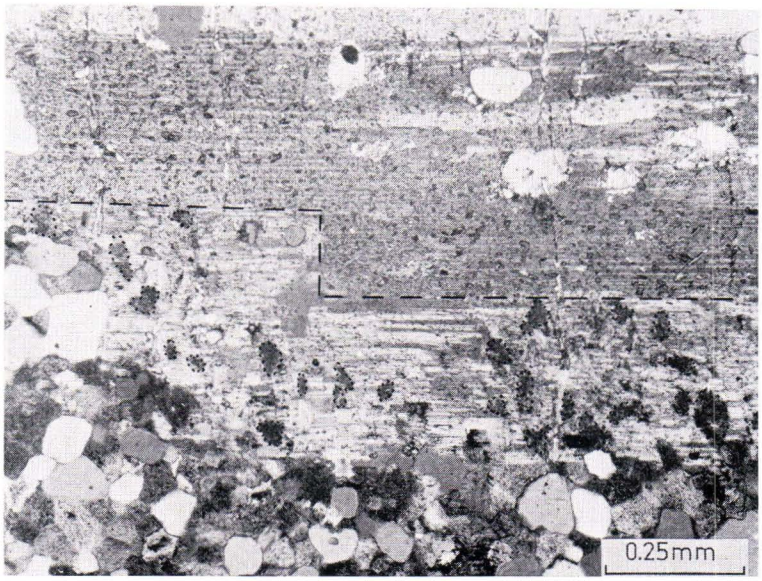

Fig. 58. Part of a plagioclase megacryst in a quartz porphyry dike. Turbid, conspicuously altered plagioclase core (upper part of the photograph) is rimmed by less turbid, discontinuously twinned albite, which contains small uniformly oriented inclusions (relicts) of K-feldspar. The boundary between the turbid core plagioclase (albite) and the marginal discontinuously twinned albite is marked with a broken line, and the K-feldspar inclusions are accentuated with a dotted line. Dike QP III, sample 126/IH/67.

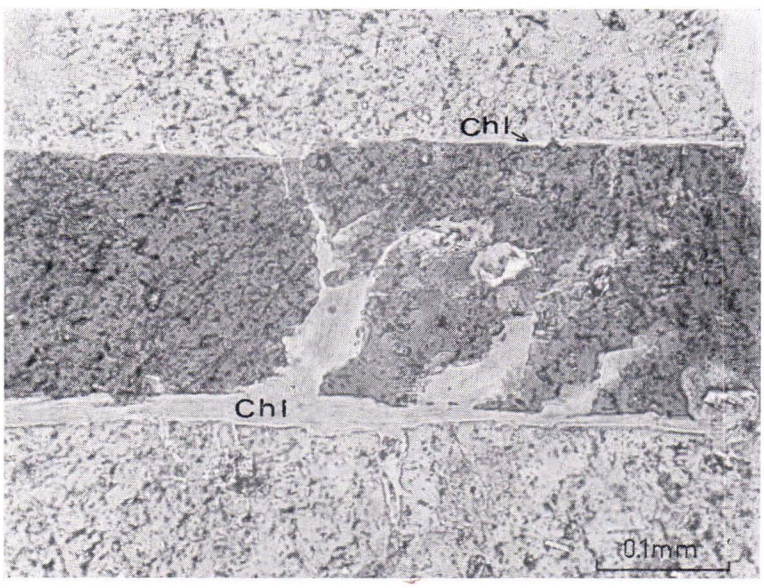

Fig. 59. Replacement of plagioclase by chlorite (Chl) along twin boundaries and fractures. Porphyritic type of Väkkärä granite, sample 274/PL/68.

Fig. 60. Replacement of plagioclase by white mica. The dark tongues at the left margin are topaz. Prominently greisenized porphyritic type of Väkkärä granite, sample 376/PL/68.

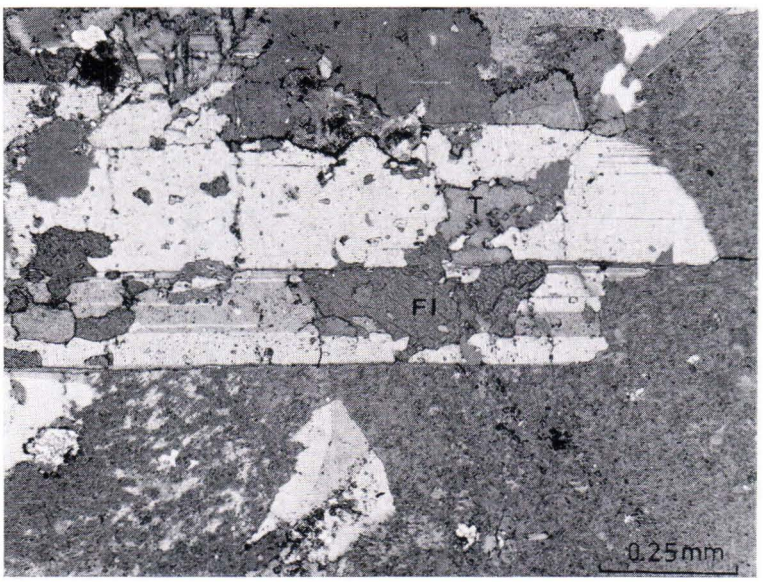

Fig. 61. Replacement of plagioclase by irregular grains of topaz (T) and fluorite (Fl). Conspicuously altered porphyritic type of Väkkärä granite, sample 366/PL/68.

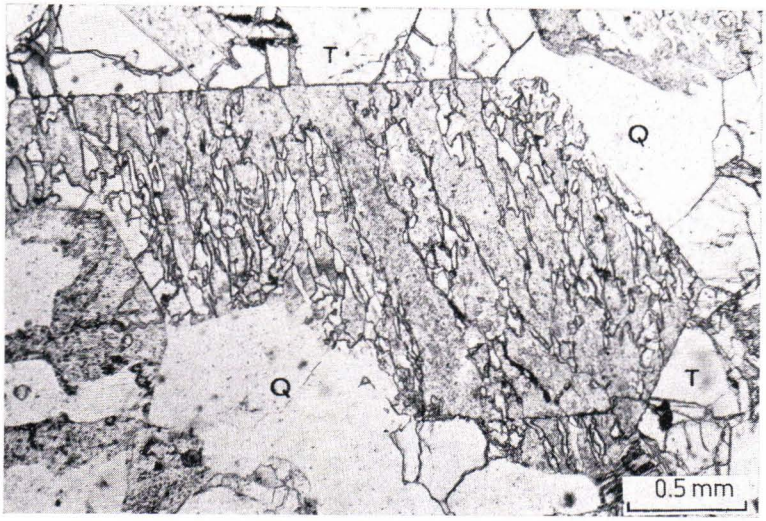

Fig. 62. Replacement of K-feldspar by topaz and quartz. Most of the vein-like strings are topaz, some quartz. Greisenized Väkkärä granite, sample 304/PL/68. The K-feldspar megacryst is surrounded by quartz (Q) and topaz (T). The dark veins in topaz are sericite. One nicol. Photo E. Halme.

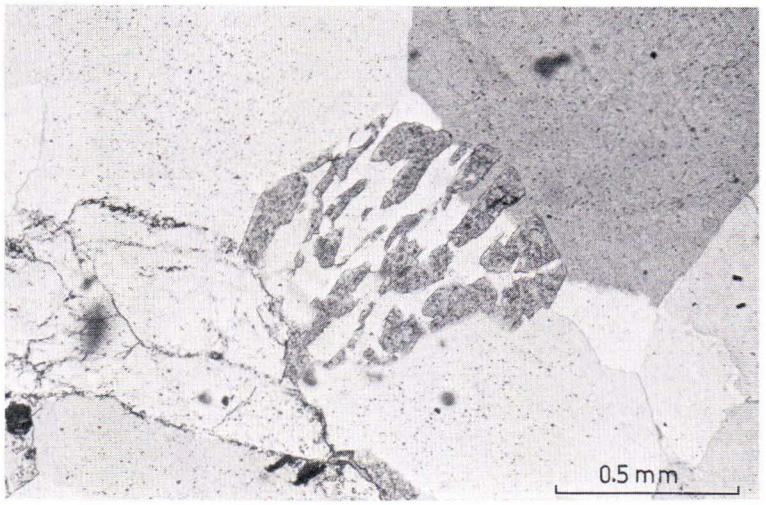

Fig. 63. Advanced replacement of K-feldspar by quartz. The original form of the K-feldspar grain is still detectable. The same sample as in Fig. 62. One nicol. Photo E. Halme.

in the Väkkärä granite are in general formed by exsolution and that a large part of the exsolution took place across the grain boundaries (p. 87). This is indicated by, among other things, the internal texture of the perthite grains and by the results of microprobe analyses of feldspars. However, in some samples there occur, besides the normal film—string—vein—patch perthite, also broad albite veins and patches, which can be best explained as a result of metasomatic albitization (Figs. 56 and 57). Sometimes the albite veins are seen to continue across grain boundaries, and can be followed in quartz grains as mineral veins or as planes of secondary fluid inclusions (p. 65); but in many cases the albitization is restricted in thin sections to one grain or to a few adjacent alkali feldspar grains. In some samples of the even-grained Väkkärä granite, all the gradations can be seen from alkali feldspar grains with a normal, finely developed perthite texture to grains with approximately equal amounts of K-feldspar and finely twinned albite veins, further to albite containing only small relicts of K-feldspar and finally to pure albite. Typically, the replacing albite is finely but uncontinuously twinned chessboard albite (Fig. 56). Thus albite formed by replacement can be distinguished from the primary plagioclase on the basis of the twin texture, even though no relict K-feldspar is visible. The intergranular water-clear albite of the topaz-bearing Väkkärä granite is obviously produced partly by exsolution, partly by metasomatic replacement, and it sometimes exhibits a rudimentary chessboard texture. In some exceptional cases, the textural relations even suggest replacement of quartz by albite.

A peculiar example of obvious albitization was observed in the quartz porphyry dike QP III (Fig. 58). The alteration involved a zoned feldspar megacryst with a plagioclase core and alkali feldspar mantle. The plagioclase core has been partly replaced by very small grains of topaz, fluorite, quartz and sericite, and in connection with these reactions the plagioclase has probably deanorthitized (see p. 61). The regular albite twinning of the core plagioclase has been preserved. The K-feldspar mantle is nearly totally replaced by a chessboard albite, in which small remnants of uniformly oriented K-feldspar are still present.

The alteration of biotite is a very complex process. Dark brown biotite has sometimes altered to green or greenish biotite. Very common alteration products are chlorite and muscovite, which often occur interleaving each other and biotite. In many cases, the textural relations indicate that chloritization took place before muscovitization. Especially in the even-grained and contact types, chlorite with or without muscovite and relict biotite forms aggregates, which also contain grain accumulations of anatase and iron oxide, obviously formed by decomposition of biotite and ilmenite. Also in the topaz-bearing Väkkärä granite, the dark mica is commonly replaced partly, sometimes totally, by chlorite and muscovite, and not infrequently the chlorite-mica intergrowths are overgrown and partly replaced by pale brown mica (lithian siderophyllite/protolithionite). This secondary pale brown mica is typically devoid of or poor in pleocroic halos. Anatase and iron oxide may be found in small amounts in the intergrowths, but the anatase is much rarer than in the even-

grained and contact type granites. Chlorite, muscovite and pale brown biotite occur also in feldspar replacing it along fractures, twin boundaries and cleavages in more conspicuously metasomatized (greisenized) granite (Fig. 59 and 60).

Topaz and fluorite often show modes of occurrence that indicate a replacement origin. The very small inclusions of fluorite and topaz, with or without sericite, chlorite and quartz, in the turbid plagioclase probably result from the reaction between plagioclase and fluorine-rich fluids (e.g., $CaAl_2Si_2O_8 + 4HF \rightarrow CaF_2 + Al_2F_2SiO_4 + SiO_2 + H_2O$). It should be noted that such deanorthitization of plagioclase, if it occurs, involves a rearrangement (recrystallization) of the alumosilicate framework. The twin texture of the turbid plagioclase is in general relatively clearly defined and regular. In certain instances, topaz and fluorite replace the feldspar together or separately as coarser irregular grains (Fig. 61). In strongly metasomatized granite, topaz and quartz are often seen to replace the alkali feldspar, producing perthite-like textures (Fig. 62). Topaz has been noted to occur also as irregular grains in microfractures of quartz.

Small-scale quartzification along microfractures and grain margins is visible occasionally in all types of Väkkärä granite, but a more intense secondary addition of quartz occurs in the greisenized granite. Here quartz replaces alkali feldspar often together with and in the same manner as topaz (Figs. 62 and 63). The ultimate product of such quartzification, topazization, micatization and chloritization is greisen.

In otherwise well-preserved granite, topaz has often been observed to have altered along grain margins and fractures or cleavages to micaceous material (sericite and some clay mineral). Feldspars, especially plagioclase, have commonly partly sericitized; also kaolinite has been identified as an alteration product of feldspar. Locally, also other alterations (e.g., hematitization) may be of some importance.

Microscopic replacement veins

In many thin sections of the Väkkärä granite, there are microscopic veins that cut the mineral grains and continue over boundaries from one grain to another. The veins consist of albite, quartz, K-feldspar, chlorite, sericite, biotite, topaz and fluorite. The mineral composition of the veins varies depending on the host mineral. Thus, for example, one and the same vein can be followed as albite vein (oriented like perthite albite) in K-feldspar, as a quartz and water-clear albite vein in turbid plagioclase, and as planes of secondary fluid inclusions in quartz. Typical examples of the microscopic veins are presented in Figs. 64—70.

The common occurrence of microscopic veins of feldspar $\pm$ quartz $\pm$ mica (as in Fig. 64) in the even-grained type of Väkkärä granite may be related to the emplacement of the topaz-bearing types. Fluids emating from the crystallizing residual magma have escaped into fractures of the already consolidated even-grained granite and caused the observed replacement phenomena.

Fig. 64. Replacement vein of albitic plagioclase in perthitic microcline. The plagioclase grains show the same or nearly the same optical orientation as the perthite albite. Some of the plagioclase grains are visibly zoned. The vein continues in the adjacent quartz grain as planes of secondary fluid inclusions and as a K-feldspar vein. Even-grained type of Väkkärä granite, sample 394/PL/68.

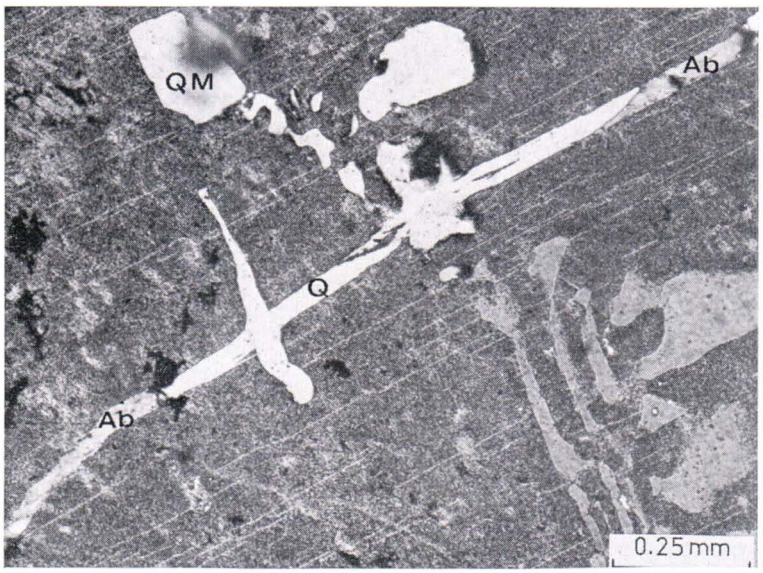

Fig. 65. Albite—quartz vein intersecting perthitic microcline. The vein is composed mainly of albite (Ab) oriented as the perthite albite, but in the zone containing micrographic quartz (MQ), it consists of quartz (Q) oriented according to the quartz units intersected by the vein. In quartz grains, the vein disappears or can be followed as planes of secondary fluid inclusions. Even-grained type of Väkkärä granite, sample 207/IH/67.

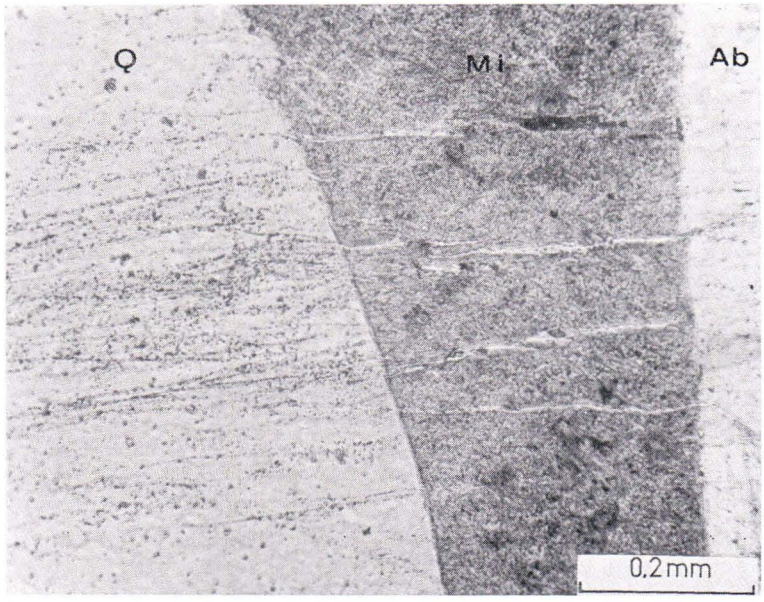

Fig. 66. Planes of secondary fluid inclusions (ancient fractures) in quartz (Q) continue as chlorite or kaolinite veins in perthitic microcline (Mi) and albite (Ab). In microcline, the veins are thicker than in albite. Coarse-grained type of Väkkärä granite, sample 1/IH/72).

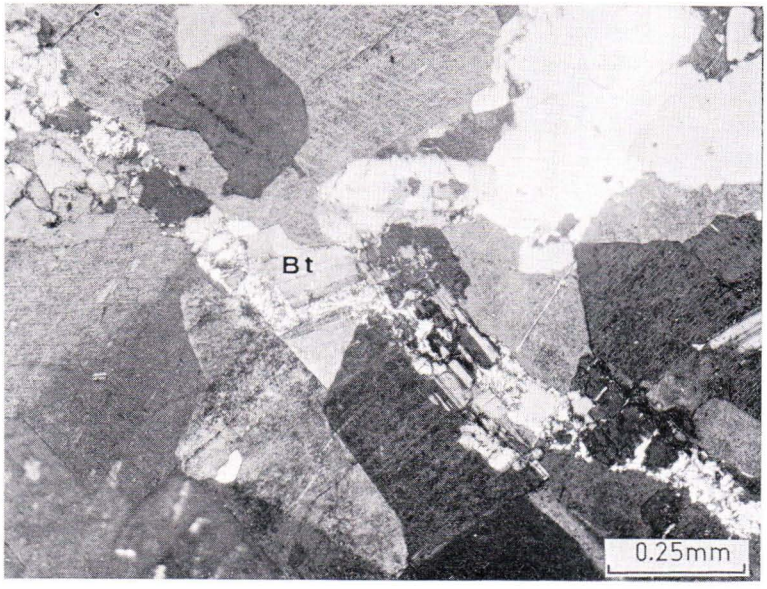

Fig. 67. Sericitization of plagioclase (twinned), microcline and biotite (Bt) along a fracture. In plagioclase, the sericitization is weaker than in microcline. In biotite, the sericitization has proceeded along the basal cleavage. Porphyritic type of Väkkärä granite, sample 13 a/PL/68.

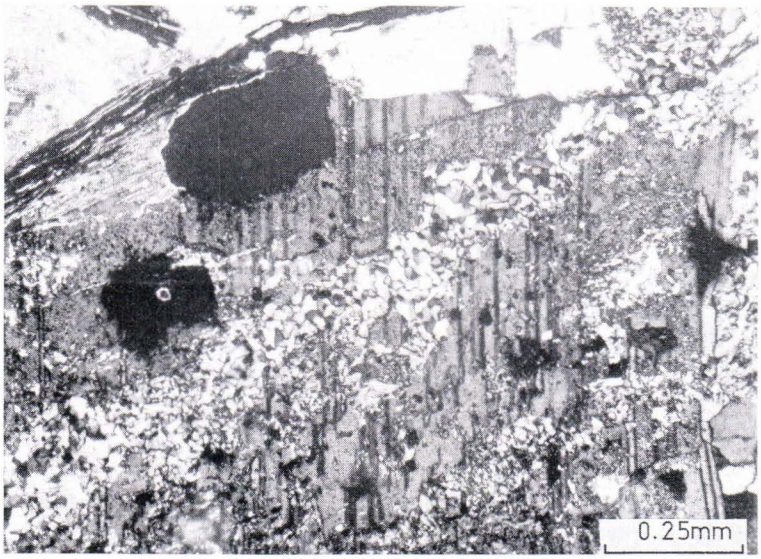

Fig. 68. Replacement of plagioclase by cryptocrystalline quartz along fractures. Porphyritic type of Väkkärä granite, sample 644/PL/69.

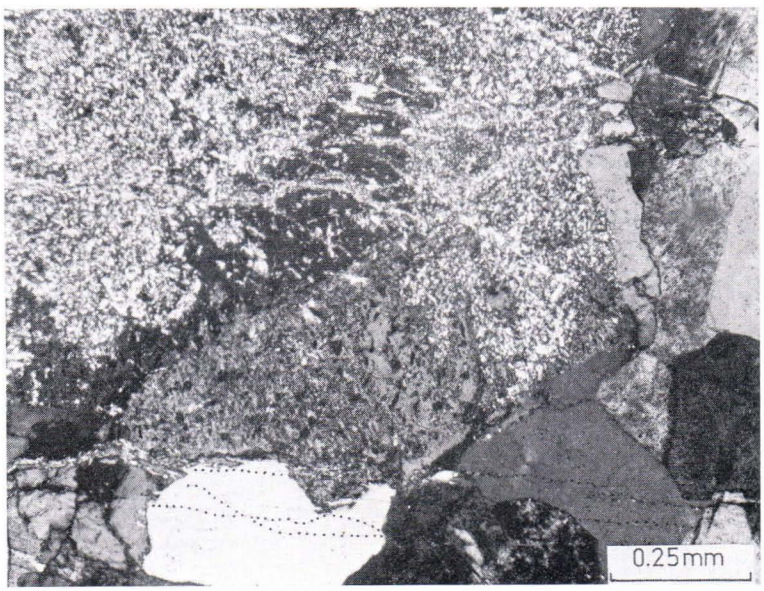

Fig. 69. Fracture-controlled replacement of plagioclase by sericite, leading to nearly uniform sericitization. In quartz, the sericite veins can be traced as planes of secondary fluid inclusions (accentuated with dotted lines in the lower part of the photograph). The same sample as in Fig. 66.

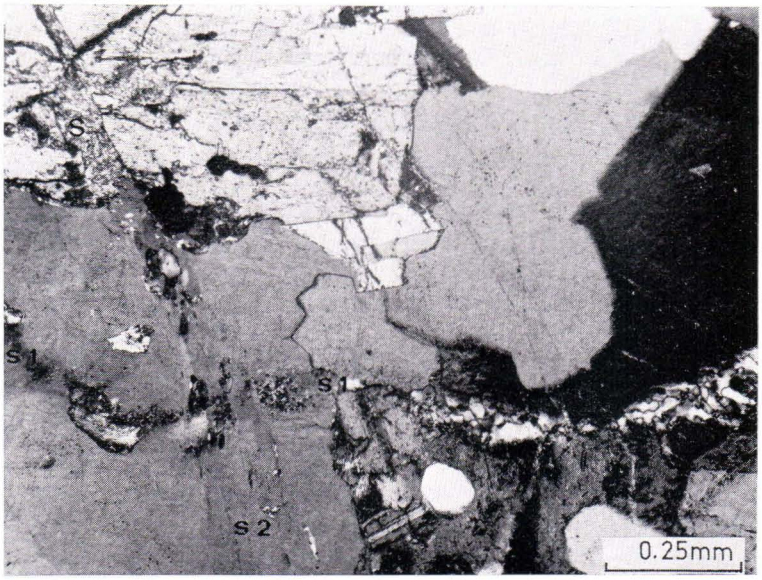

Fig. 70. In subhorizontal direction a fracture (s 1) along which silification of plagioclase and K-feldspar has taken place (see Fig. 66). This fracture is intersected by a later fracture (s 2) along which sericitization of feldspars has taken place. S sericite vein in plagioclase. The same sample as in Fig. 68.

Fig. 65 represents an albite (—quartz) vein intersecting K-feldspar, which contains as inclusions micrographic quartz. In the neighborhood of the quartz rods, the veins also consist of quartz with the same optical orientation as the rods. This gives the false impression that part of the micrographic quartz intersects as veins the host alkali feldspars. When the albite—quartz vein approaches another, differently oriented quartz inclusion in the same feldspar grain, it consists of quartz oriented according to this quartz individual. This phenomenon shows that the albite—quartz veins described are younger than the micrographic quartz.

Some of the veins depicted may be essentially fracture fillings (*cf.* Fig. 65), but most of them are formed by replacing pre-existing minerals. This is indicated by, among other things, the uniform continuation of obliquely intersecting textures (cleavage, fractures, grain borders) without »displacements» on both sides of the veins and by the occurrence of uniformly oriented inclusions of the host mineral in the veins. The vein material is derived partly from the host minerals (e.g., the albite of the veins may be derived by exsolution from the host alkali feldspar; sericite components are largely derived from the host feldspar, etc.), and partly from the circulating fluids. In quartz, the fluids commonly have not been able to cause replacement reactions, and during healing of the fracture they have been trapped into it as secondary fluid inclusions (Figs. 66 and 69). These inclusions are thus relicts of the fluids that caused albitization, sericitization, chloritization, argillitization, etc., along the microfractures. In some cases, the veins so formed are microscopic equivalents of greisen veins.

The planes of the secondary fluid inclusions are quite abundant in the granites of the Eurajoki stock, and often they form subparallel microscopic lines in different quartz grains of the thin sections. These planes run, at least in some places, parallel to the nearby greisen and quartz veins. It is possible that the orientation of the planes of secondary fluid inclusions could be used to evaluate the tectonic history of these granites, although no foliation or related deformation textures are visible.

GREISEN

Mode of occurrence

Greisen bodies occur in different parts of the Eurajoki stock. In the Tarkki granite, they are almost always replacement veins, often forming swarms of nearly parallel veins. The directions of the veins and lodes differ in different parts of the stock. Many of the veins run parallel or perpendicular to the contacts of the stock. In the vein swarms and lodes there are commonly minor veins arranged en echelon and associated with major veins (Figs. 71 and 73). In the vein swarm between the villages of Lapijoki and Hankkila (Fig. 71), the direction of the major veins is N75°E — E-W, 75°N—90°. These veins represent ancient shear joints (faults). Both the numerous observed displacements (Fig. 72a) and the en echelon structure of minor veins and joints (Figs. 72b and c) give consistently the same right-lateral movement direction: the northern side has moved to the east in relation to the southern side. The same movement direction is observed occasionally also from the internal texture of the quartz veins occurring at the center of the greisen veins (obliquely cutting fractures and beryl crystals, Fig. 72d). In such a case, the direction of the shear was evidently the same both before and after the mineralization, but probably the time interval between these events was short. In another well-developed vein swarm (Fig. 73), located 1.5 km to the north of the Eurajoki church, the main vein direction is nearly the same (N75°E, 90°) as in the Lapijoki—Hankkila vein swarm, but the prevailing en echelon pattern of the minor veins suggests an opposite, left-lateral movement direction: the northern side has moved to the west in relation to the southern side.

The width of the veins varies, being usually on the order of 20 cm or less, but veins up to 2 m in width do occur. Deep drillings have shown that at least some of the vein swarms and single veins can be followed in depth more than 100 m and in a horizontal direction more than 300 m.

In the Väkkärä granite, the veins tend to be more irregularly oriented (sparse stockwork) than in the Tarkki granite, and in addition lensoid, rounded and irregular greisen bodies of varying size occur.

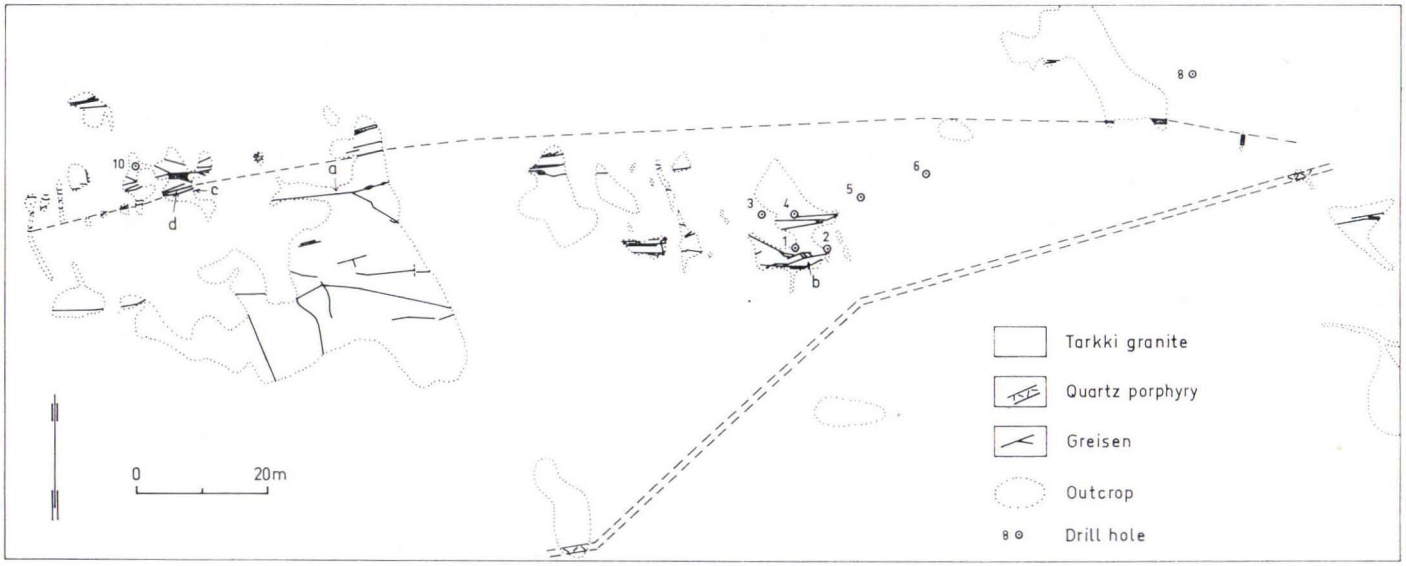

Fig. 71. Swarm of greisen veins in Tarkki granite between the villages of Lapijoki and Hankkila (x ~ 6 787.25, y ~ 533.0). Letters a—d refer to more detailed sketches in Fig. 72.

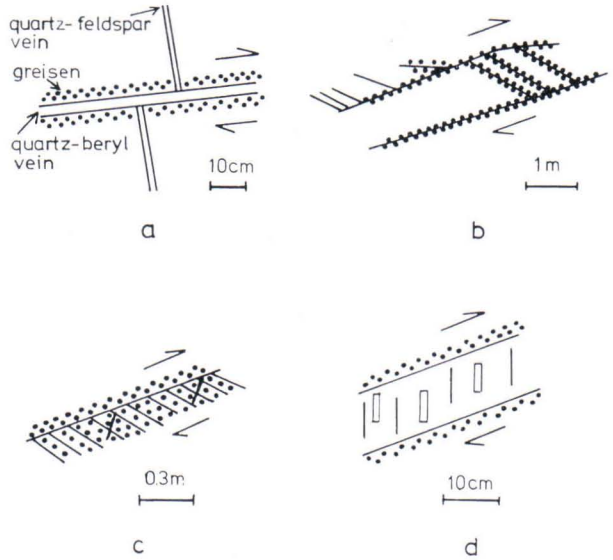

Fig. 72. Sketches of some details in the vein swarm of Fig. 71, indicating directions of shear movement. In *a* the movement is visible from the displacements, in *b* and *c* from the en echelon structure of minor veins and joints, and in *d* from the deformed texture of the central quartz—beryl vein (orientation of beryl crystals and cross joints).

Internal structure and mineral associations

The major gangue minerals of the greisens are quartz, white and dark mica and iron-rich chlorite. In many cases, the greisens also contain abundant topaz, fluorite, garnet (usually almandine, sometimes spessartine), beryl, genthelvite and bertrandite. Baryte and carbonate have been found in some cavities in the greisen veins. The most common ore minerals are sphalerite, cassiterite, chalcopyrite, wolframite, gahnite, molybdenite, rutile, secondary iron oxide, pyrite, pyrrhotite, marcasite, arsenopyrite and galena. As rarities, argentite, tetrahedrite and native bismuth have been found.

The internal structure of the greisen veins varies in broad limits. A central quartz vein with or without beryl, cassiterite, wolframite, molybdenite, sulphides and mica is commonly but not always present (*cf.*, Figs. 74 and 75). Many of the veins show a zoned structure, examples of which are presented in Fig. 76. The zoned structure of a genthelvite-bearing greisen is described by Haapala and Ojanperä (1972). Beryl, wolframite and molybdenite occur typically in the central quartz veins, cassiterite and Zn-, Cu- and Fe-sulphides are met with both in the central quartz veins and in the surrounding greisens. Gahnite is typically associated with sphalerite and almandine

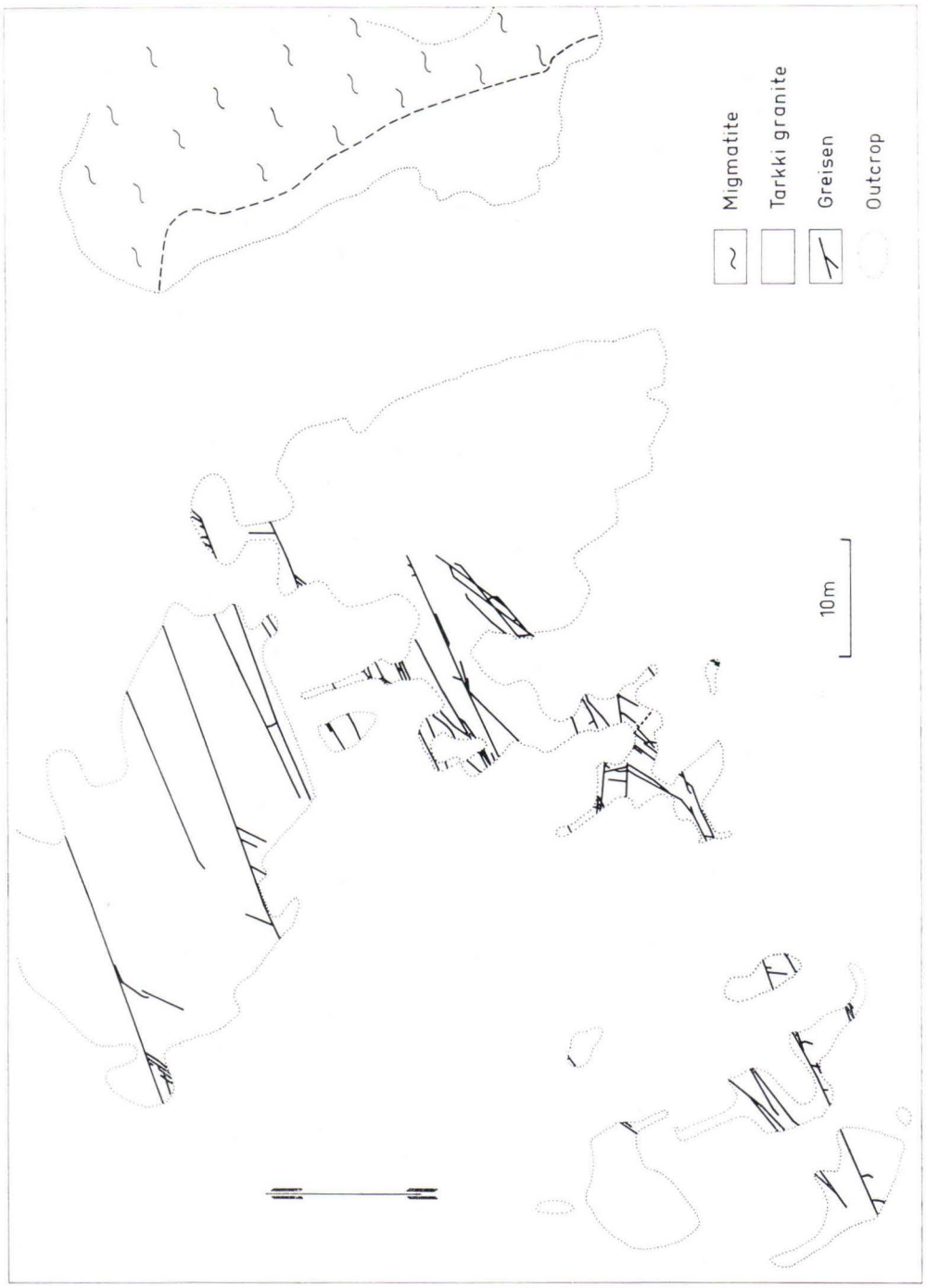

Fig. 73. Swarm of greisen veins in the Tarkki granite, about 1.5 km north of Eurajoki church (x ~ 6 789.9, y ~ 539.3).

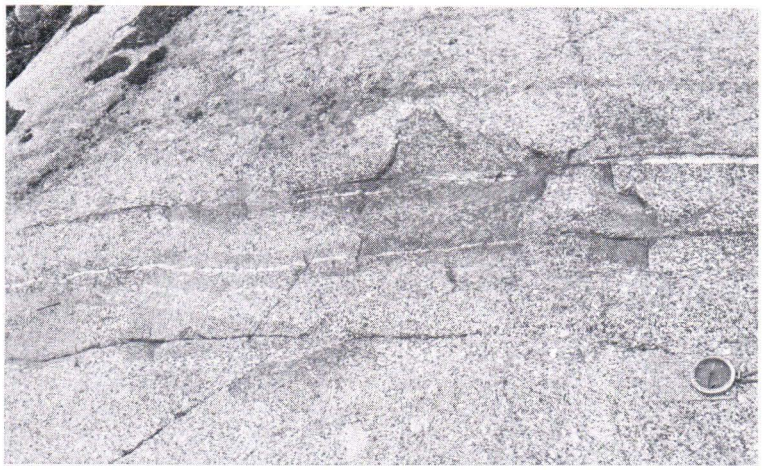

Fig. 74. Greisen veins with the central quartz(—beryl) veinlets in the Tarkki granite. Outcrop 107/1H/67.

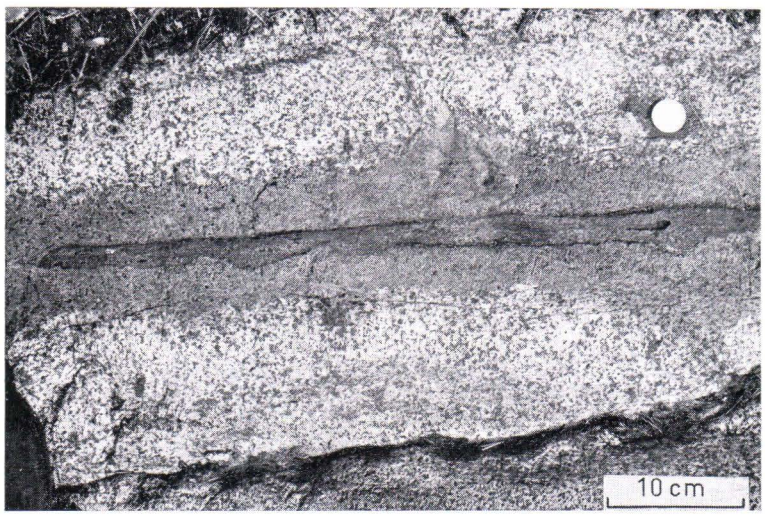

Fig. 75. Zoned greisen vein with core of dark garnet—chlorite (—gahnite) rock, intersecting the Tarkki granite. Outcrop 139/MK/67.

in the greisen. Genthelvite occurs together with quartz, sericite, chlorite and topaz (Haapala and Ojanperä 1972). Bertrandite occurs in greisen and very intensely greisenized Väkkärä granite with the mineral association quartz—bertrandite—topaz—albite—microcline—white mica—chlorite—cassiterite. Around the greisen bodies, there is usually a red-colored zone, which is caused by iron oxide pigment in alkali feldspar. In this zone, plagioclase is commonly very intensely sericitized.

Marked differences occur in the mineral composition between the greisens of different areas of the Eurajoki stock. Garnet, gahnite, beryl and wolframite have been found only in the greisen and associated quartz veins intersecting the Tarkki granite

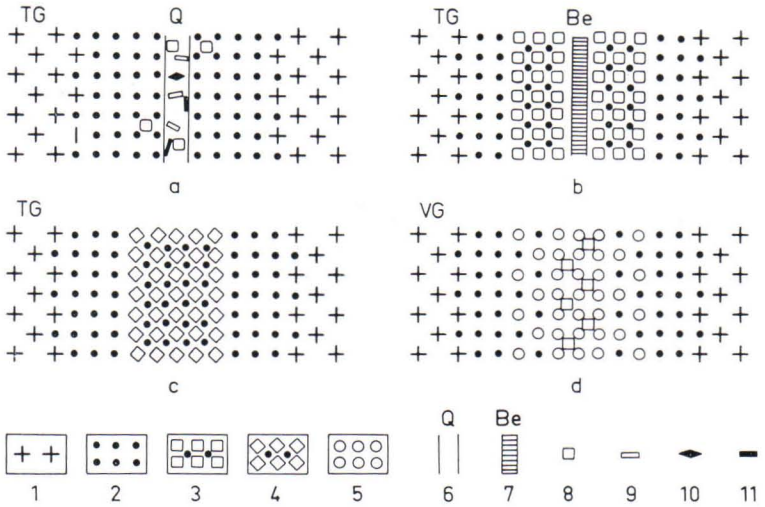

Fig. 76. Schematic examples, without scale, of the zoned structure of the greisen veins of the Eurajoki area. Explanation of the symbols: 1) granite (TG Tarkki granite, VG Väkkärä granite); 2) quartz—mica—chlorite greisen; 3) mica—cassiterite (—quartz) greisen; 4) garnet—chlorite (—gahnite) rock; 5) topaz—quartz—mica greisen; 6) quartz vein; 7) beryl vein; 8) cassiterite; 9) beryl; 10) wolframite; 11) molybdenite.

(beryl and wolframite only in the southwestern part of the stock), genthelvite and bertrandite only in the greisens of the Väkkärä granite. Cassiterite appears to be more commonly present in the greisens of the Väkkärä granite than in those of the Tarkki granite, but very high contents have been found only in the greisens intersecting the Tarkki granite. There ore shoots containing as much as 20 wt-% Sn have been found. Sphalerite is more common in the greisens of the Tarkki granite.

Tin, beryllium and tungsten are the economically interesting elements of the greisens. Although separate rich ore shoots are not rare, economically minable units have not been found. The presumably more intensively greisenized and mineralized elevations of the Väkkärä granite are removed by erosion.

Fluid inclusion studies

The author has carried out some fluid inclusion studies of minerals of the greisen vein swarm in the Tarkki granite around coordinates x = 6 787.3, y = 533.0 using the Leitz 350 and 1 350 heating stages and the freezing stage described by Roedder (1962). According to these preliminary studies, the presumably primary inclusions in cassiterite fill by disappearance of the gas phase at temperatures of 300—380°C (45 observations), those in the greisen quartz at 310—335°C and those in beryl of the central veinlets at 370—390°C (30 observations). These are minimum trapping

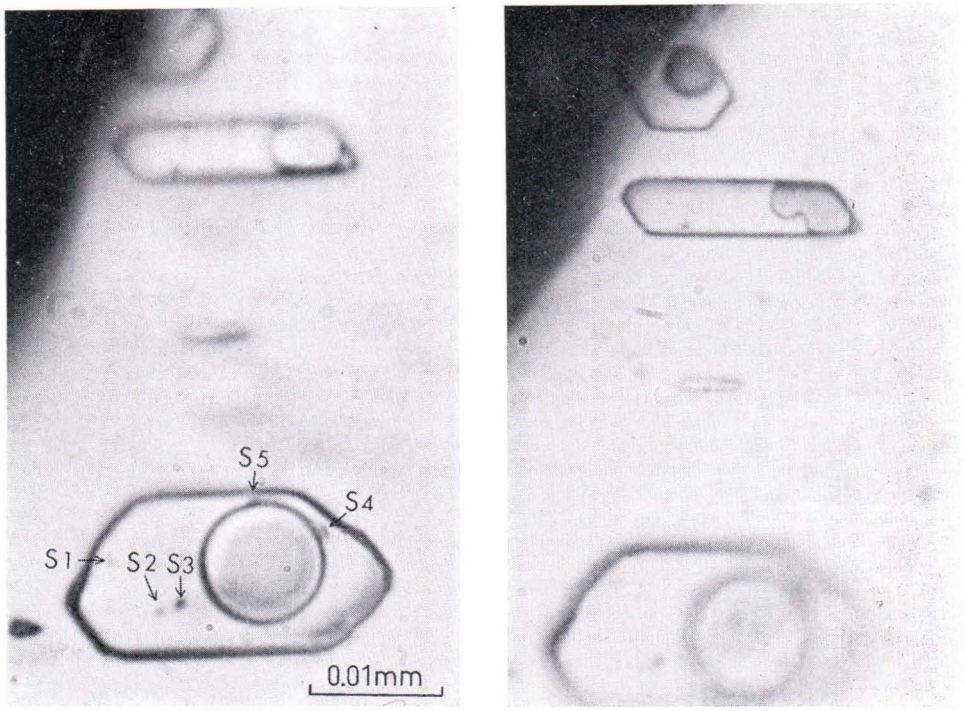

Fig. 77. Zone-controlled primary fluid inclusions in greisen cassiterite, sample 108 C/IH/67. Figure *a* shows the inclusions before the heating and freezing experiments. The figure is focused on the large inclusion. The inclusions contain liquid, vapor bubble and small daughter minerals (S_1—S_5). In *b*, the inclusions are shown two months after the homogenization heating. A colorless isotropic daughter mineral with practically the same refractive index as that of the liquid is visible from its contact with the gas bubble. Before heating, this daughter mineral was not detectable, but reprecipitation into a favorable place after heating made it visible. The inclusions homogenized to liquid at 315—317°C. The bigger inclusion had a freezing temperature of —7.7°C; beginning of melting of the ice was at about —29.5°C.

temperatures, without pressure corrections. Some of the apparently primary inclusions in the beryl of the central veinlets homogenize to gas at approximately the same temperature (380—400°C) as most of the inclusions of the same crystals do to a liquid. This might indicate crystallization from a boiling liquid, but also other interpretations (small differences in time and temperature of trapping, leakage) are possible. It is also possible that the differences in the filling temperatures (390—300°C) are largely due to differences in confining pressure, which may well have fluctuated between lithostatic and hydrostatic during greisenization and the formation of the central quartz—beryl veinlets into opened fractures (*cf.*, Kelly and Turneaure 1970, p. 669; Roedder 1971, p. 110).

The freezing temperature of the liquid could be determined only for a few larger inclusions. For four apparently primary inclusions in cassiterite, the freezing temperature was —7.9 to —7.35°C, corresponding to a salinity of 11.8—11.0 wt-% NaCl,

and for eight inclusions (homogenization to liquid) in beryl —7.3 to —4.4°C, corresponding to a salinity of 11.0—7.1 wt-% NaCl. The fluid inclusions usually contained some small unidentified daughter minerals (not halite or sylvite). One visually isotropic colorless daughter mineral occurring in a zone-controlled primary fluid inclusion in cassiterite had almost exactly the same refractive index as that of the liquid (n 1.34—1.35). These properties fit cryolite Na_3AlF_6 (α 1.338, γ 1.339), hieratite K_2SiF_6 (n 1.340) and cryolithionite $Li_3Na_3Al_2F_{12}$ (n 1.339). The presence of the mineral was recognized from its angular contact with the gas bubble (Fig. 77). In a couple of inclusions, liquid carbon dioxide was also observed. These observations indicate that at least during some stage in the development of the greisen, the ore fluid contained substantial amounts of fluorine and carbon dioxide in saline aqueous solution.

ALKALI FELDSPARS

In connection with the petrographic description of the rocks, the modes of occurrence and some general characteristics of the alkali feldspars were also given. In this section, a more detailed description will be given of the microscopic textures (perthite texture, interstitial albite) and some data on the structural state of K-feldspar. The obliquity (triclinicity) has been determined from the separation of $d_{131} - d_{\bar{1}31}$ in the X-ray powder diagram, and the results are summarized in a map in Fig. 78.

Perthite texture and structural state

In the Tarkki granite, the alkali feldspar has typically a faintly developed perthite texture. It is often more clearly visible at the marginal parts of the grains, whereas the central parts, sometimes also whole grains, may appear homogeneous under the microscope. The albite component occurs typically as very thin films (width typically < 1—2 μm), strings (1—5 μm) or veins (2—10 μm), film perthite being the prevailing type (Fig. 79). Locally, also much coarser perthite veins occur. K-feldspar is nearly always pigmented, especially at the margins of the albite veins, owing to minute iron oxide inclusions. The obliquity Δ is typically 0 or very low. From the 24 samples studied, 15 gave the result 0.0 and five 0.0—0.2. Only in two samples, taken from the margins of greisen veins, higher obliquities (0.6 and 0.8) were obtained. The optic axial angle $2V\alpha$ was determined from five samples with $\Delta = 0.0$—0.1, and it varied between 50° and 76° (averages 55, 57, 65, 66 and 68°).

In the contact type of Väkkärä granite, both the megacryst and ground mass alkali feldspars are perthitic. The albite occurs mainly as very thin films (width 1—2 μm), stringlets (≤ 2 μm) and veins (4—10 μm), but also more irregular, coarser intergrowths occur. The obliquity determination of the potassic phase including both ground mass and phenocryst material of one sample (309/PL/68/IH) gave the result

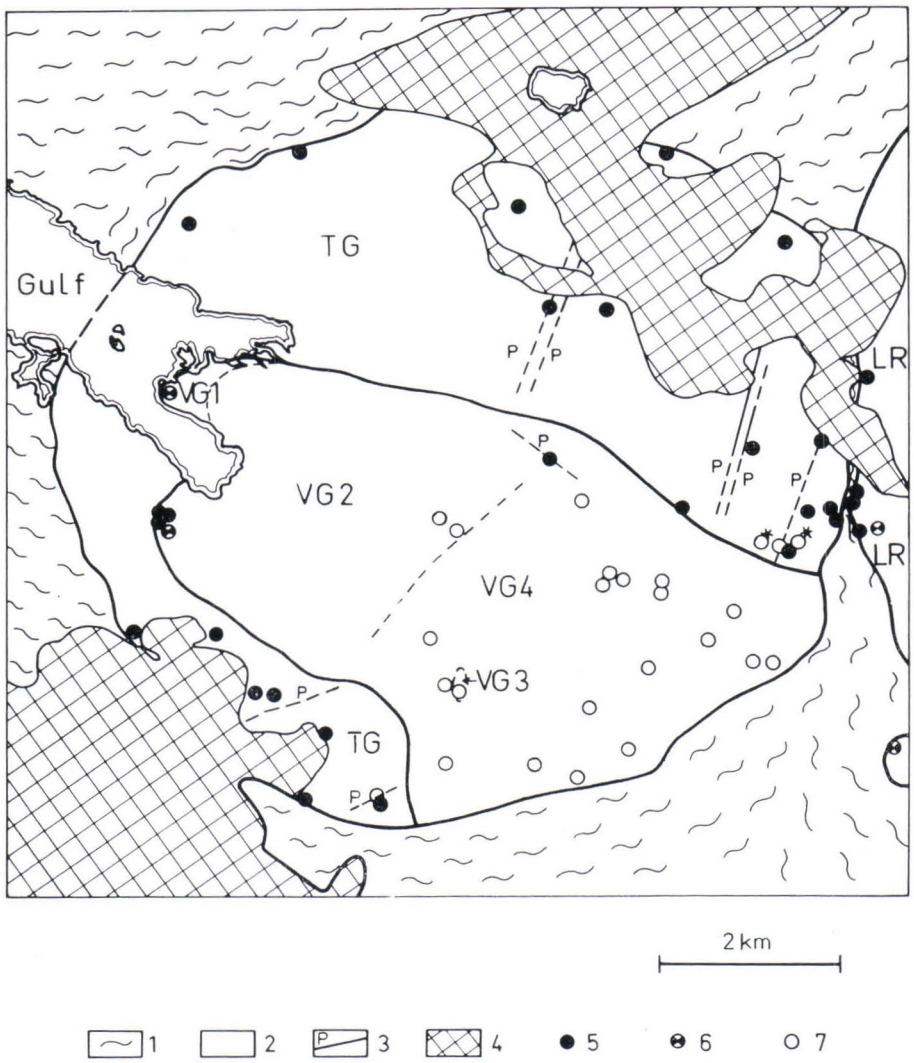

Fig. 78. Lithologic map of the Eurajoki area showing obliquity (Δ) of K-feldspar in the granites and porphyry dikes. Symbols: 1, migmatite; 2, rapakivi granite; 3, porphyry dike; 4, diabase; 5, K-feldspar with Δ 0.0—0.2; 6, K-feldspar with intermediate (Δ 0.3—0.6) or mixed obliquities; 7, K-feldspar with Δ 0.65—1.0. LR, Laitila rapakivi granite; TG, Tarkki granite; VG, Väkkärä granite (VG 1, contact type; VG 2, even-grained type; VG 3, coarse-grained VG 4, porphyritic type). The obliquity observations marked with asterisks are from the border of greisen veins.

Δ = 0.0—0.8 (three maxima, the strongest one at 0.6). The $2V\alpha$ of a megacryst of the same sample was 72° and that of a ground-mass alkali feldspar 62—82°, the average being 73°. K-feldspar is strongly pigmented by minute inclusions, as it commonly is also in the other types of Väkkärä granite.

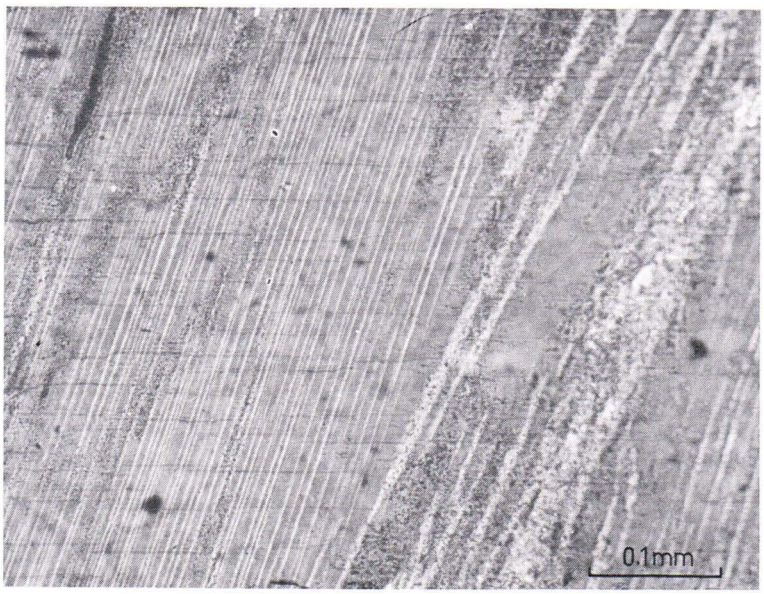

Fig. 79. Unusually well-developed film and vein perthite in the alkali feldspar of the Tarkki granite. Sample 221/IH/68.

In the even-grained type of Väkkärä granite, the albite component of perthite occurs typically as films or strings, 1—10 μm or less in width, often also as small roundish lenses or drops (Ø 2—12 μm) or as veins (width 2—20 μm), sometimes as patches (Ø up to 200 μm). Regular coarse film—vein perthite occurs at the central parts of the stock (outcrops 17, 393 and 394/PL/68 near coordinates x = 6 789.3 y = 535.0). The obliquity varies between 0.0 and 0.8. Low values (0.0—0.5) were obtained for the K-feldspar in the outcrops near the Tarkki granite, whereas higher values (0.7—0.8) occur in the even-grained granite at the central parts of the stock. The average $2V\alpha$ varies between 56 and 75°, in general increasing with increasing obliquity.

In the topaz-bearing (porphyritic and coarse-grained) types, the alkali feldspar generally shows a coarse, well-developed perthite texture. The nature of perthite varies depending on the location of the sample and the size of the alkali feldspar grain. In larger grain, a combination of a string perthite (width of albite lamellae 1—10 μm) and coarser vein perthite (2—20 μm) is common. Together with them or separately, there also occur patch perthite (Ø 10—100 μm). The perthite texture is typically well developed at the central parts of the grains (Fig. 31). In the marginal parts of the K-feldspar megacrysts, the perthite texture is commonly weakly developed or lacking. This is due either to the exsolution across the grain borders or to the crystallization under subsolvus conditions. Often the different types of perthite grade into each other. In the alkali feldspar of the finer-grained ground mass, the perthite texture is represented usually by sparse albite veins or patches, or they may even be

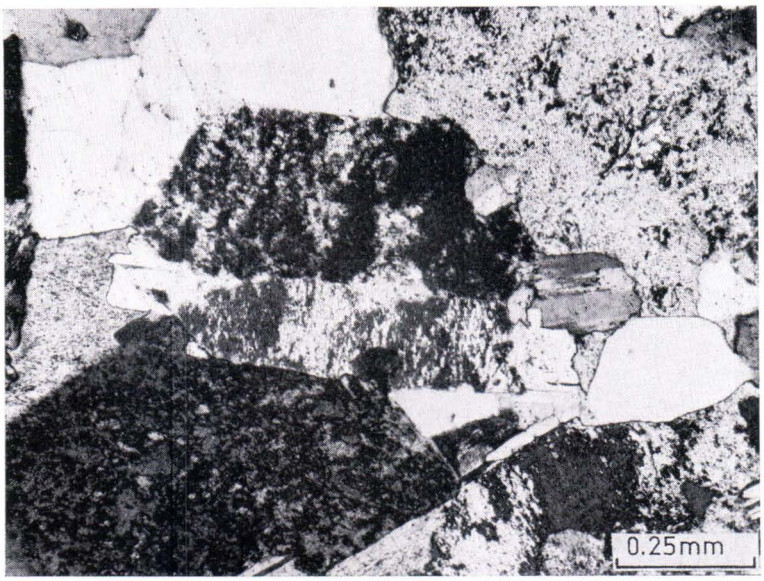

Fig. 80. Unusually coarse and well-developed patchy twinning in microcline. In the Karlsbad twin, the dark and the light units have slightly different extinctions in different Karlsbad twin units. Porphyritic type of the Väkkärä granite, sample 17/MK/67.

lacking, so that the feldspar is homogeneous, nearly pure K-feldspar. Probably the exsolution of albite here took place largely over the grain boundaries (*cf.*, Vorma 1971, p. 31). The obliquity of the K-feldspar varies between 0.65 and 0.95, the most typical values being 0.8—0.9. The average $2V\alpha$ varies between 72 and 82° with the maximum frequency at 73—74°. The single $2V\alpha$ determination for the megacrysts and ground mass of the same thin section overlap, but the average $2V\alpha$ is 1—5° higher for the ground mass in the three samples from which the $2V\alpha$ was determined both for the ground mass and megacrysts. In conspicuously chloritized and greisenized granite samples, the alkali feldspar is homogeneous microcline (Δ 0.9, average $2V\alpha$ 71—74°) or it contains only a few albite patches.

In the quartz porphyry dikes, the perthite texture of the alkali feldspar megacrysts varies from film perthite to a very irregular, coarse vein and patch perthite. Obliquity Δ is typically 0.7—0.8. The obliquity of the ground mass K-feldspar was determined from only one sample (229B/IH/67); in this case, it was the same (0.7) as that of the megacrysts. Only in one sample, taken from the immediate vicinity of a horizontal diabase dike (sample 231/IH/67, x = 6 790.13, y = 539.06) a monoclinic symmetry ($\Delta = 0.0$) was observed. This is caused by the heating effect of the diabase (*cf.*, Lundqvist 1973). In the dark porphyry dikes, the alkali feldspar megacrysts are either homogeneous or show a development of thin (1—2 μm) albite strings and veins along irregular cutting zones. In such zones also incipient cross-hatching may be visible. The obliquity Δ of K-feldspar from dike DP III is 0.0 and $2V\alpha$ 64°.

Cross-hatched twinning is practically lacking in the Väkkärä granite. Of the 47 samples studied, well-developed cross-hatching was observed in only one, the country rock of the dark porphyry dike DP III (outcrop 1/IH/75). Instead of cross-hatching, the microcline of the topaz-bearing Väkkärä granite often shows a peculiar patchy extinction texture (patchy twinning) which is visible between crossed nicols as an intimate irregular intergrowth of two differently oriented units (Fig. 80). The optical orientation of the perthite albite differs from the orientation of the K-feldspar units. This patchy twin texture is especially well developed in the greisenized granite.

Intergranular albite in the Väkkärä granite

Water-clear albite occurs in the Väkkärä granite typically at the interfaces between K-feldspar and turbid (clouded by inclusions) plagioclase or between two adjacent K-feldspar grains. Very thin albite rims occur in some places in the contact type, and somewhat thicker rims can be found in the even-grained type, but in the topaz-bearing types the albite rims and grain rows are much more pronounced. The mode of occurrence of the albite rims greatly resembles that of the myrmekite and sodic plagioclase rims in the Tarkki granite (p. 19).

Between pigmented (primary) plagioclase and potassic alkali feldspar, the water-clear albite occurs in crystallographic continuation with the core plagioclase. The turbid core has nearly always a euhedral or subhedral form (Figs. 81 and 82). The K-feldspar—rim boundary is commonly irregular, and if it is regular it does not necessarily follow the outline of the core plagioclase. The rims are generally narrow on the (010) faces of the plagioclase laths, and thick at the ends of the laths. In some samples of the contact type, the core plagioclase clearly differs in composition from the albite rims; but in the topaz-bearing types, there is only a very small or no compositional difference between the core and the rim, as can be easily observed from the extinction angles. The twinning of the core commonly continues uniformly to the rim, but at some points the rim shows a different (usually more irregular) twin texture (Figs. 83 and 84).

The water-clear albite rims occur as well between independent plagioclase and microcline grains as between a turbid plagioclase inclusion and the K-feldspar host. In the latter case, the number of perthite albite strings and veins is usually lower near the differently oriented inclusions than farther away from them. This is especially well illustrated when the plagioclase inclusions form zone-controlled inclusion rows. This is in agreement with the hypothesis (p. 87) that the rim albite has exsolved from the host alkali feldspar.

Sometimes the rim albite is seen to contain small inclusions of differently oriented albite. Usually these inclusions have the same optical orientation and form as the perthite albite of the adjacent (replaced) perthite grain (Fig. 83), and are thus obviously relicts of the perthite. Occasionally also single, arbitrarily oriented albite inclusions can be found in the rim albite (Fig. 84). Such inclusions probably represent the

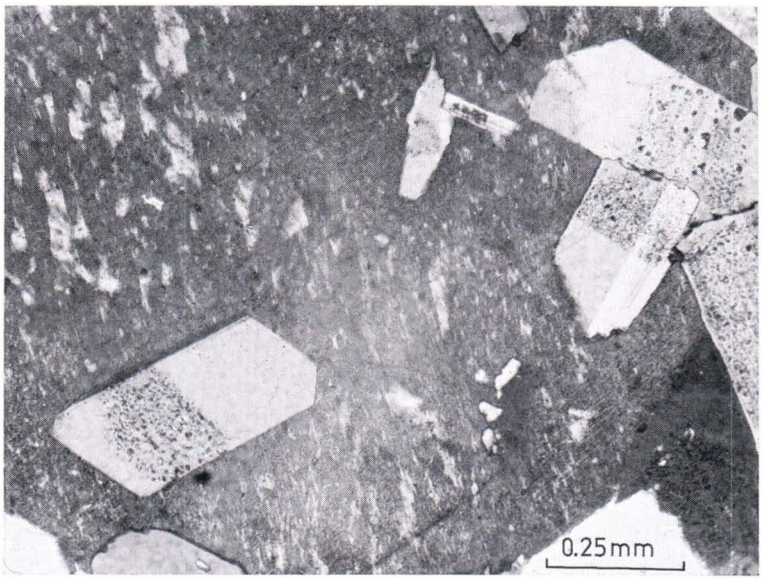

Fig. 81. Differently oriented albite inclusions in microcline perthite megacryst. The turbid cores of the inclusions are surrounded by water-clear albite margins. The perthite texture is weakly developed near the inclusions. Porphyritic type of Väkkärä granite, sample 301/PL/68.

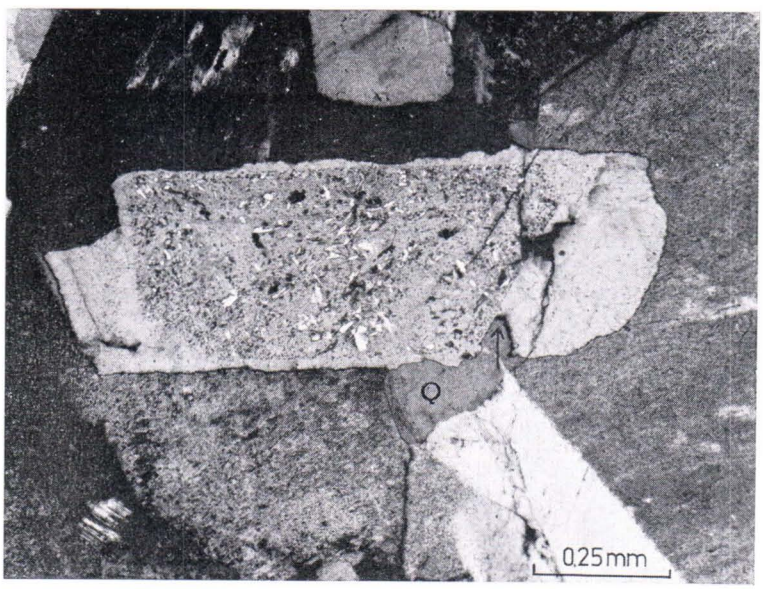

Fig. 82. Albitic plagioclase with turbid core and water-clear margin against microcline. The boundary between turbid plagioclase and quartz (Q) continues linearly as a boundary between turbid plagioclase and water-clear albite (see arrow). Porphyritic type of Väkkärä granite, sample 37/MK/67.

Fig. 83. Uniformly oriented perthite albite inclusions in water-clear albite surrounding turbid plagioclase core. Note the somewhat discontinuous twinning and incipient mosaic texture in the water-clear albite. Coarse-grained type of the Väkkärä granite, sample 1/IH/72.

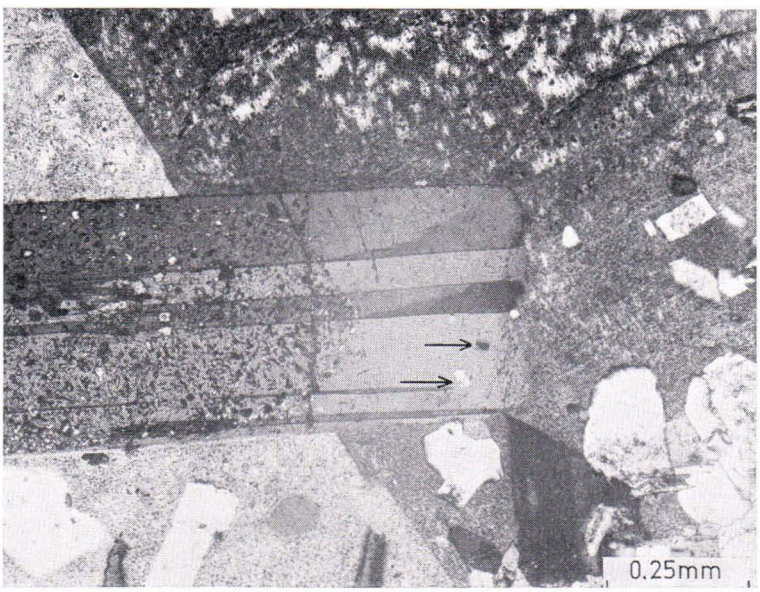

Fig. 84. Small, randomly oriented plagioclase inclusions (marked with arrows) in the water-clear albite surrounding the turbid (inclusion-rich) plagioclase core. Porphyritic type of Väkkärä granite, sample 98/MK/67/ER.

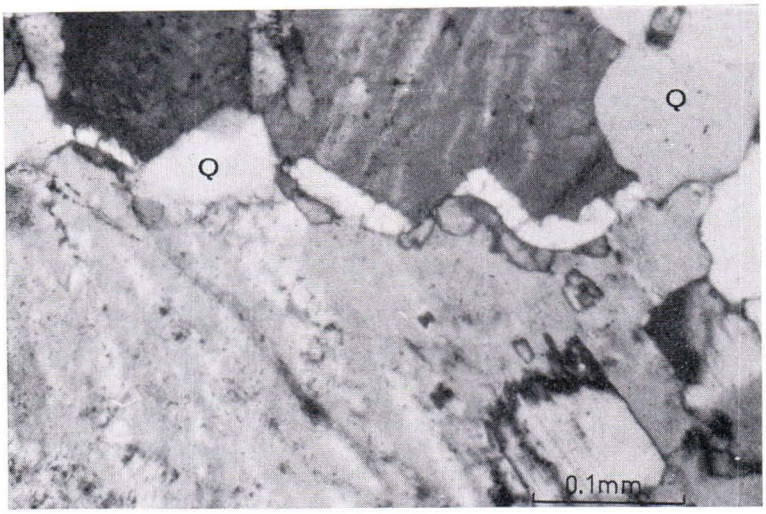

Fig. 85. Swapped albite rims between two microcline perthite grains. The intergranular rim albite units have the same optical orientation as the perthite albite on the opposite side of the rim. Q quartz. Väkkärä granite, sample 16/PL/68.

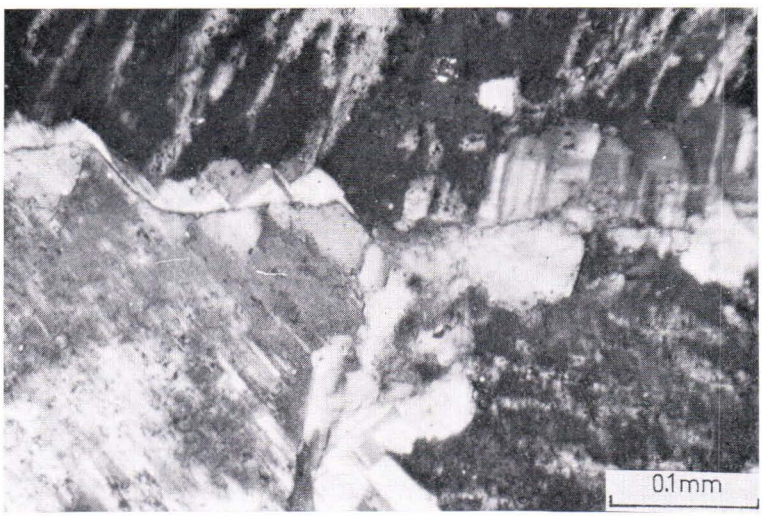

Fig. 86. Swapped albite rims between three differently oriented microcline perthite grains. Each of the rim albite units have the same optical orientation as the perthite albite on the opposite side of the rim. Väkkärä granite, sample 16/PL/68.

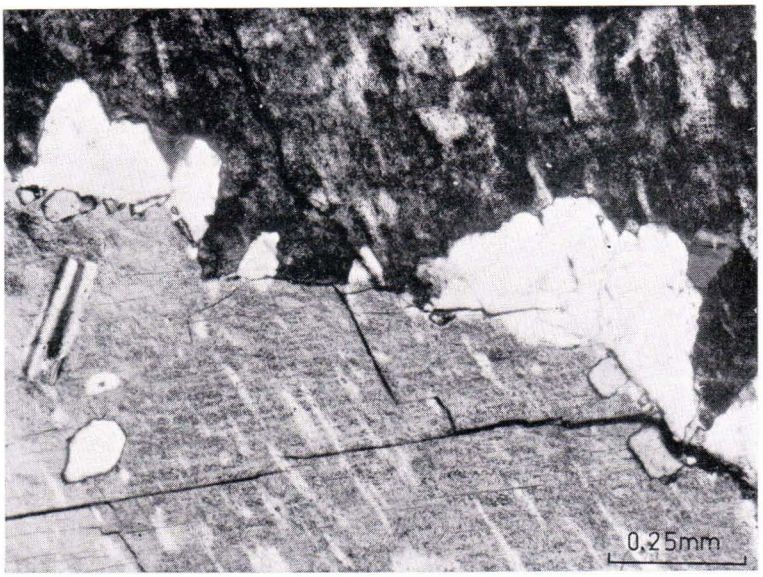

Fig. 87. Irregular intergranular albite grains in two different orientations, corresponding to the orientation of the perthite albites. Inclusions of perthite albite in the large intergranular albite grain. Porphyritic type of Väkkärä granite, sample 37/MK/67.

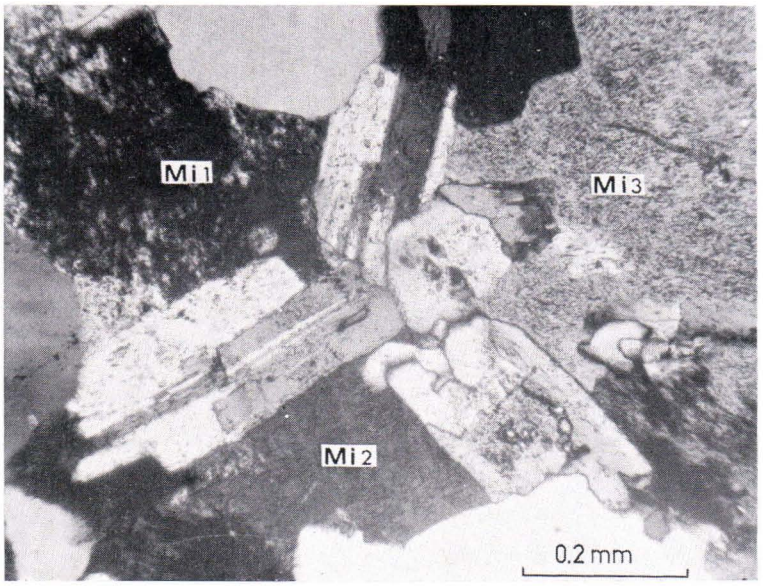

Fig. 88. Single subhedral albite grains between three microcline (Mi 1—Mi 3) grains. At least two of the albite laths are oriented according to the adjacent microcline grains, as can be verified from the sparse perthite albite patches in microcline. Conspicuously autometamorphosed Väkkärä granite, sample 104 A/IH/67.

original plagioclase inclusions of the replaced K-feldspar. Also K-feldspar inclusions oriented like the adjacent K-feldspar grain, can be found occasionally in the rim albite. The perthite albite strings and other albite inclusions are found only in the rim albite, not in the turbid core plagioclase. If the perthite albite inclusions in the rim albite were formed by later infiltration of albite into older plagioclase (see Drescher-Kaaden 1969, p. 364), they would obviously sometimes continue also to the turbid plagioclase core.

Between two K-feldspar (perthite) grains, the albite occurs as double rims or double rows of grains or as single grains. In the double rims and grain rows, the albite units have nearly always become oriented according to the alkali feldspar on the opposite side of the rows (swapped albite rims, Figs. 85—87). The albite twinning is usually well-developed, sometimes irregular and discontinuous. Perthite albite inclusions of the adjacent perthite grain are occasionally present. Myrmekite quartz has been found in only a couple of thin sections of Väkkärä granite in very small amounts. In conspicuously autometamorphosed or greisenized granite, clear interstitial albite rims are generally not present; but between the microcline grains, there are bigger single albite grains or laths, which have commonly become oriented crystallographically after either one of the microcline grains (Fig. 88).

Exceptions to the general rules presented do occur. Occasionally there is a thin, water-clear albite rim between microcline and quartz, between two turbid plagioclase grains, between plagioclase and quartz and between plagioclase and topaz. Exceptionally, water-clear albite may occur also as veins in turbid plagioclase (Fig. 89).

The data presented indicate that the water-clear albite of the Väkkärä granite is younger than the associated turbid plagioclase (albite) and K-feldspar grains. Between plagioclase and K-feldspar, the rim albite normally nucleated on the plagioclase, adopting its orientation and grew into the K-feldspar, and between two adjacent K-feldspar grains, the albite nucleated on one of the grains and grew into another (see Ramberg 1962). The occurrence of perthite albite inclusions in the interstitial albite indicates that some perthite albite is older than the interstitial albite.

Electron microprobe analyses

To obtain some information concerning the composition of alkali feldspar and plagioclase, polished thin sections were prepared from representative samples of different rock types, and the feldspars were analyzed with an electron microprobe. The perthite analyses were carried out using a beam diameter of 70 μm; the composition of plagioclase and separate phases of coarse perthite were determined using a beam diameter of 2—5 μm. Chemically analyzed orthoclase, oligoclase and labradorite were used as standars. The results are presented in Table 6 together with the obliquity and $2V\alpha$ determinations of the K-feldspar. The composition of coarse perthites was calculated from the average of analyses made at 2—3 adjacent points. Although the

Table 6

Partial electron-microprobe analyses of feldspars and structural state of K-feldspar from the rocks of the Eurajoki stock. Microprobe runs by Jaakko Siivola.

No*	Mineral	Remarks	Type of perthite	Potassic phase: Obliq. (Δ)	Potassic phase: 2V$_a$(°)	Beam diam. (μm)	Na_2O	K_2O	CaO	Ab	Or	An
Tarkki granite, sample 44/PL/68 (x = 6 792.35, y = 531.64)												
1	Kf		faint f	0.0	60—70 (mean 66)	70	2.6	13.4	0.3	22.5	76.1	1.4
2	Kf		h			70	3.3	12.4	0.8	27.7	68.5	3.8
3	Kf		f, v			70	2.1	14.2	0.1	18.3	81.2	0.5
4	Kf		h			70	2.9	13.1	0.2	24.9	74.1	1.0
5	Pl					2—5	7.0	0.5	8.0	59.5	2.8	37.7
6	Pl					2—5	6.6	0.7	7.9	57.8	4.0	38.2
7	Pl					2—5	5.9	0.2	10.6	49.6	1.1	49.2
8	Pl					2—5	5.8	0.3	10.4	49.4	1.7	48.9
Tarkki granite, sample 188/IH/67 (x = 6 789.34, y = 539.18)												
9	Kf		h	0.0	62—76 (mean 68)	70	2.4	13.2	0.1	21.5	78.0	0.5
10	Kf		f, v			70	1.9	14.2	0.1	17.9	81.6	0.5
11	Kf		f			70	2.9	12.7	0.1	25.6	73.9	0.5
12	Kf		faint f			70	3.2	13.3	0.2	26.5	72.5	0.9
13	Pl					2—5	6.1	0.4	8.8	54.3	2.3	43.3
14	Pl					2—5	6.4	0.4	8.5	56.4	2.3	41.4
Contact type of Väkkärä granite, sample 309/PL/68/IH (x = 6 790.71, y = 531.77)												
15	Kf	M	f, v	0.0—0.8 (maximum at 0.6)	72 (mean 73)	70	2.8	13.8	0.1	23.5	76.1	0.5
16	Kf	M	f, v			70	3.5	12.2	0.2	30.0	69.0	1.0
17	Kf	GM	f, s		62—80	70	1.6	12.9	0.0	15.9	84.1	0.0
18	Kf	GM	f, s			70	1.7	14.0	0.5	15.2	82.4	2.4
19	Pl	M, cent. part				2—5	11.1	0.0	0.1	99.5	0.0	0.5
20	Pl	M, cent. part				2—5	12.0	0.0	0.1	99.5	0.0	0.5
21	Pl	M, cent. part				2—5	11.8	0.0	0.1	99.5	0.0	0.5
22	Pl	M, cent. part				2—5	11.8	0.1	0.2	98.5	0.6	0.9
23	Pl	GM, pigmented				2—5	10.2	0.2	0.5	96.1	1.2	2.6
24	Pl	GM, pigmented				2—5	12.2	0.1	0.2	98.5	0.6	0.9
Even-grained type of Väkkärä granite, sample 208C/IH/67 (x = 6 789.27, y = 531.71)												
25	Kf		nearly h	0.0—0.2	60—70 (mean 65)	70	2.6	14.4	0.2	21.3	77.8	0.9
26	Kf		nearly h			70	2.3	13.9	0.1	20.0	79.5	0.5
27	Kf		f, v			70	2.2	14.4	0.1	18.8	80.8	0.5
28	Kf		v			70	1.8	14.7	0.1	15.6	83.9	0.5
29	Pl					2—5	10.7	0.2	0.4	96.8	1.2	2.0
30	Pl	intensely sericitized				2—5	9.6		0.6	96.6	0.0	3.4
31	Pl	intensely sericitized				2—5	9.8		0.9	95.2	0.0	4.8
Even-grained type of Väkkärä granite, sample 394/PL/68 (x = 6 789.38, y = 534.80)												
32	Kf		f—v	0.65	66—84 (mean 75)	70	3.8	11.3	0.2	33.5	65.5	1.0
33	Kf		v			70	3.0	11.8	0.1	27.7	71.8	0.5
34	Kf		v			70	2.9	12.2	0.2	26.3	72.7	1.0
35	Kf		v			70	1.9	12.7	0.1	18.4	81.0	0.5
36	Pl					2—5	10.9	0.2	0.9	94.6	1.1	4.3
37	Pl	pigmented				2—5	11.1	0.3	1.2	92.8	1.7	5.5
38	Pl					2—5	10.4	0.2	1.3	92.5	1.2	6.4

* Analytic points of one and the same grain are united with brackets
Mineral: Kf potassium-rich alkali feldspar, Pl plagioclase (incl. albite)
Remarks: M megacryst, GM ground mass
Type of perthite: h homogeneous or nearly homogeneous under microscope, f film perthite, s string perthite, v vein perthite, p patch perthite

Table 6, continued

No*	Mineral	Remarks	Type of perthite	Potassic phase Obliq. (Δ)	Potassic phase $2V\alpha(°)$	Beam diam. (μm)	Na_2O	K_2O	CaO	Ab	Or	An
Even-grained type of Väkkärä granite, sample 17/PL/67/IH (x = 6 789.10, y = 535.00)												
39	Kf		regular v	0.8	74, 76	70	3.8	11.7	0.3	32.6	66.0	1.4
40	Kf		coarse v			70	4.0	11.4	0.5	33.9	63.7	2.4
41	Kf		coarse v			70	3.3	12.6	0.3	28.0	7.05	1.4
42	Pl	small grain				2—5	11.7	0.1	0.4	97.6	0.6	1.9
43	Pl	large grain, central part				2—5	11.5	0.2	0.9	94.8	1.1	4.1
44	Pl	large grain, margin				2—5	11.3	0.1	0.7	96.1	0.6	3.3
45	Pl	albite rim on plag.				2—5	11.5	0.1	0.8	95.8	0.6	3.7
46	Pl	swapped albite rim				2—5	11.4	0.1	0.3	98.0	0.6	1.4
47	Pl	perthite albite vein				2—5	12.0	0.2	0.4	97.1	1.0	1.8
48	Pl	perthite albite vein				2—5	11.8	0.2	0.4	97.1	1.1	1.8
Porphyritic type of Väkkärä granite, sample 98/MK/67 (x = 6 787.94, y = 537.79)												
49	Kf	M, centr. part	v	0.8	70	70	2.6	13.2	0.0	23.0	77.0	0.0
50	Kf	M, margin	nearly h			70	1.8	14.7	0.0	15.7	84.3	0.0
51	Kf	M	v			70	2.2	13.7	0.0	19.6	80.4	0.0
52	Kf	GM	h		68—80	70	0.3	16.1	0.0	2.7	97.3	0.0
53	Kf	GM	h		(mean 75)	70	0.5	15.8	0.0	4.6	95.4	0.0
54	Pl	M, pigm. centr. part				2—5	11.1	0.1	0.0	99.4	0.6	0.0
55	Pl	M, clear margin				2—5	10.7	0.2	0.1	98.3	1.2	0.5
56	Pl	M, pigm. centr. part				2—5	11.3	0.1	0.1	98.9	0.6	0.5
57	Pl	M, clear margin				2—5	11.2	0.1	0.1	98.9	0.6	0.5
58	Pl					2—5	11.4	0.1	0.1	98.9	0.6	0.5
Porphyritic type of Väkkärä granite, sample 301/PL/68 (x = 6 787.38, y = 534.90)												
59	Kf	M	coarse v	0.85	70—76 (mean 73)	70	2.6	13.8	0.1	22.1	77.4	0.5
60	Kf	M	v, p			70	2.7	13.7	0.1	23.0	76.6	0.5
61	Kf	GM				70	0.8	15.7	0.0	7.2	92.8	0.0
62	Kf	GM				70	0.0	15.9	0.0	9.5	90.5	0.0
63	Kf	M	(sparse p)			2—5	0.3	17.0	0.0	2.6	97.4	0.0
64	Pl	M, pigm. centr. part				2—5	11.4	0.0	0.0	100.0	0.0	0.0
65	Pl	M, pigm. centr. part				2—5	11.3	0.1	0.3	98.0	0.6	1.5
66	Pl	GM, clear margin				2—5	11.4	0.1	0.2	98.4	0.6	1.0
Porphyritic type of Väkkärä granite, sample 73/MK/67 (x = 6 787.14, y = 536.27)												
67	Kf	M, centr. part	v, p	0.90	68—76 (mean 71)	70	2.4	13.2	0.1	21.5	78.0	0.5
68	Kf	M, margin	nearly h			70	0.9	16.2	0.0	7.8	92.2	0.0
69	Kf	M, centr. part	v, p			70	2.8	12.9	0.3	24.5	74.1	1.5
70	Kf	M, margin	v			70	1.3	15.9	0.1	11.0	88.5	0.5
71	Kf	M	(sparse p)			2—5	0.4	16.5	0.1	3.6	95.9	0.5
72	Kf	GM	sparse p, v		60—80 (mean 72)	70	0.4	16.5	0.1	3.6	95.9	0.5
73	Pl	pigm. centr. part				2—5	11.1	0.1	0.0	99.4	0.6	0.0
74	Pl	clear margin				2—5	10.7	0.2	0.1	98.3	1.2	0.5
75	Pl	M, pigm. centr. part				2—5	11.3	0.1	0.1	98.9	0.6	0.5
76	Pl	M, clear margin				2—5	11.2	0.1	0.1	98.9	0.6	0.5
77	Pl					2—5	11.4	0.1	0.1	98.9	0.6	0.5

Table 6, continued

No*	Mineral	Remarks	Type of perthite	Potassic phase: Obliq. (Δ)	Potassic phase: 2Vα(°)	Beam diam. (μm)	Na_2O	K_2O	CaO	Ab	Or	An
		Porphyritic type of Väkkärä granite, sample 17/MK/67 (x = 6 786.49, y = 535.86)										
78	Kf	M	coarse p, v		70, 76	70	1.3	14.6	0.0	11.9	88.1	0.0
79	Kf	GM	h	0.90	68—80 (mean 74)	70	0.3	15.2	0.0	2.9	97.1	0.0
80	Kf	GM	h			70	0.3	16.6	0.1	2.6	96.9	0.5
81	Kf	GM	h			70	0.5	15.2	0.0	4.8	95.2	0.0
82	Kf	M	(h)			2—5	0.3	16.1	0.0	2.7	97.3	0.0
83	Kf	GM	(h)			2—5	0.3	15.6	0.0	2.8	97.2	0.0
84	Pl	M				2—5	11.9	0.1	0.0	99.4	0.6	0.0
85	Pl	GM				2—5	12.5	0.1	0.3	98.2	0.5	1.3
86	Pl	GM				2—5	12.5	0.1	0.3	98.2	0.5	1.3
87	Pl	Incl. in Kf M				2—5	12.2	0.1	0.5	97.2	0.5	2.2
88	Pl	Incl. in Kf M				2—5	11.6	0.2	0.3	97.5	1.1	1.4
89	Pl	Incl. in Kf M				2—5	11.7	0.0	0.1	99.5	0.0	0.5
90	Pl	Exsol. (?) patch in Kf				2—5	10.5	0.2	0.2	97.7	1.2	1.0
91	Pl	Exsol. (?) patch in Kf				2—5	12.6	0.1	0.1	99.0	0.5	0.4
92	Pl	Exsol. (?) vein in Kf				2—5	12.3	0.1	0.1	99.0	0.5	0.4
93	Pl	Exsol. (?) vein in Kf				2—5	11.9	0.1	0.1	99.0	0.6	0.5
		Porphyritic type of Väkkärä granite, chloritized, sample DH 311/48.7 m										
94	Kf	M	h			70	0.5	16.8	0.0	4.3	95.7	0.0
95	Kf	GM	h	0.90	60—72 (mean 67)	70	0.4	17.2	0.1	3.4	96.1	0.5
96	Kf	GM	h			70	0.3	17.1	0.0	2.6	97.4	0.0
97	Pl	GM				2—5	11.1	0.1	0.2	98.4	0.6	1.0
98	Pl	GM				2—5	12.4	0.1	0.0	99.5	0.5	0.0
99	Pl	GM				2—5	11.9	0.1	0.1	99.0	0.6	0.5
		Greisenized Väkkärä granite, sample 204/PL/68 (x = 6 788.08, y = 534.55)										
100	Kf		h		68—74 (mean 71)	70	0.2	17.1	0.5	1.7	93.8	4.6
101	Kf		h			70	0.3	16.2	0.0	2.7	97.3	0.0
102	Kf		h			70	0.7	15.3	0.1	6.5	93.0	0.5
103	Pl					2—5	11.3	0.1	0.1	98.9	0.6	0.5
104	Pl					2—5	11.9	0.0	0.1	99.5	0.0	0.5
		Greisenized Väkkärä granite, sample 376/PL/68 (x = 6 787.55, y = 534.34)										
105	Kf		h	0.90	70—82 (mean 74)	70	0 4	16 8	0 0	3 5	96 5	0 0
106	Kf		h			70	0.3	17.5	0.0	2.5	97.5	0.0
107	Pl					2—5	11.6	0.1	0.1	98.9	0.6	0.5
108	Pl					2—5	11.9	0.1	0.1	98.5	1.1	0.5
		Topaz-bearing quartz porphyry, dike QP I, sample 97B/IH/67 (x = 6 787.16, y = 532.68)										
109	Kf	M	f		82—85	70	6.5	6.8	0.1	58.9	40.6	0.5
110	Kf	M	f			70	2.3	12.9	0.0	21.3	78.7	0.0
111	Kf	M	f			70	3.6	10.9	0.0	33.4	66.6	0.0
112	Pl	M				70	10.9	0.7	0.4	94.1	4.0	2.0
113	Pl	M, cross hatched				70	11.3	0.7	0.1	95.6	3.9	0.5
114	Pl	M, cross hatched				70	11.8	0.2	0.1	98.4	1.1	0.5
115	Pl	M, core				70	11.3	0.3	0.1	97.8	1.7	0.5
116	Kf	M, mantle				70	5.1	8.3	0.7	46.6	49.9	3.5
117	Pl	M, core				70	11.1	1.0	0.0	99.4	0.6	0.0
118	Kf	M, mantle				70	2.8	11.5	0.2	26.7	72.2	1.1
		Dark porphyry, dike DP III, sample 1C/IH/75 (x = 6 789.97, y = 536.00)										
119	Kf	M	h	0.0	64	70	2.4	12.6	0.1	22.3	77.2	0.5
120	Kf	M	f			70	2.2	13.3	0.1	20.0	79.5	0.5
121	Pl	M				70	4.2	0.5	11.8	38.0	3.0	59.0
122	Pl	M				70	4.6	0.5	11.7	40.4	2.9	56.7

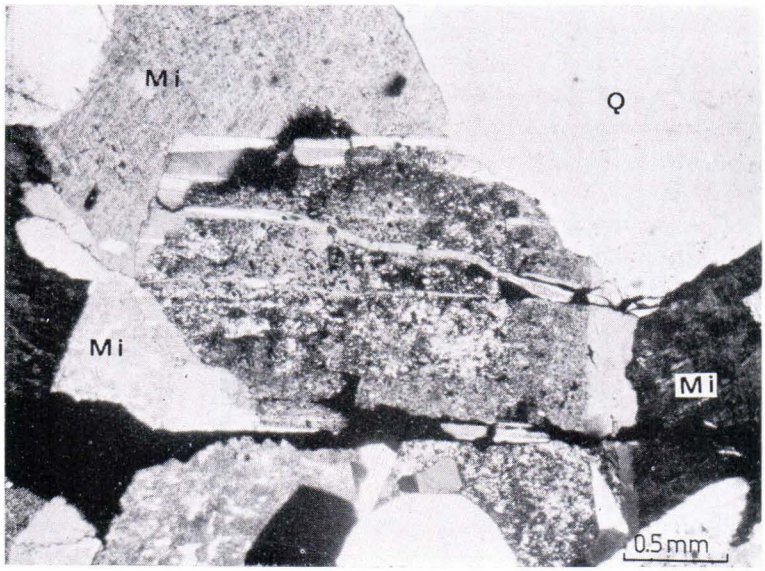

Fig. 89. Water-clear albite intersecting turbid plagioclase as veins. Water-clear albite also between turbid plagioclase and microcline (Mi). Coarse-grained type of Väkkärä granite, sample 1/IH/72.

compositions arrived at for the coarse perthites cannot be very accurate, they do show the main chemical characteristics of the alkali feldspars of the different granites.

In the Tarkki granite samples, the alkali feldspar has a bulk composition of $Ab_{18-28}Or_{82-68}An_{0\cdot5-4}$. The analyses show that homogeneous or nearly homogeneous alkali feldspar has a higher content of Ab (possibly also An) than perthitic feldspar of the same sample. This suggests that 1) the perthite is of exsolution origin, and 2) some exsolution of albite to or across the grain borders has occurred. The associated unaltered plagioclase has a composition of $Ab_{49-60}Or_{1-4}An_{49-38}$. The Ab content increases towards the margins, sometimes with oscillatory zoning. The average Ab content of plagioclase is in sampe 44/PL/68 54 %, in sample 188/IH/67 55 %. A plot of these values on Stormer's (1975) feldspar composition—temperature diagram for 1 000 bars pressure gives a modal equilibrium temperature of 740—750°C; for 2 000 bars pressure, the temperatures would be 20°C higher.

In the sample of the contact type of Väkkärä granite studied (sample 309/PL/68/IH), the megacryst alkali feldspar has a composition of $Ab_{23-30}Or_{69-76}An_{0.5-1}$. In the ground-mass alkali feldspar, the Ab content is lower, 16—15 mole %, probably owing to exsolution across the grain boundaries. The An content of plagioclase is, according to the microprobe analyses, only 0.5—3 %, but refractive indice determinations of the same sample indicate that there is also plagioclase with 13—15 % An (α 1.531, γ 1.545).

Notable variation occurs in the composition of the alkali feldspar of the even-grained type. In sample 208C/IH/67 (near the Tarkki granite contact), the Ab content

of perthite is 21—16 %, decreasing from nearly homogeneous alkali feldspar to vein perthite. In samples 394/PL/68 and 17/PL/68/IH, taken from the central parts of the Väkkärä granite formation, somewhat higher Ab contents (31—18 %) were observed. The An content of coexisting separate plagioclase is 6—2 %.

In the topaz-bearing Väkkärä granite, the bulk composition of perthite varies in very broad limits. In apparently well-preserved samples (98/MK/67/ER, 301/PL/68 and 73/MK/67), the coarsely perthitic central parts of the alkali feldspar megacrysts show notably high Ab contents (20—25 %), but in the marginal parts of the megacrysts and in the ground mass the Ab contents is much lower. The analyses made from the K-feldspar host phase by using the small beam diameter (samples 301/PL/68, 73/MK/67 and 17/MK/67) show very small Ab contents, about 2.6—3.6 %. The plagioclase of these samples, regardless of the mode of occurrence (individual plagioclase grains, inclusions in K-feldspar, intergranular albite and perthite albite), is always albite with less than 5 % An.

In the non-perthitic K-feldspar of the association K-feldspar—quartz—plagioclase—chlorite—topaz (transitional to greisenized granite, sample DH 311/48.7 m) and of the greisenized granite (samples 304/PL/68 and 376/PL/68), the Ab content is 2—6 %. The associated plagioclase is nearly pure albite.

In the quartz porphyry dikes, the composition of the perthite megacrysts appears to vary in wide limits, but the plagioclase phase, which occurs either as individual megacrysts or as the cores of zoned feldspar megacrysts, is always nearly pure albite. In the studied sample of the dark porphyry dike, the alkali feldspar has the composition $Ab_{22-20}Or_{77-79}An_{0.5}$, and the associated unaltered plagioclase $Ab_{38-40}Or_3$ An_{59-57}.

Interpretations

Some of the most important characteristics of the alkali feldspars of the Eurajoki granites and the writer's opinion of their development are presented schematically in Fig. 90.

Exsolution of the plagioclase component from alkali feldspar has obviously been the most important factor in the development of the perthite texture and the intergranular albite and myrmekite. Exsolution across the grain borders from the high-temperature (presumably Ca-rich) alkali feldspar of the Tarkki granite has led to the formation of myrmekite, whereas corresponding exsolution from the lower-temperature alkali feldspar of the Väkkärä granite has produced intergranular albite. The exsolution and ordering were catalyzed by the fluid phase (Tuttle and Bowen 1958, p. 129, Ragland 1969, Vorma 1971, Martin 1974). The coarseness of the perthite texture, the amount of intergranular albite, and the obliquity of the K-feldspar tend to increase concomitant with the supposed increasing activity of the fluid phase towards the latest granite differentiates. In the well-preserved samples, the exsolution across the

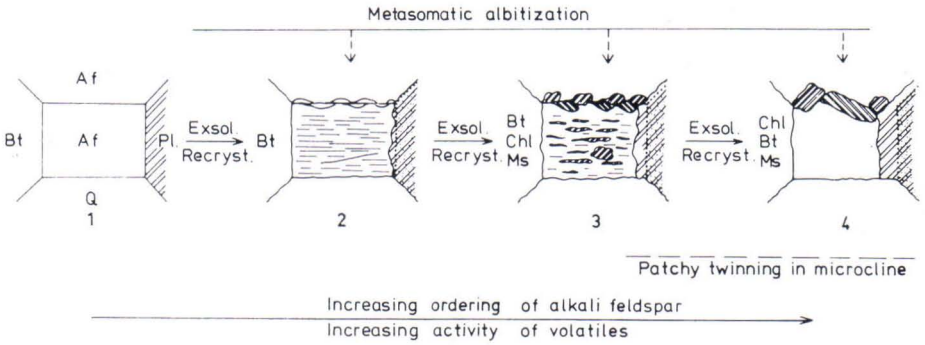

Fig. 90. Model of the development of some characteristics of the alkali feldspars of the granites of the Eurajoki stock. Af, potassic alkali feldspar; Q, quartz; Pl, plagioclase; Bt, biotite; Chl, chlorite; Ms, muscovite.

grain borders has been more intense in the ground-mass alkali feldspar, as might be expected (large surface area, short distances to diffuse). In the chloritized and greisenized granite, the albite component has exsolved nearly totally out of the alkali feldspar. Locally, however, the perthite texture and intergranular albite have developed by (auto)metasomatic albitization. Recrystallization of plagioclase along fractures and grain margins may also produce water-clear (inclusion poor) albite (e.g., water-clear veins in turbid plagioclase, Fig. 89; see also Vernon 1975), but this mechanism appears to be of minor importance.

The alkali feldspar of the Tarkki granite represents stages 1 and 2 in Fig. 90. In the even-grained type of Väkkärä granite, stage 2 is typical, but also coarse vein perthite (type 3) occurs. The alkali feldspar of the topaz-bearing Väkkärä granite is characterized by development stage 3, but with increasing alteration (chloritization of biotite etc.) and recrystallization stage 4 is achieved. In the greisenized granite, textures of stage 4 are typical. In stages 1 and 4, the alkali feldspar is homogeneous or nearly so, but in the alkali feldspar of stage 1, the Na content is high, in stage 4 very low.

One characteristic feature of the topaz-bearing Väkkärä granite is the patchy twin texture of the microcline. Microcline with a patchy extinction texture or four-ling twinning has been described by Heinrich and Moore (1970) in metasomatic rocks associated with igneous alkaline complexes. Barth (1959) described microcline with »twin texture consisting of lozenge-shaped areas or of irrational curved boundaries» from a chlorite schist in Norway (cited from Smith 1974, p. 384). Barth suggested primary growth in the stability field of microcline. Authigenic microcline grown in solid tends to show four-ling twinning, commonly with irregular twin boundaries. (Baskin 1956, Smith 1974, pp. 258—261, 382). The common existence of unoriented, often zone-controlled inclusions of plagioclase in the microcline of the Väkkärä granite (p. 36) can best be explained to be due to accidental trapping during crystallization from a melt. Typical four-ling twinning is not present. The intimate texture of the twinned microcline might indicate inversion. Perhaps this curious

patchy twinning is produced by strong recrystallization, possibly coupled with inversion, the process being catalyzed by fluorine-bearing fluids. Microcline with similar patchy twinning has been found by the author also in the even-grained topaz-bearing granite from Kymi in the Wiborg rapakivi massif.

COMPOSITION OF BIOTITE

The chemical composition of the dark micas of the Tarkki and Väkkärä granites were studied by using electron microprobe and wet chemical methods. In the microprobe analyses, chemically analyzed biotite were used as standards. In computing the analyses, the raw counts were corrected according to the method of Bence and Albee (1968). For the wet chemical analyses, dark mica was separated by using heavy liquids and a Franz isodynamic separator. The mica concentrates were ground very carefully in an agate mortar to loosen inclusions (zircon, apatite, cassiterite, etc.), and the grinding—separation treatment was repeated several times. Finally, visible impurities were removed under a stereo microscope. Unfortunately, it was not possible to remove all the chlorite intergrown with the biotite of the Tarkki granite.

The general modes of occurrence of the mica minerals are given in connection with the petrographic description of the rocks. The microscopic characteristics observed from thin sections and from separated mica fractions are summarized here for the wet-chemically analyzed micas:

Sample 85/IH/67. Anhedral (interstitial), partly chloritized dark brown flakes. Abundant ilmenite inclusions as well as zircon and apatite inclusions surrounded by pleochroic halos.

Sample 98/MK/67/ER. Anhedral, well-preserved, medium-brown flakes. Color zoning sometimes present but is not typical. Sometimes very weak alteration to pale green mica (anal. 8 in Table 7) or muscovite. Abundant pleochroic halos around small inclusions (zircon, monazite, etc.). A very small percentage of mica occurs as small dark brown inclusions in quartz megacrysts (anal. 7, Table 7).

Sample 10/PL/68/IH. Anhedral to subhedral well-preserved flakes, which often show a color zoning: the pale brown flakes ($2V\alpha \sim 0°$) are surrounded by a thin seam of white mica ($2V\alpha$ 18—22°). Pleochroic halos are not common.

Sample 1/IH/72. Anhedral to subhedral brownish green flakes ($2V\alpha \sim 0$) are surrounded in some cases by a thin seam of white mica ($2V\alpha$ 20—28°). Very small inclusions surrounded by pleochroic halos, also some streaks of iron oxide as inclusions.

The general formula of trioctahedral micas can be written as $X_2Y^{[6]}_6Z^{[4]}_8(OH)_4$ where X = K, Na, Ca; Y = Fe^{2+}, Mg^{2+}, Mn^{2+}, Li^{+}, Fe^{3+}, Al^{3+}, Ti^{4+} and Z = Si^{4+} (6—5) Al^{3+} (2—3), Ti^{4+}. Anions F^- and Cl^- can substitute for OH. The occupation of the octahedral sites is usually not complete, the sum of the Y group elements being less than in the ideal formula. In addition, the dark micas contain a number of trace elements. Their position in the mica formula and structure is as follows (Tischendorf *et al.* 1969):

X group: Rb^{+}, Cs^{+}, Tl^{+}, Sr^{2+}, Ba^{2+}, Pb^{2+}, Pb^{2+}
Y group: Zn^{2+}, Co^{2+}, Ni^{2+}, Sc^{3+}, Cr^{3+}, V^{3+}, In^{3+}, Sn^{4+}, Zr^{4+}, Mo^{4+}, Nb^{5+}, Ta^{5+}
Z group: Be^{2+}, Ga^{3+}, Ge^{4+}

The usefulness of the electron microprobe analyses is limited because they do not give the contents of such important elements as Li and F nor the oxidation state of iron. However, the microprobe analyses (Table 7) and the wet-chemical analyses (Table 8) show clearly that all the micas analyzed have very high Fe/(Fe + Mg) ratios and that the biotite of the Tarkki granite has lower contents of Al_2O_3 and higher contents of TiO_2 and MgO than the dark micas of the Väkkärä granite. The biotite of the Tarkki granite does not contain octahedrally coordinated aluminum. There are also systematic compositional differences between the dark micas of the different types of Väkkärä granite: SiO_2 and Al_2O_3 contents increase and TiO_2 and MgO contents decrease in the order contact type → even-grained type → coarse-grained and porphyritic (topaz-bearing) types, following the supposed order of development of the granite types. The differences are not great between the biotites of the contact type and the even-grained type, but the dark micas of the topaz-bearing types differ

Table 7

Electron microprobe analyses of dark micas and chlorite from the Tarkki and Väkkärä granites. Anal. Tuula Paasivirta.

	1	2	3	4	5	6	7	8	9
SiO_2	36.3	36.9	33.5	34.5	35.8	35.4	39.8	40.3	23.5
TiO_2	4.7	4.3	3.0	2.5	3.1	2.7	0.2	0.4	0.1
Al_2O_3	12.0	11.8	17.8	18.0	19.0	19.4	19.9	20.4	20.4
FeO (tot. iron)	33.0	34.4	29.9	32.4	31.0	31.6	21.3	20.0	44.6
MnO	0.2	0.3	0.1	0.3	0.3	0.3	0.6	0.8	0.3
MgO	3.4	2.4	2.5	0.9	2.2	0.9	0.1	0.2	0.7
CaO	0.0	0.0	0.3	0.5	0.1	0.2	0.1	0.5	0.1
Na_2O	0.0	0.0	0.0	0.2	0.0	0.0	0.0	0.0	0.1
K_2O	8.4	8.5	8.5	8.5	8.6	8.1	9.8	9.1	0.1
Σ	98.0	98.6	95.6	97.8	100.1	98.6	91.8	91.7	89.9
Y ~ Z	d.br.	d.br.	d.br.	br.	d.r.br.	d.br.	d.br.	p.br.gr.	br.gr.

d. dark; br, brown, brownish; r. reddish; gr. green, greenish

1. Biotite (lepidomelane), anhedral flake. Tarkki granite, sample 44/PL/68 (x = 6 792.35, y = 531.64)
2. Biotite (lepidomelane), anhedral flake. Tarkki granite, sample 188/IH/67 (x = 6 789.34, y = 539.18)
3. Biotite, euhedral flake. Contact type of Väkkärä granite, sample 309/PL/68/IH (x = 6 790.71, y = 531.77)
4. Biotite, euhedral aggregate. Even-grained type of Väkkärä granite, sample 208C/IH/67 (x = 6 789.27, y = 531.71)
5. Biotite, euhedral flake (1st generation) } Even-grained type of Väkkärä granite, sample
6. Biotite, anhedral interstitial aggregate (2nd generation) } 17/PL/68/IH (x = 6 789.10, y = 535.00)
7. Biotite (protolithionite), inclusion in a quartz megacryst (1st generation) } Porphyritic type of Väkkärä granite, sample 98/MK/67/ER (x = 6 787.94,
8. Biotite (protolithionite), leached anhedral flake } y = 537.79)
9. Chlorite. Even-grained type of Väkkärä granite, sample 208C/IH/67

Table 8

Chemical composition and physical properties of dark micas from the granites of the Eurajoki stock. Wet-chemical analyses by Pentti Ojanperä, emission spectrographic determinations (trace elements given in ppm) by Ringa Danielsson.

Weight per cent	1 W	2 W	3 W	4 W
SiO_2	34.37	39.43	39.12	40.30
TiO_2	3.32	0.73	0.59	0.64
Al_2O_3	11.99	19.43	20.80	20.13
Fe_2O_3	5.95	5.08	2.77	4.04
FeO	27.30	17.68	19.04	16.53
ZnO	0.11	0.44	0.42	0.40
MnO	0.21	0.91	1.00	0.95
MgO	3.83	0.11	0.08	0.10
CaO	0.40	0.18	0.06	0.08
BaO *)	0.09		0.00	
SrO*)	0.00		0.00	
Li_2O	0.03	1.18	1.36	1.63
Na_2O	0.11	0.27	0.22	0.18
K_2O	8.00	9.14	9.30	9.22
Rb_2O *)	0.056	0.76	0.73	0.90
Cs_2O *)	0.007	0.025	0.02	0.024
ZrO_2*)	0.00		0.00	
Nb_2O_5*)	0.003		0.004	
CO_2	0.00	0.00	0.00	0.00
Cl	0.09		0.003	
F	0.39	4.30	4.83	4.90
P_2O_5	0.07	0.06	0.05	0.06
H_2O+	2.75	1.84	0.98	1.55
H_2O-	0.53	0.01	0.26	0.01
	99.606	101.644	101.637	101.575
$-O = F_2$	0.16	1.81	2.04	2.06
$-O = Cl_2$	0.02			
	99.426	99.765	99.597	99.584

Trace in ppm	1 W	2 W	3 W	4 W	
V	180		n.o.		
Cr	89		n.o.		Z
Ni	40		n.o.		
Co	15		n.o.		
Cu	19		33		
Pb	15	83	11	19	
Mo	10		n.o.		Y
Be	n.o.	10	11	17	
B	n.o.	40	n.o.	33	
Sc	30	270	140	230	
Ga	80	650	520	630	
Sn	35	500	600	300	
Physical properties					X
Sp.gr.	3.25	3.11	3.11	3.09	
Y ~ Z	Dark brown	Light green	Light brown	Brown	
$\beta \sim \gamma$		brown			
($\pm$0.003)	1.690	1.625	1.615	1.610	
2Va	12—18°	~ 0	~ 0	0—8°	
Polytype	1M		1M, 3T		

Atomic ratios on the basis of 24 (O, OH, F, Cl)	1 W	2 W	3 W	4 W
Si	5.65	5.99	6.01	6.07
Al[4]	2.32	2.01	1.99	1.93
Ti[4]	0.03	0.00	0.00	0.00
Al[6]	0.00	1.47	1.77	1.64
Ti[6]	0.38	0.08	0.07	0.07
Fe^{3+}	0.74	0.58	0.32	0.46
Fe^{2+}	3.75	2.25	2.45	2.08
Zn	0.01	0.05	0.05	0.05
Mn	0.03	0.12	0.13	0.12
Mg	0.94	0.03	0.02	0.02
Li	0.02	0.72	0.84	0.99
Ca	0.07	0.03	0.01	0.01
Ba	0.01		0.00	
Na	0.04	0.08	0.07	0.05
K	1.68	1.77	1.82	1.77
Rb	0.01	0.07	0.07	0.09
O	20.76	20.07	20.65	20.11
OH	3.01	1.86	1.00	1.56
F	0.20	2.07	2.35	2.33
Cl	0.03		0.00	
Z	8.00	8.00	8.00	8.00
Y	5.87	5.30	5.65	5.43
X	1.81	1.95	1.97	1.92

n.o. not observed; *) X-ray fluorescence determination by V. Hoffrén and Maija-Leena Hagel-Brunnström

1. Biotite (lepidomelane), Tarkki granite, sample 85/IH/67 (x = 6 785.98, y = 534.18)
2. Lithian siderophyllite (protolithionite), coarse-grained type of Väkkärä granite, sample 1/IH/72 (x = 6 787.29, y = 535.04)
3. Lithian siderophyllite (protolithionite), porphyritic type of Väkkärä granite, sample 10/PL/68/IH (x = 6 787.54, y = 535.00)
4. Lithian siderophyllite (protolithionite), porphyritic type of Väkkärä granite, sample 98/MK/67/ER (x = 6 787.94, y = 537.79)

from them markedly. Analyses No. 5 and No. 6 (Table 7) are from one and the same sample (17/PL/68/IH), but the biotite of anal. No. 6 is of an earlier generation (note slightly higher TiO_2 and MgO contents). Similarly, microprobe analyses No. 7 and No. 8 and wet-chemical analysis No. 4W (Table 8) are from one and the same sample (see description of sample 98/MK/67/ER). Although the mica of anal. No. 7 is obviously of an earlier generation and the colors of the micas are different, the analyses are nearly identical. Probably there are differences in the oxidation state of the iron. The Li_2O and F contents are evidently very high in the micas of anal. No. 7 and No. 8.

The wet-chemical analyses (Table 8) show considerable differences also in the minor and trace element contents between the biotites of the Tarkki granite and topaz-bearing Väkkärä granite. The last-mentioned dark micas are heavily enriched in Zn, (Mn), Li, Rb, Sc, F, Sc, Ga and Sn and impoverished in Ti, Ba, V, Cr and Ni compared with the biotite of the Tarkki granite and most dark micas in general. The greenish color of mica anal. No. 2W is obviously due to higher Fe^{3+}/Fe^{2+} ratio of this mica.

The dark micas of the topaz-bearing Väkkärä granite have compositions intermediate between siderophyllite and zinnwaldite. According to the terminology of Foster (1960), these micas are protolithionites (Li 1 $\pm$ 0.5 per unit cell), members of the ferrous lithium mica series. According to the nomenclature suggested by Rieder (1970), they are lithian siderophyllites and members of the biotite group. The mineral name protolithionite is widely used by tin granite specialists, but commonly used mineralogical handbooks such as Deer, Howie and Zussman (1963), Strunz (1970) and Fleischer (1971) do not mention protolithionite as a mineral species.

The compositional variation of the dark micas of the Eurajoki granites can be visualized in an Al_2O_3—FeO(total iron)—MgO diagram (Fig. 91). The three fields (I—III) show the biotite compositions for different mineral associations according to Nockolds (1947):

I biotite associated with muscovite, topaz, etc.
II biotite unaccompanied by other mafic minerals
III biotite associated with hornblende, pyroxene and/or olivine

The analytic points of the biotite of the Tarkki granite fall into field III, very close to each other, and into the same part (association with hornblende) as the previously published biotite analyses of the Finnish rapakivi granites (see Simonen and Vorma 1969). Biotites of the contact type and even-grained type of Väkkärä granite fall at the border between fields II and I. In these granites, biotite and its alteration products are the only mafic minerals; and in sample 17/PL/68/IH, there is a little topaz in close association with the interstitial biotite (anal. No. 6). The dark micas of the coarse-grained and porphyritic (topaz-bearing) types fall into field I.

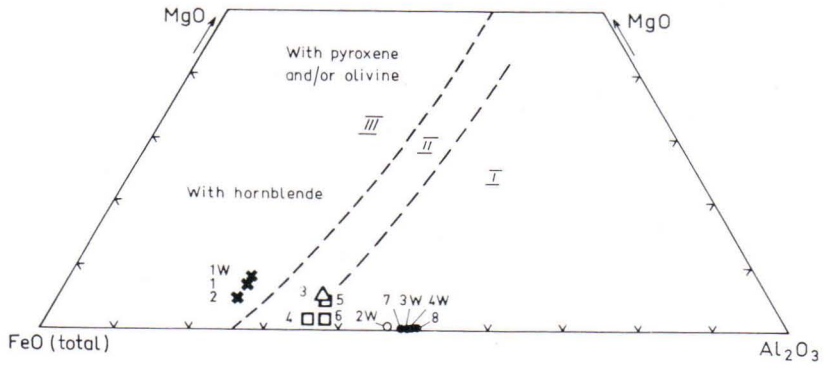

Fig. 91. Proportions of FeO (total iron), Al_2O_3 and MgO weight percentages in the biotites of the Tarkki and Väkkärä granites. The numbering of the analyzed samples is the same as in Tables 7 and 8. The fields I—III show biotite compositions for different mineral associations according to Nockolds (1947) (see text).

Lithium-iron micas with high Sn contents are typical of tin-bearing granites in different parts of the world, e.g., Erzgebirge (Tischendorf *et al.* 1969), Lost River area in Alaska (Sainsbury 1969), Pitkäranta in Soviet Karelia (Rub *et al.* 1974). In many studies, the Li micas of granitoids are believed to be of metasomatic origin (e.g., Stemprok 1974). However, Rub (1972) and Rub *et al.* (1974) offered evidence for the primary magmatic origin of Li-rich micas of some granitic rocks of the USSR. In the Väkkärä granite, the protolithionite/lithian siderophyllite occurs partly as individual flakes (also as small zone-controlled inclusions in quartz megacrysts) without any evidence of a replacement origin, but in part it replaces dark brown mica and its alteration products, and in the greisenized granite also feldspars.

COMPOSITION OF CASSITERITE

Among the accessory minerals of the Väkkärä granite, the occurrence of cassiterite is of special interest. It occurs dispersed in very small amounts throughout the topaz-bearing Väkkärä granite (an area of more than 10 km²). Higher concentrations occur in the small pegmatite veins and pockets in the Väkkärä granite and in the greisen bodies. In thin sections made from granite samples, cassiterite has been found as small inclusions at the borders of euhedral quartz grains, in a matrix embedded in altered biotite or in contact with fluorite. It shows simple crystal forms and is very dark brown in color. In pegmatite and, especially, in greisen, cassiterite is lighter and the color zoning is more clearly visible. In greisen, cassiterite is commonly twinned, the different individuals forming radial intergrowths.

In the literature, there is considerable evidence that the chemical composition of cassiterite reflects the type of occurrence. It is known that cassiterite from pegmatite has higher contents of Ta, Nb, Fe, Mn, etc., than cassiterite from greisens and related

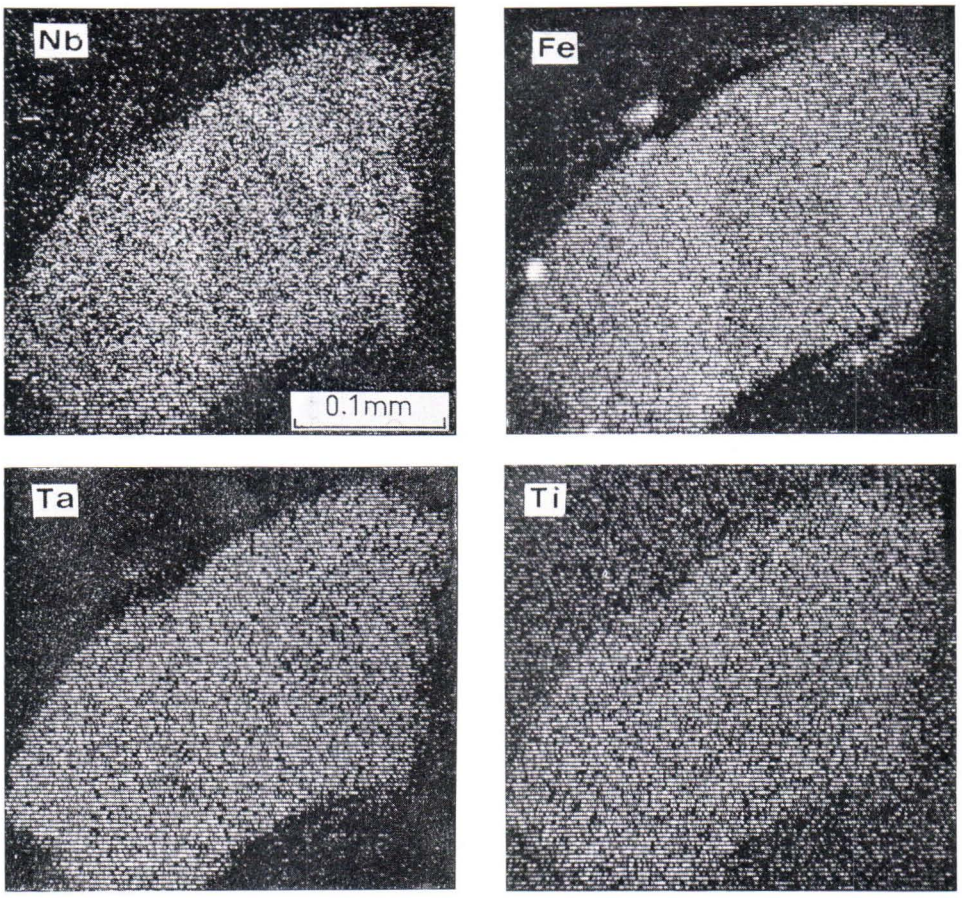

Fig. 92. Electron-probe scanning pictures showing distribution of Nb, Fe, Ta and Ti in a cassiterite grain from the Väkkärä granite (porphyritic type, sample 98/MK/67/ER).

low-temperature occurrences (e.g., Dudykina 1959, Dolomanova *et al.* 1969). To clarify the chemical composition (and genesis) of the cassiterite from the Eurajoki occurrences, polished sections were prepared 1) from five cassiterite fractions separated from the topaz-bearing types of Väkkärä granite 2) from two samples of cassiterite-bearing pegmatite veins intersecting the porphyritic type of Väkkärä granite and 3) from five cassiterite-bearing greisen samples. The cassiterite sections were checked for inclusions using routine microscopic and electron microprobe techniques. In reflecting light, most of the cassiterite grains of granite and pegmatite samples appeared homogeneous, but some grains contained inclusions identified by the microprobe as Fe-Ta-Nb-Ti oxide (tapiolite—mossite or tantalite—columbite) and iron oxide (probably magnetite). The cassiterite from greisens in the Tarkki granite contained some inclusions of niobian rutile (electron microprobe analysis: TiO_2 82 %, Nb_2O_5 12 %, Ta_2O_5 0.7 %, FeO 6 %, Σ 100.7) and iron oxide in fracture fillings.

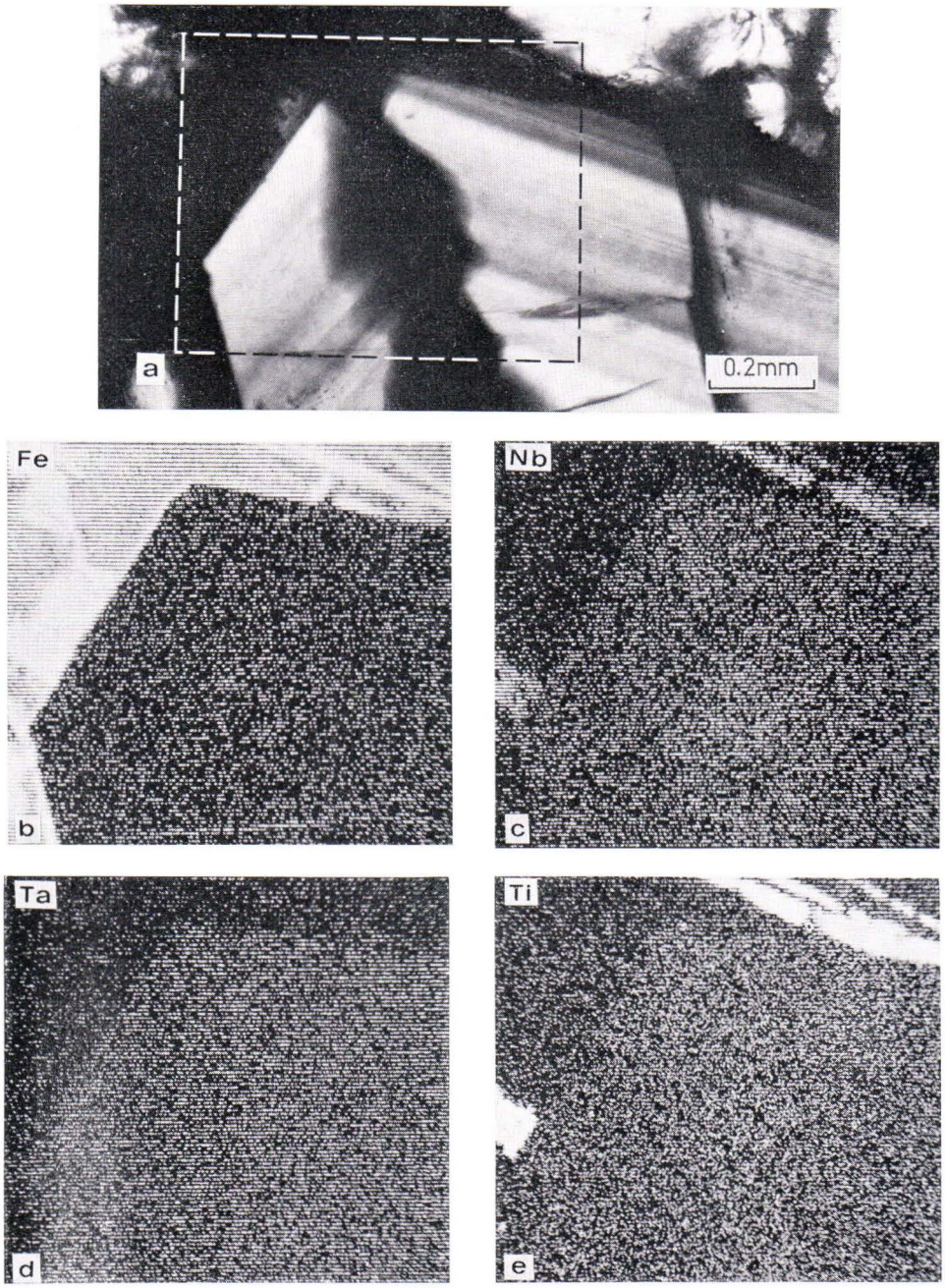

Fig. 93. Photomicrograph (transmitted light, one nicol) of a zoned cassiterite grain from a greisen vein in the Tarkki granite (*a*), and electron-probe scanning pictures showing distribution of Fe, Nb, Ta and Ti (*b*—*e*) in the area indicated in figure *a*. The mineral rich in Ti and Nb is niobian rutile. Sample 108 C/1H/67.

Electron-probe scanning pictures showed that the distributions of the elements were relatively homogeneous in most of the samples studies, but some of the cassiterite grains from granite and, especially, those from pegmatite were notable inhomogeneous (Fig. 92). The inhomogeneity of element distributions was not always related to the color banding visible under the microscope. The cassiterite of the greisen bodies did not show marked compositional zoning for the elements analyzed, although the color zoning was conspicuous (Fig. 93).

The cassiterite samples were analyzed for Nb_2O_5, Ta_2O_5, FeO (total iron), MnO and TiO_2 using the electron microprobe. Also Zr, W and Sc were sought in most of the samples, but none was found. To diminish the effect of compositional inhomogeneities, four to seven analyses were made from different cassiterite grains and/or zones of each sample, after which the averages were calculated. The analyses (Table 9) must be regarded as only semiquantitative, and the actual mode of occurrence (homo-

Table 9

Semiquantitative electron microprobe analyses (corrected for the background error) of cassiterite from different types of occurrences in the Eurajoki area. Analyses by Tuula Paasivirta.

	Coarse-grained type of Väkkärä granite		Porphyritic type of Väkkärä granite								Pegmatite	
Field No.	I/IH/72		98/MK/67/ ER		301/PL/68		277/PL/68/ IH		10/PL/68/ IH		328A/IH/69	
Map x .	6 787.29		6 787.94		6 787.38		6 786.55		6 787.54		6 788.53	
coord. y .	535.04		537.79		534.92		534.83		535.00		536.75	
	Range	Mean	Range	Mean	Range	Mean	Range	Mean	Range	Mean	Range	Mean
Nb_2O_5 ..	2.8—4.9	3.9	3.3—5.8	4.9	2.6—3.6	3.1	2.5—3.5	3.0	1.9—3.7	2.8	2.0—3.1	2.7
Ta_2O_5 ...	0.5—3.5	2.5	2.5—3.1	2.9	0.8—5.5	2.7	1.8—2.6	2.4	0.9—2.4	2.0	0.2—0.5	0.3
FeO (tot. Fe)	1.2—2.0	1.7	1.9—2.7	2.4	1.2—2.1	1.6	1.6—2.2	1.8	1.2—1.7	1.4	1.2—1.5	1.4
MnO	0.0	0.0	0.0	0.0	0.0	0.0	0.0	0.0	0.0	0.0	0.0	0.0
TiO_2	0.3—0.6	0.4	0.3	0.3	0.0—0.1	0.1	0.1—0.3	0.3	0.1—0.2	0.2	0.5—0.6	0.6
Σ		8.5		10.5		7.5		7.5		6.4		5.0

	Pegmatite		Greisen in Tarkki granite						Greisen in Väkkärä granite			
Field No.	104/MK/67/ IH		8H/IH/67		105X/IH/67		108C/IH/67		DH 309/ 72.0 m		DH 310/ 121.0 m	
Map x .	6 788.60		6 786.08		6 787.25		6 787.25					
coord. y .	536.78		533.29		532.90		533.02					
	Range	Mean	Range	Mean	Range	Mean	Range	Mean	Range	Mean	Range	Mean
Nb_2O_5 ..	0.3—3.2	1.6	0.0—0.1	0.0	0.2—0.3	0.2	0.0—0.3	0.2	0.3—1.0	0.5	0.2—1.0	0.6
Ta_2O_5 ...	0.0—2.7	0.7	0.0—0.1	0.0	0.0—0.1	0.1	0.0	0.0	0.0	0.0	0.0	0.0
FeO (tot. Fe)	0.2—1.5	0.9	0.1—0.4	0.3	0.1	0.1	0.0—0.1	0.1	0.0—0.1	0.1	0.2—0.3	0.2
MnO	0.0	0.0	0.0	0.0	0.0	0.0	0.0	0.0	0.0	0.0	0.0	0.0
TiO_2	0.1—1.1	0.5	0.4—1.2	0.8	0.5—0.6	0.6	0.4—0.6	0.5	0.1—0.2	0.2	0.1	0.1
Σ		3.7		1.1		1.0		0.8		0.8		0.9

geneous mixture or very fine mechanical mixture) of the elements analyzed in the cassiterite is not known. However, the analyses show the compositional differences between granite cassiterite (Σ Nb_2O_5, Ta_2O_5, FeO and TiO_2 = 10.5—6.4 wt %), pegmatite cassiterite (Σ = 5.0 and 3.7 %) and greisen cassiterite (Σ = 1.1—0.8 %). The observed differences in chemical composition and other properties of the cassiterites from different types of occurrences indicate differences in the physicochemical conditions of their formation. Thus, in the Eurajoki area, cassiterite was not formed during one single process (e.g., greisenization) but crystallized in several different stages. If it is assumed that the Nb, Ta, Ti, etc., contents of cassiterite increase with increasing crystallization temperature (see Dudykina 1959, Dolomanova *et al.* 1969, Singh and Bean 1967), then it is obvious that the granite cassiterite (referring to the analyzed samples) crystallized at a slightly higher temperature than the pegmatite cassiterite and at a much higher temperature than the greisen cassiterite. Either the granite cassiterite studied is a primary constituent of the rock or it was formed at the beginning of autometasomatic alteration which preceded fracturing and the development of pegmatite and still later greisen veins.

GEOCHEMISTRY

Major elements

In connection with the studies carried out by the author, new total wet-chemical analyses were made from eight rock samples (weight 10—15 kg) representing the main granite types and one topaz-bearing quartz porphyry dike of the Eurajoki area. These analyses are presented in Table 10 together with the old analyses of the Tarkki granite, Väkkärä granite and normal Laitila rapakivi granite published by Laitakari (1928) from the Eurajoki area. Included in the table are also the Niggli values, Köhler-Raaz values and weight norms, as well as for the newly analyzed samples also the modes, specific gravities and magnetic susceptibilities. In calculating the norms, fluorine has been omitted because in many cases the atomic percentage of fluorine is more than twice that of calcium. Fluorite is the only fluorine-bearing mineral of the norms; however, in the Eurajoki granites fluorine occurs not only in fluorite but also in topaz and mica.

The chemical composition of the Tarkki granite is quite similar to that of tirilite (dark hornblende-bearing granite) and dark wiborgite of the Wiborg rapakivi massif (see analyses in Vorma 1971). Tarkki granite thus represents the most basic members of the Finnish rapakivi granites. Significant differences occur in the composition of the different types of Väkkärä granite, but they are all much more acidic than the Tarkki granite, corresponding roughly to the pyterlite—biotite rapakivi—porphyry aplite group of the Wiborg massif. Of the old analyses of the Laitila massif, those of the »rapakivi aplite» of Liesjärvi and »dotted granite» of Kodisjoki (Eskola 1928)

Table 10

Chemical composition, Niggli values, Köhler-Raaz values, weight norms, modes and accessory heavy minerals of the granites and a topaz-bearing quartz porphyry dike from the Eurajoki area.

Weight percentages

	1	2	3	4	5	6	7	8	9	10	11
SiO_2	65.87	64.96	73.02	74.20	75.32	74.60	74.40	74.63	74.57	73.59	68.79
TiO_2	0.79	0.85	0.31	0.36	0.17	0.07	0.07	0.06	0.03	0.02	0.38
Al_2O_3	13.61	14.26	12.95	12.48	12.27	13.08	13.25	13.82	14.26	15.04	14.44
Fe_2O_3	1.68	1.25	1.12	0.77	0.55	1.64	0.80	0.37	0.55	0.52	1.61
FeO	5.49	6.02	1.76	1.63	1.39	0.20	0.86	0.62	0.43	0.14	3.01
MnO	0.08	0.10	0.03	0.02	0.02	0.04	0.04	0.04	0.03	0.02	trace
MgO	0.75	0.54	0.38	0.15	0.04	0.01	0.01	0.01	0.03	0.00	0.49
CaO	1.98	2.45	0.80	1.08	0.97	0.99	1.14	0.68	0.60	0.38	1.33
BaO	0.16		0.06		0.01	0.02	0.01	0.00	0.00	0.03	
Li_2O	0.02		0.01		0.01	0.05	0.04	0.05	0.10	0.01	
Na_2O	2.43	2.80	2.47	2.32	2.55	2.92	2.68	3.72	3.72	4.80	2.95
K_2O	4.97	5.23	5.55	6.01	5.22	5.02	5.01	4.90	4.48	4.13	6.85
Rb_2O	0.020		0.038		0.051	0.107	0.094	0.119	0.092	0.078	
P_2O_5	0.30	0.05	0.17	0.02	0.07	0.10	0.10	0.01	0.01	0.11	trace
F	0.25		0.39		0.67	0.88	1.33	1.06	0.90	0.30	
CO_2	0.00		0.00		0.00	0.00	0.00	0.00	0.00	0.00	
H_2O+	1.26	1.20	1.00	0.65	0.63	0.47	0.64	0.38	0.51	0.57	} 0.50
H_2O-	0.10	0.13	0.14	0.22	0.07	0.03	0.08	0.06	0.07	0.09	}
	99.76	99.84	100.19	99.91	100.01	100.22	100.55	100.53	100.33	99.82	100.35
$-O = F_2$	0.11		0.16		0.28	0.37	0.65	0.45	0.38	0.13	
Σ	99.65		100.03		99.73	99.85	99.99	100.08	100.00	99.69	
Density (g/cm^3)	2.72		2.63		2.62	2.62	2.62	2.62	2.62	2.60	
Magn. suscept. (SI units)	172		16		8	10	11	7	9	8	

Niggli values

si	288	271	420	442	478	455	456	450	450	429.3	318
al	35.1	35.1	43.9	43.8	45.9	47.0	47.9	49.1	50.7	51.7	39.4
fm	30.8	28.7	16.7	13.0	10.5	8.85	8.40	5.10	5.09	3.06	20.6
c	9.6	11.0	5.1	6.90	6.62	6.52	7.51	4.39	3.87	2.44	6.6
alk	24.4	25.3	24.3	36.3	37.0	37.6	36.2	41.4	40.3	42.8	33.4
qz	90.9	70.2	183	197	230	205	211	184	188	158	84.4
mg	0.16	0.12	0.19	0.10	3.61	0.01	0.01	0.02	0.05	0.0	0.16
k	0.57	0.55	0.59	0.63	0.57	0.52	0.54	0.45	0.43	0.36	0.60
o	0.09	0.07	0.14	0.13	0.13	0.43	0.22	0.16	0.25	0.37	0.14
ti	2.60	2.67	1.34	1.61	0.81	0.32	0.32	0.27	0.14	0.09	1.32
p	0.56	0.09	0.41	0.05	0.19	0.26	0.26	0.03	0.03	0.27	0.0
f_2	1.73		3.55		6.72	8.49	12.9	10.1	8.58	2.77	
h	18.4	16.7	19.2	12.9	13.3	9.6	13.1	7.6	10.3	11.1	7.7

Köhler-Raaz values

qz	49.5	42.8	65.1	67.3	70.7	68.7	69.4	66.0	66.5	61.6	46.9
f	28.8	37.6	23.7	27.0	23.7	25.0	23.7	29.0	25.7	30.6	40.8
fm	21.7	19.5	11.2	5.7	5.6	6.3	6.9	5.1	7.8	7.8	12.3

Table 10, continued

Weight norms

	1	2	3	4	5	6	7	8	9	10	11
Q	24.29	18.93	34.50	34.40	37.48	35.72	36.39	31.60	32.95	29.07	20.35
or	29.80	30.91	33.10	35.51	31.18	30.91	30.63	30.24	28.61	24.82	40.48
ab	20.56	23.69	20.90	19.63	21.58	24.71	22.68	31.48	31.48	40.62	24.96
an	8.22	10.90	3.00	5.23	4.37	4.29	5.02	3.31	2.91	1.22	5.93
C	1.14	0.00	1.73	0.24	0.76	1.04	1.39	0.95	1.83	2.15	0.00
en	1.87	1.34	0.95	0.37	0.10	0.02	0.02	0.02	0.07	0.00	1.22
fs	7.54	8.80	1.85	1.80	1.85	0.00	0.88	0.81	0.34	0.00	3.57
wo	0.00	0.39	0.00	0.00	0.00	0.00	0.00	0.00	0.00	0.00	0.28
ap	0.71	0.12	0.40	0.05	0.17	0.24	0.24	0.02	0.02	0.26	
il	1.50	1.61	0.59	0.68	0.32	0.13	0.13	0.11	0.06	0.04	0.72
mt	2.44	1.81	1.62	1.12	0.80	0.57	1.16	0.54	0.80	0.46	2.33
zr	0.12		0.04		0.04	0.00	0.02	0.00	0.00	0.00	
hm	0.00	0.00	0.00	0.00	0.00	1.25	0.00	0.00	0.00	0.00	0.00
DI (Q + or + ab)	74.65	73.52	88.49	89.54	90.23	91.33	89.68	93.32	93.02	94.42	85.79

Table 10 continued on p. 100.

1. Tarkki granite. No. 85/IH/67 (x = 6 785.98, y = 534.18). Anal. P. Ojanperä (Haapala 1974)
2. Tarkki granite (x ~ 6 786.9, y ~ 533.4). Anal. E. Nordensvan (Laitakari 1928)
3. Väkkärä granite, contact type. No. 309/PL/68/IH (x = 6 790.71, y = 531.77). Anal. P. Ojanperä (Haapala 1974)
4. Väkkärä granite, even-grained type. (x = 6 789.3, y = 531.7). Anal. E. Nordensvan (Laitakari 1928)
5. Väkkärä granite, even-grained type. No. 17/PL/68/IH (x = 6 789.10, y = 535.00). Anal. P. Ojanperä (Haapala 1974)
6. Väkkärä granite, coarse-grained type. No. 1/IH/72 (x = 6 787.29, y = 535.04). Anal. P. Ojanperä (Haapala 1974)
7. Väkkärä granite, porphyritic type. No. 277/PL/68/IH (x = 6 785.55, y = 534.83). Anal. P. Ojanperä (Haapala 1974)
8. Väkkärä granite, porphyritic type. No. 98/MK/67/ER (x = 6 787.94, y = 537.79). Anal. P. Ojanperä
9. Väkkärä granite, porphyritic type (fine-grained, slightly porphyritic variety). No. 10/PL/68/IH (x = 6 787.54, y = 535.00). Anal. P. Ojanperä (Haapala 1974)
10. Quartz porphyry (topaz-bearing quartz keratofyre). No. 97B/IH/67 (x = 6 787.16, y = 532.68). Anal. P. Ojanperä
11. Normal rapakivi granite. (x ~ 6 787.3, y ~ 546.2). Anal. Naima Sahlbom (Laitakari 1928)

resemble the major element analyses of the Väkkärä granite, the most obvious difference being the higher fluorine content of the Väkkärä granite.

Within the Väkkärä granite formation, the contents of TiO_2, Fe_2O_3 + FeO and MgO decrease from the contact type to the porphyritic and coarse-grained (topaz-bearing) types. In the topaz-bearing types and in the quartz porphyry dike, the contents of the granitophobe elements mentioned are extremely low, and the fluorine content anomalously high, compared with normal rapakivi granites and the average contents of granitic rocks (see Turekian and Wedepohl 1961, Vinogradov 1962). They differ from normal rapakivi granites also in the combination of relatively high Al_2O_3 contents (13.08—13.26 wt-%) to high SiO_2 contents (74.40—74.63 wt-%). In the quartz porphyry dike analyzed, these characteristics are still more pronounced.

The Niggli values of the contact type and the even-grained type of Väkkärä granite are comparable with those of other acidic rapakivi granites with the same *si* values (Fig. 94), but the topaz-bearing types and the quartz porphyry show

Table 10, continued

Modes (vol. %)

	1	2	3	4	5	6	7	8	9	10	11
Quartz	22.7		31.1		33.0	36.7	39.9	37.3	33.0	see	
Alkali fs.	38.0		40.7		56.1	32.2	28.1	26.8	27.8	Table 4	
Plagioclase	20.3		18.3		7.3	24.5	18.0	28.8	28.4		
(An %)	(40—50)		(0—5)		(0—5)	(0—5)	(0—5)	(0—5)	(0—5)		
Hornblende	3.9		—		—	—	—	—	—		
Biotite	8.7		1.0		1.4	3.3	6.6	3.6	3.3		
Chlorite	3.8		6.1		0.6	—	1.6	—	0.7		
Fayal.+ iddings.	0.4		—		—	—	—	—	—		
Fluorite	0.5		1.2		1.4	1.5	3.6	1.2	3.9		
Topaz	—		—		trace	0.7	2.1	2.2	2.7		
Opaque	1.0		1.2		0.2	1.1	0.1	—	0.2		
Others	0.8		0.1		—	—	—	—	—		

Accessory heavy minerals

+++ abundant, ++ common, + sparse in heavy mineral fraction (Density > 3.1 g/cm³)

Iddingsite	+++										
Danalite	+										
Perrierite—chevkinite	+										
Apatite	+++		++							+	
Zircon	+++		++		++	+	+	++			
Ilmenite	+++				+				+		
Magnetite	+(+)		+		+		+				
Hematite						++	+		+		
Rutile								+			
Anatase			++		+(+)			+	+		
Cassiterite					+	+	++	++	++		
Columbite						+	+	+	+		
Monazite			+		+	+	++	++	++		
Xenotime			++			+			+		
Bastnaesite					+	+	++	+	++		
Thorite						+		+			
Pyrrhotite			+			+					
Pyrite			+					+		+	
Chalcopyrite					+	+					
Molybdenite					+			+			
Arsenopyrite					+						
Fluorite	++		++		++	++	++	++	++	++	
Topaz					++	+++	+++	+++	+++	+++	

anomalously high *al* values as well as unusually low *mg* and *fm* values. Two of the porphyritic Väkkärä granite samples (anal. Nos. 8 and 9) and the quartz porphyry show in addition anomalously low *k* and high *alk* values.

The Köhler-Raaz (1951) values of the Väkkärä granite fall within or at the border of the field determined by Sattran and Klominsky (1970) as the field of the »petrometallogenic Sn series».

The differentiation index of Thornton and Tuttle (1960) (DI = sum of normative albite, orthoclase and quartz) is for the Tarkki granite 73.5—74.7, for the normal

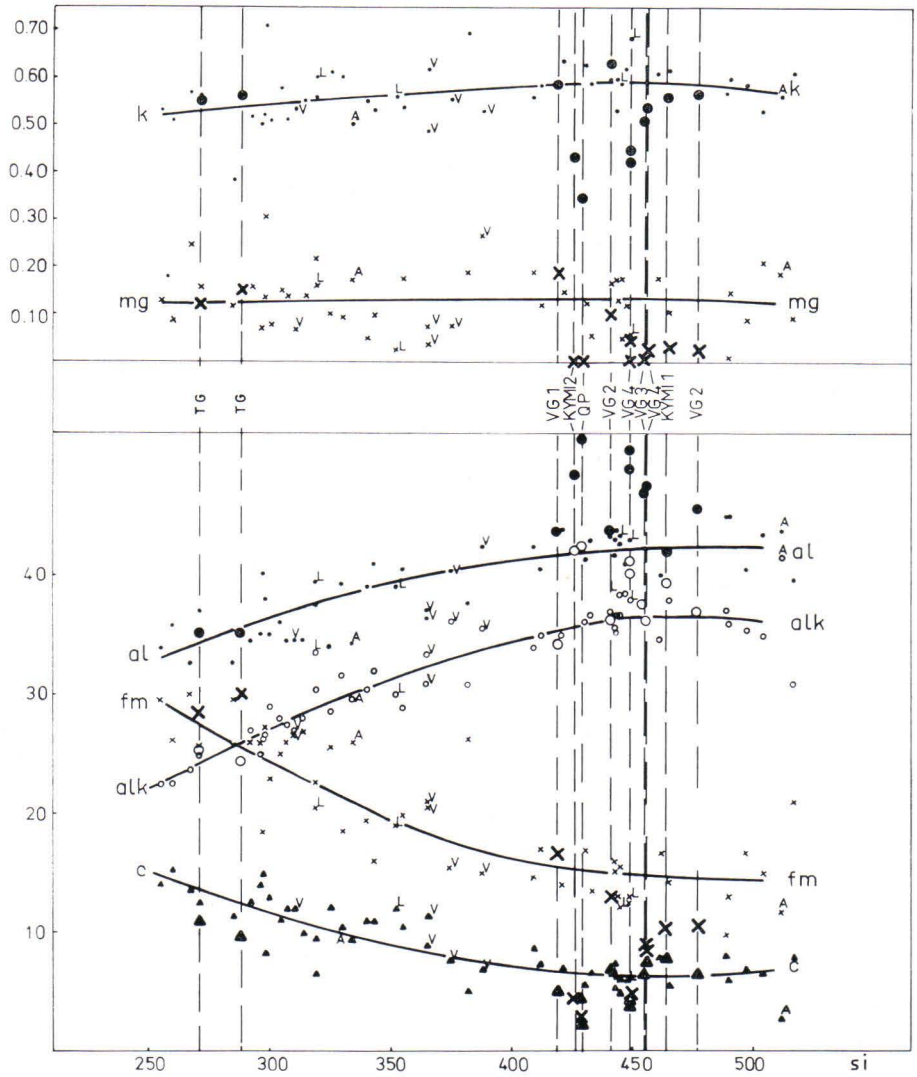

Fig. 94. Niggli diagram of the rapakivi granites of Finland. The approximating curves are based on the rapakivi analyses published by Sahama (1945), Savolahti (1965), Lehijärvi and Lonka (1964), Simonen and Vorma (1969) and Vorma (1971), excluding the tin-bearing granites of the Eurajoki and Kymi areas. The composition points of the different rapakivi massifs are indicated by small letters: L, Laitila massif; V, Vehmaa massif; A, Åland massif; composition points without any letters, Wiborg massif. The composition points of the Eurajoki granites are marked with large symbols. TG, Tarkki granite; VG, Väkkärä granite (VG 1, contact type; VG 2, even-grained type; VG 3, coarse-grained type; VG 4, porphyritic type); QP, topaz-bearing quartz porphyry dike. Kymi 1 and Kymi 2 represent granites of the Kymi cupola (Haapala 1974).

Laitila rapakivi granite 85.8 and for the Väkkärä granite 88.5—93.3, increasing from the contact type through the even-grained type to the average of topaz-bearing types. A normative albite—orthoclase—quartz diagram of the Väkkärä granite and the quartz porphyry dike is presented in Fig. 101 together with the H_2O-saturated ternary minima (Tuttle and Bowen 1958, Luth *et al.* 1964) and the minima of the An-bearing systems (James and Hamilton 1969). The analytic points of the Väkkärä granite fall near the ternary minima for systems with An 0—5 per cent and P_{H_2O} about 1 kb. The analyses of the Väkkärä granite and the quartz porphyry dike contain normative corundum (in the topaz-bearing Väkkärä granite 0.94—1.83 %, in the quartz porphyry 2.15 %). The excess of alumina is bound to topaz and mica. Oversaturation in alumina is a typical feature of subsolvus granites, and it is obviously related to the increased volatile content of the magmas (Luth *et. al.* 1964).

Trace elements

Methods

The trace elements Li, Be, Rb, Sr, Ba, Ga, Zr and Nb were analyzed for in 57 granite samples of the Eurajoki stock. The samples were taken from a typical granite, not close to any quartz or greisen veins. In addition, Sn and Be were determined from more than 500 other granite samples in different parts of the Eurajoki stock.

The elements Be, Ga and Sn were analyzed using an emission spectrograph (analysts: Ringa Danielsson, Anneli Savola, Arvo Löfgren, Ari Puisto), elements Rb, Sr, Ba, Zr and Nb with an X-ray fluorescence spectrograph (analysts: Maija-Leena Hagel, Väinö Hoffrén), and Li (and some Rb) with an atomic absorption spectrograph (analysts: Maria Hynönen, Risto Saikkonen). The contents of some of the elements were in many samples below the detection limits (Be 3 ppm, Sn 3—5 ppm, Sr, Zr, and Nb 30—40 ppm and Ba 110 ppm). The basic standard used for the Rb, Sr, Ba and Zr determinations was the USGS granite standard G-1. For Be and Ga, synthetic standards were prepared and compared with the international standard. The analytic points of rock standards W-1 (USGS, 16 ppm Ga) and DR-N (ANRT, France, 25 ppm Ga) fitted on the line drawn for the synthetic Ga standard. For Sn determinations, standard were prepared by mixing natural, analyzed samples. The reproducibility of the determinations was calculated for Be, Ga and Sn with the following result:

	mean (ppm)	coefficient of variation (%)	number of exposures
Be	7.3	10.1	14
Be	42.8	4.9	14
Ga	23.8	10.4	29
Ga	57.6	12.5	29
Sn	12.4	20.7	10
Sn	49.3	17.9	11

Trace-elements contents of the rocks

The results of the trace-element analyses of the different rocks of the rapakivi suite from the Eurajoki area are listed in Table 11. In calculating the averages, the following values were used for the contents below the limit of detection: Be 1.5, Sn 2.5, Sr, Zr and Nb 20 ppm and Ba 50 ppm. In addition to the means and medians, also standard deviations and coefficients of variation are listed for the analyses of the Tarkki granite and porphyritic Väkkärä granite. The linear and logarithmic correlation coefficients between Li, Ga, Rb, Sn and Zr of the Väkkärä granite are listed in Table 12.

The trace-element contents of the Tarkki granite show only slight variation, regardless of the fact that the samples are from different parts of the granite body, thus reflecting the general homogeneity of the rock. Only one Sn content is very high (sample 221/IH/68), and it is obviously related to the contamination from the numerous thin greisen veins occurring in the outcrop. The frequency distribution of the trace-element contents are presented in Fig. 95. Compared with the normal (ovoidal) Laitila rapakivi of the Eurajoki area, the Tarkki granite is characterized by lower Rb and higher Sr, Ba and Zr contents, which is in agreement with the more basic nature of the Tarkki granite. The Ba and Zr contents are also markedly higher than the averages of granitic rocks according to Turekian and Wedepohl (1961) and Vinogradov (1962). Also a relatively high Ga content appears to be typical of the Tarkki granite, as well as of the Finnish rapakivi granites in general.

In the Väkkärä granite, the trace-element contents vary widely, but systematically. There is some overlapping, but the average contents of Li, Ga, Rb and Sn increase, while the Sr, Ba and Zr contents decrease, following the probable order of development of the Väkkärä granite complex: contact type → even-grained type → porphyritic and coarse-grained (topaz-bearing) types. The trace-element contents of the contact type are nearly similar to the contents of the normal Laitila rapakivi granite of the Eurajoki area, and of the same order of magnitude as the averages of granitic rocks. The topaz-bearing types are geochemically highly specialized. Compared with the averages of the Ca-poor granites (Turekian and Wedepohl 1961), the concentration factors for the mean values in the porphyritic Väkkärä granite are: Sn 25—30, Li 6.2, Rb 5.0, Ga 3.9, Nb 2.6, Be ~ 1, Sr ~ 0.4, Zr ~ 0.4 and Ba ~ 0.1. The trace-element distributions indicate a more or less normal distribution for Li, Ga and Nb, and log normal for Zr and Sn (Fig. 96). In the coarse-grained type, the trace-element contents appear to be closely similar to those of the porphyritic type.

The quartz porphyry dikes show much the same geochemical characteristics as the topaz-bearing Väkkärä granite: anomalously high Ga, Sn and Rb contents and low Sr, (Ba) and Zr contents. The most marked difference is the distinctively lower Li contents and higher Ba contents of most of the quartz porphyry samples analyzed. The average Ga content is still slightly higher than in the topaz-bearing Väkkärä granite, which may be related to the high albite content of the rock. The dark porphyry

Table 11

Trace element contents (in ppm) of the granites porphyry dikes and greisen, of the Eurajoki area. Emission spectrographic analyses (Be, Ga, Sn) by Ringa Danielsson, Anneli Savola and Arvo Löfgren, X-ray fluorescence analyses (Rb, Sr, Ba, Zr, Nb and high Sn values) by Väinö Hoffrén and Maija-Leena Hagel, atomic adsorption spectrographic analyses (Li and part of Rb determinations) by Risto Saikkonen and Marja Hynönen.

Sample	x	y	Be	Li	Ga	Sn	Rb	Sr	Ba	Zr	Nb
Normal (ovoidal) Laitila rapakivi granite											
161/MK/67	6 789.16	539.65	5	19	35	10	360	80	600	330	< 40
8/RS/68	6 790.85	539.52	< 3	28	36	< 5	350	60	800	280	< 40
463/PL/69	6 792.38	539.70	4	37	44	< 5	360	80	500	330	< 40
628/PM/69	6 792.95	539.83	< 3	23	30	< 5	410	70	500	250	< 40
Mean				27	36		370	73	600	300	
Median				26	36	< 5	360	75	550	310	< 40
Fine-grained equigranular granite from the Vuojoki station											
4/IH/75	6 786.72	539.82	6	12	35	10	530	30	200	210	< 40
Tarkki granite											
8/IH/67	6 786.10	533 30	< 3	25	40	< 5	210	180	2 000	500	< 40
*85/IH/67	6 785.98	534.18	8	38	28	< 5	180	210	1 600	610	< 40
107/IH/67	6 787.25	532.98	< 3	39	31	6	230	180	1 900	470	< 40
18/IH/67	6 787.30	532.75	< 3	39	30	< 5	240	150	1 900	460	< 40
166/IH/67	6 787.96	532.31	< 3	37	25	8	240	160	1 700	440	< 40
204/IH/67	6 789.98	539.05	< 3	31	41	5	240	220	2 000	480	< 40
221/IH/68	6 790.05	538.28	< 3	27	29	36	310	150	1 400	460	< 40
256/IH/68	6 790.95	538.56	< 3	40	42	5	140	170	1 300	450	< 40
260/IH/68	6 790.76	536.58	3	19	36	5	180	170	1 300	370	< 40
295/IH/68	6 790.60	536.63	< 3	31	28	< 5	240	200	1 700	410	< 40
314/IH/68	6 792.75	535.69	< 3	24	25	5	220	160	1 300	360	< 40
42/RS/68	6 792.75	534.50	< 3	24	33	6	230	190	1 400	400	< 40
50E/RS/68	6 793.43	533.40	< 3	32	35	5	190	180	1 900	480	40
38/PL/68	6 790.36	532.17	< 3	31	41	5	180	170	1 200	400	< 40
104/PL/68	6 791.26	531.23	< 3	33	27	5	220	190	1 700	470	< 40
184/PL/68	6 791.44	533.56	< 3	27	27	6	280	130	1 200	350	< 40
206/PL/68	6 789.85	531.27	4	20	32	< 5	200	170	1 700	480	< 40
502/PL/69	6 793.38	537.30	< 3	23	34	< 5	170	180	1 800	510	< 40
624/PL/69	6 792.37	538.51	< 3	24	26	< 5	190	190	1 800	450	< 40
Mean				30	32	6	215	176	1 621	450	
Median			< 3	31	31	5	220	180	1 700	460	< 40
Standard deviation				6.7	5.7	7.4	40.2	21.7	276.0	60.8	
Coeff. of variation				0.23	0.18	1.24	0.19	0.12	0.17	0.14	
Standard error of the mean				1.5	1.3	1.7	9.2	5.1	63.3	14.1	
Väkkärä granite, contact type											
310/PL/68	6 790.63	531.83	< 3	32	33	5	290	90	700	260	< 40
313A/PL/68	6 790.70	531.72	4	33	29	< 5	300	60	900	240	< 40
314/PL/68	6 790.57	531.73	< 3	33	29	7	320	80	700	220	< 40
369/PL/68	6 790.71	531.99	< 3	20	24	5	380	110	500	190	< 40
370/PL/68	6 790.63	531.89	< 3	33	29	5	350	80	600	200	< 40
*309/PL/68/IH	6 790.71	531.77	< 3	25	21	< 5	350	100	540	200	< 40
1/IH/74	6 790.70	531.79	< 3	20	18	< 5	290	90	500	200	< 40
Mean				28	26	4.2	326	87	634	216	
Median			< 3	32	29	5	320	90	600	200	< 40

Table 11, continued

Sample	x	y	Be	Li	Ga	Sn	Rb	Sr	Ba	Zr	Nb
Väkkärä granite, even-grained type											
208C/IH/67	6 789.27	531.71	< 3	25	28	11	370	40	100	150	< 40
209/IH/67	6 789.10	531.85	< 3	30	29	16	370	50	200	270	< 40
634/PL/69	6 789.29	531.79	< 3	20	20	46	390	70	200	210	< 40
17/PL/68	6 789.00	535.00	7	70	34	12	480	< 40	200	250	< 40
*17/PL/68/IH	6 789.10	535.01	3	60	35	13	470	20	100	220	< 40
393/PL/68	6 789.28	534.80	8	70	27	11	540	< 40	100	190	< 40
Mean			3.4	46	29	18	440	37	150	220	
Median			2.3	45	28.5	12.5	430	30	150	215	< 40
Väkkärä granite, porphyritic type											
13/MK/67	6 791.42	535.61	6	47	44	20	670	< 40	< 100	120	80
38/MK/67	6 791.50	536.92	< 3	60	78	19	700	< 40	< 100	60	< 40
72/MK/67/IH	6 787.12	536.45	42	240	63	35	770	< 40	< 100	90	< 40
77/MK/67/IH	6 787.17	535.60	< 3	280	62	84	860	< 40	< 100	50	60
79/MK/67/IH	6 787.57	537.13	< 3	130	60	14	610	< 40	< 100	90	60
80A/MK/67/IH	6 787.50	537.12	< 3	190	38	31	670	< 40	< 100	140	100
80B/MK/67/IH	6 787.53	537.14	6	120	56	26	590	< 40	< 100	120	60
81/MK/67/IH	6 787.45	536.92	< 3	180	76	120	750	< 40	< 100	50	< 40
82/MK/67/IH	6 787.46	537.01	< 3	160	64	28	640	< 40	< 100	110	60
85/MK/67/IH	6 788.23	538.06	< 3	350	67	100	1 230	< 40	< 100	50	60
86/MK/67/IH	6 788.10	537.95	< 3	300	71	56	870	< 40	< 100	50	60
88/MK/67/IH	6 787.66	538.30	< 3	290	67	110	1 100	< 40	< 100	40	60
89/MK/67/IH	6 787.64	538.19	< 3	360	49	130	1 130	< 40	< 100	40	< 40
92/MK/67/IH	6 787.80	538.13	4	300	64	56	1 130	< 40	100	< 40	60
98/MK/67/IH	6 787.90	537.81	7	230	81	76	800	< 40	< 100	50	60
99/MK/67/IH	6 787.84	537.88	< 3	590	91	240	1 250	< 40	< 100	< 40	< 40
100/MK/67/IH	6 787.84	537.96	< 3	300	64	120	950	< 40	< 100	< 40	70
109/MK/67/IH	6 788.50	536.62	< 3	90	51	38	640	< 40	100	150	60
2/IH/72	6 787.30	535.05	< 3	350	78	160	890	< 40	< 100	40	70
3/IH/72	6 787.26	535.18	< 3	370	78	130	880	< 40	< 100	40	60
644/PL/69	6 789.47	537.29	16	160	50	120	730	< 40	< 100	150	80
*10/PL/68/IH	6 787.54	535.00	3	480	100	100	840	< 40	< 100	< 40	70
277A/PL/68/IH	6 786.55	534.83	< 3	200	78	80	700	< 40	< 100	110	40
*277/PL/68/IH	6 786.55	434.83	< 3	160	64	140	860	< 40	100	80	60
385/PL/68/IH	6 786.89	534.64	< 3	200	56	70	750	< 40	< 100	70	60
*98/MK/67/ER	6 787.94	537.79	5	240	75	36	1 090	< 40	< 100	< 40	50
389/PL/68/IH	6 788.03	534.82	< 3	290	80	150	950	< 40	< 100	50	60
390/PL/68/IH	6 787.95	534.70	< 3	230	68	50	880	< 40	< 100	60	< 40
Mean				246	67	84	855			68	54
Median			< 3	230	66	78	850	< 40	< 100	50	60
Standard deviation				121.6	14.0	54.2	189.7			41.0	21.8
Coeff. of variation				0.49	0.21	0.65	0.22			0.60	0.41
Standard error of the mean				23.0	2.6	10.2	35.8			7.8	4.1
Väkkärä granite, coarse-grained type											
*1/IH/72	6 787.29	535.04	5	210	82	30	1 070	< 40	200	60	60
1A/IH/72	6 787.29	535.04	< 3	280	54	130	880	< 40	< 100	90	70
4/IH/72	6 786.72	539.82	< 3	220	54	64	750	< 40	< 100	100	60
Mean				237	63	75	900			83	63
Median			< 3	210	54	64	880	< 40	< 100	90	60

Table 11, continued

Sample	x	y	Be	Li	Ga	Sn	Rb	Sr	Ba	Zr	Nb
					Quartz porphyry dikes						
85B/IH/67 (dike QP I)	6 786.00	534.15	6	380	51	35	1 160	50	300	230	60
*97B/IH/67 (dike QP II)	6 787.16	532.68	< 3	130	120	100	710	10	300	24	80
228A/IH/68 (dike QP IV chilled margin) ..	6 789.88	538.15	< 3	22	100	82	790	30	200	< 40	60
228B/IH/68 (dike QP IV, central part)	6 789.88	538.15	< 3	19	83	24	800	< 40	< 100	50	40
229A/IH/68 (dike QP V,chilled margin, 0—5 cm from the contact)	6 789.97	538.04	< 3	13	100	125	640	30	200	40	60
229B/IH/68 (dike QP V, 5—10 cm from the contact)	6 789.97	538.04	< 3	21	71	31	840	< 40	100	50	< 40
229C/IH/68 (dike QP V, central part)	6 789.97	538.04	11	11	38	12	410	< 40	200	150	< 40
231A/IH/68 (dike QP III)....	6 790.13	539.06	14	19	78	25	600	40	300	90	40
243/IH/68 (dike QP V)	6 790.90	538.31	< 3	10	63	41	500	100	500	50	40
Mean				69	78	53	717	36	239	78	47
Median			< 3	19	78	35	710	30	200	50	40
					Dark porphyry dikes						
269/IH/68 (dike DP I)	6 791.55	536.16	6	49	59	< 5	460	300	2 100	720	< 40
271/IH/68 (dike DP II)	6 791.62	536.04	5	35	54	< 5	210	320	1 300	630	< 40
1A/IH/75 (dike DP III, endocontact zone)	6 789.97	536.00	3	44	56	37	170	330	1 200	690	< 40
1C/IH/75 (dike DP III, central part)	6 789.97	536.00	6	51	55	< 5	170	320	1 300	650	< 40
2/IH/75(dike DP III, central part, with big K-feldspar megacrysts	6 790.03	535.92	6	75	45	6	320	280	1 400	560	< 40
Mean			5.2	51	54	~10	266	310	1 460	650	
Median			6	49	55	< 5	210	320	1 300	650	< 40
					Greisenized Väkkärä granite (porphyritic type)						
B30/PL/68	6 787.45	534.80	< 3	720	85	190	1 100	< 40	< 100	< 40	50
B34/PL/68	6 787.28	535.04	10	300	120	620	1 160	30	< 100	< 40	60
304/PL/68	6 788.08	534.55	< 3	370	90	130	800	< 40	< 100	60	50
376/PL/68	6 787.55	534.34	< 3	100	130	140	810	30	< 100	40	50
385/PL/68	6 786.86	534.60	8	110	100	50	720	< 40	< 100	70	60
Mean				320	105	226	918	24		42	54
Median			< 3	300	100	140	810	< 40	< 100	40	50

Table 11, continued

Sample	x	y	Be	Li	Ga	Sn	Rb	Sr	Ba	Zr	Nb
Greisen in Väkkärä granite											
B23/PL/68	6 788.15	534.55	4	300	95	240	1 210	100	< 100	30	40
B32/PL/68	6 787.32	535.07	24	200	125	520	1 360	< 40	< 100	< 40	30
B38/PL/68	6 787.25	535.09	5	300	90	660	1 420	< 40	< 100	< 40	30
B39/PL/68	6 787.25	535.09	5	100	90	280	1 220	< 40	< 100	< 40	30
283/PL/68/IH	6 786.51	534.59	1 400	1 000	90	77	1 830	50	< 100	74	50
Mean			288	380	98	355	1 408				30
Median			5	300	90	280	1 360	< 40	< 100	< 40	30
Average contents of Ca-poor granites (Turekian and Wedepohl 1961)											
			3	40	17	3	170	100	840	175	21
Average contents of felsic rocks (Vinogradov 1962)											
			5.5	40	19	3	200	300	830	200	20

* Wet-chemical analysis in Table 10

Table 12

Coefficients of correlation between Li, Ga, Sn, Rb and Zr in the Väkkärä granite, based on 44 analyses. Linear correlation coefficients above and logarithmic ones below

	Li	Ga	Sn	Rb	Zr
Li	1 1				
Ga	0.797 0.885	1 1			
Sn	0.821 0.861	0.648 0.783	1 1		
Rb	0.865 0.928	0.791 0.861	0.727 0.865	1 1	
Zr	—0.821 —0.832	—0.868 —0.816	—0.667 —0.733	—0.889 —0.863	1 1

dikes differ in their trace-element geochemistry from all the other rocks of the Eurajoki area. The distribution of the elements appears also be more irregular than in the Väkkärä granite.

The trace-element contents of the greisenized Väkkärä granite and greisen have not been studied systematically, but the available data indicate that they are enriched in Sn, Rb and Ga in relation to the unaltered granite. The increase in Rb and Ga is obviously related to the development of secondary mica. The exploration work has shown that the contents of Be, Sn and other ore elements vary in very wide limits.

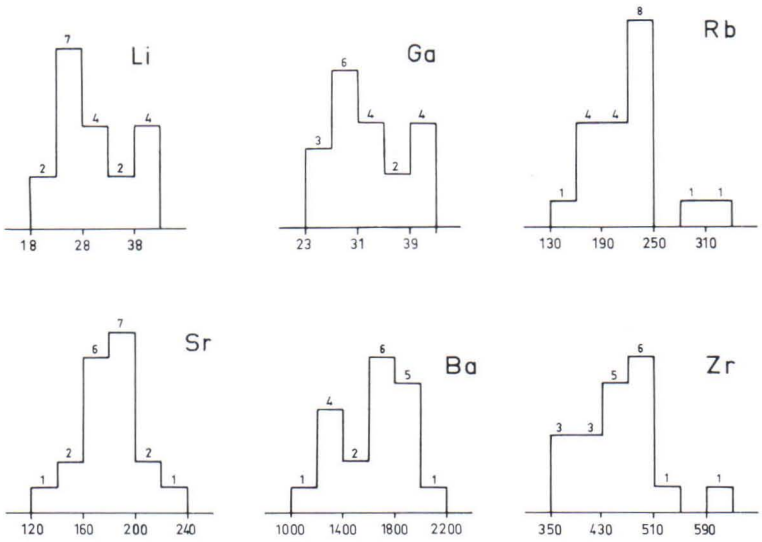

Fig. 95. Frequency histogram of the trace elements Li, Ga, Rb, Sr, Ba and Zr in the Tarkki granite. Contents in ppm.

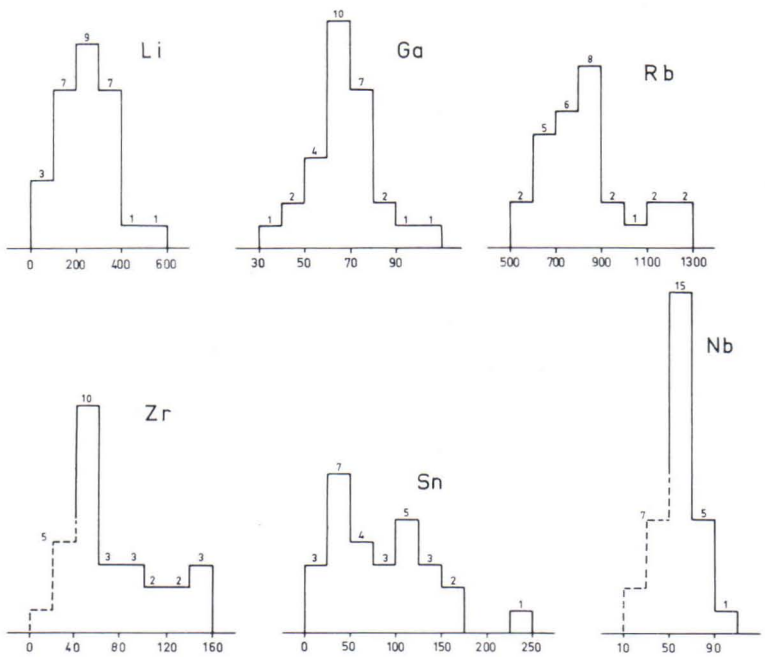

Fig. 96. Frequency histogram of Li, Ga, Rb, Zr, Sn and Nb in the porphyritic type of the Väkkärä granite. Contents in ppm. In the diagrams for Zr and Nb the parts below the limits of detection are hypothetical and marked with broken line.

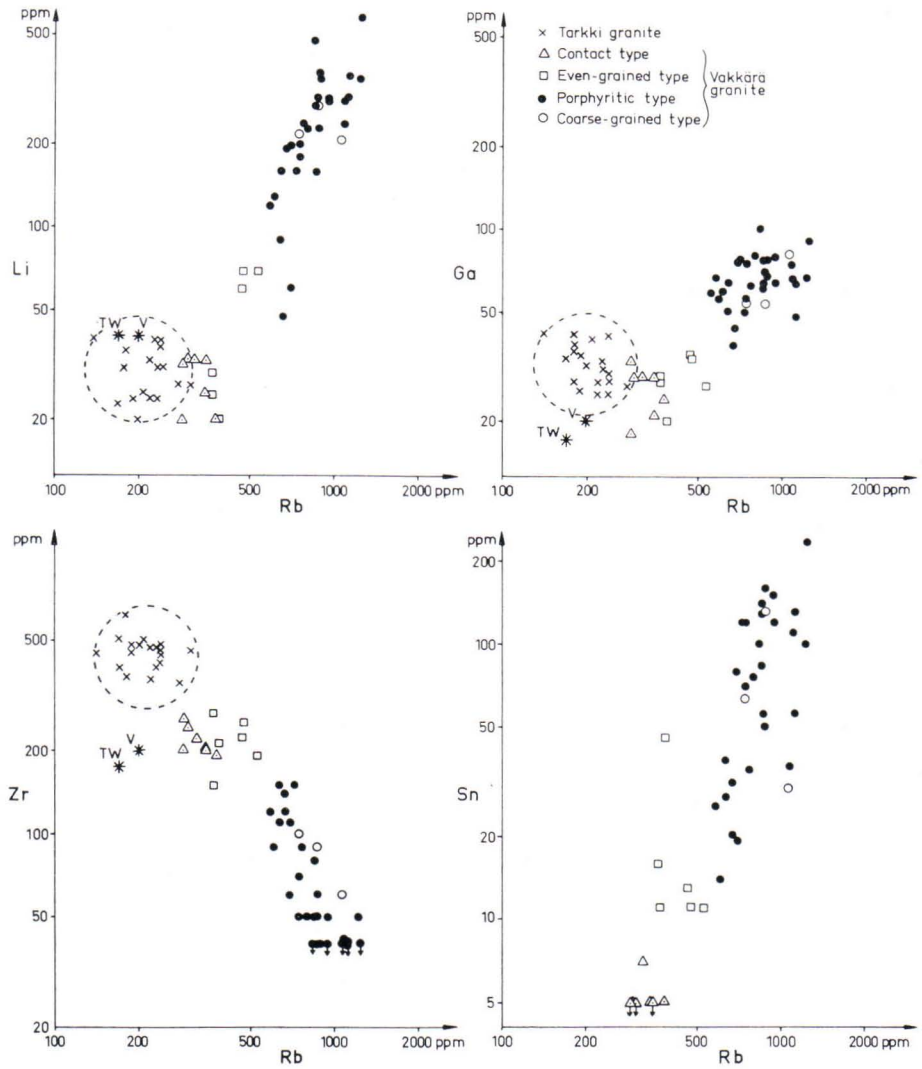

Fig. 97. Relations Li—Rb, Ga—Rb, Zr—Rb and Sn—Rb in the main granite types of the Eurajoki stock.

The relationships between element pairs Li—Rb, Ga—Rb, Zr—Rb and Sn—Rb in the granites of the Eurajoki stock are presented graphically in Fig. 97 (logarithmic scale). In the diagrams, the Tarkki granite has its own field, without any marked internal differentiation. The diagrams also illustrate the systematic change of the trace elements of the Väkkärä granite formation (contact type → even-grained type → topaz-bearing types) and the clear positive or negative correlation between the elements (see also Table 12).

The wt-ratios K/Rb and (Al + Fe^{3+})/10 Ga are for the wet-chemically analyzed samples as follow: contact type 132 and 364, even-grained type 92 and 197, topaz-bearing types 48—37 and 118—98 and topaz-bearing quartz porphyry 48 and 69, respectively. These ratios as well as the trace-element distributions in general indicate extreme fractionation and possibly autometasomatism for the topaz-bearing Väkkärä granite and quartz porphyry (see Taylor 1965, Bowden 1964). Although the contents of Ba, Sr and Zr commonly increase during magmatic differentiation from gabbroic to intermediate and granitic rocks, depletion of these elements characterizes many highly fractionated granites, rhyolites and pegmatites (e.g., Tischendorf *et al.* 1969, Noble *et al.* 1972, Tauson and Kozlov 1972, Madel 1975).

Be and Sn were analyzed from practically all the granite outcrops of the Eurajoki stock; from some large outcrops, two or more samples were analyzed. The results have been presented as maps by Haapala (1973) and are reproduced here with some additional observations. Most of the analytic points are based on single determinations, but some represent averages of several analyzed samples (Figs. 98 and 99). Owing to the uneven distribution of the outcrops, the points analyzed do not form any regular network. In the Tarkki granite, the Sn content is usually less than 10 ppm and the Be content less than 3 ppm, though some much higher contents do occur (see especially the Be map, Fig. 99). Obviously, such anomalous contents are related to the contaminating action of the postmagmatic fluids, which is not always detectable in the field to the naked eye. In the topaz-bearing Väkkärä granite, the tin content is continuously anomalous, usually between 20 and 130 ppm. Also high Be contents occur, but they show no correlation to the Sn contents. The correlation coefficient between Sn and Be in the Väkkärä granite formation (based on 156 analyses) is only about 0.04. Probably the concentration of Be was controlled by late metasomatic processes more than the concentration of Sn. Conspicuously anomalous Be values were found in the Väkkärä granite outcrops 2—3 km west of the Eurajoki church (Fig. 99). In the immediate vicinity of this anomaly (metasomatic halo), a greisen stockwork containing Sn and Be (bertrandite) mineralization was found by deep drillings, although no such veins were visible in the outcrops. Attempts to clarify the carrier of Be in the anomalous granite were not succesful. In the heavy liquid separation treatment, the high Be content followed the albite and microcline fractions.

Composite granite massifs with trace element trends analogous to those of the Eurajoki stock have been described from several areas (e.g., Bowden 1964, Hall 1967, Madel 1975). Such extreme values as in the topaz-bearing Väkkärä granite are typical of the tin-bearing younger granites of Erzgebirge-Krusne hory (Lange *et al.* 1972, Klominsky and Absalonova 1974) and obviously of tin-bearing granites in general. Among the rapakivi granites of the Baltic Shield, other such late-stage granites associated with Sn and related mineralizations have been described from Kymi in Finland (Haapala and Ojanperä 1972, Haapala 1974) and from Pitkäranta in Soviet Karelia (Khazov 1973, Rub *et al.* 1974).

Partition of Ga, Be and Sn between the minerals

Because the topaz-bearing Väkkärä granite showed anomalously high contents of certain trace elements, efforts were made to determine the partition of Ga, Be and Sn between different minerals. For this purpose, the main minerals were separated from one sample of the Tarkki granite and from four samples of the topaz-bearing Väkkärä granite. From two of these samples (85/IH/67 and 1/IH/72), it was not possible to obtain plagioclase pure enough for chemical determinations. The determinations were made with an optical spectrometer by the same analysts as in the case of the whole rock analyses.

The analyses (Table 13) show clearly that Ga is contained essentially in plagioclase (albite), K-feldspar and mica, and that the high contents of Ga in the rock (topaz-bearing Väkkärä granite contra Tarkki granite) are due to the high contents in these minerals. In the topaz and the quartz, the Ga content is below the limit of detection. In the K-feldspar, the Ga content is nearly the same as in the rock as a whole. In the topaz-bearing Väkkärä granite, the Ga-content of the albite (average 137 ppm) is 1.7—1.9 times higher than of the K-feldspar (average 78 ppm). The highest contents occur in biotite (average 575 ppm), but even so 40—50 % of the Ga is contained in albite.

The Be content of dark mica in the samples of Väkkärä granite is 10—18 ppm. In the sample with an anomalously high Be content (301/PL/68), the Be probably forms a separate mineral species, which in heavy liquid separation follows the feldspar (especially albite) and quartz fractions. The Be mineral might be beryl, since the specific gravity of alkali-poor beryl (2.65) is in the same range as that of feldspars and quartz.

Sn is included in the Tarkki granite essentially in the biotite and hornblende. In the topaz-bearing Väkkärä granite, the dark mica contains only 20—60 per cent of the total tin; the other main tin carrier is cassiterite.

Separate Rb determinations of K-feldspar from samples 85/IH/67, 98/MK/67/ER, I/IH/72 and 301/PL/68 gave the results of 320, 1 660, 1 650 and 1 580 ppm, respectively. Thus, the high Ga contents are accompanied by high Rb contents in alkali feldspar.

The Ga and Rb contents of the feldspars and mica of the topaz-bearing Väkkärä granite are unusually high. The Ga contents and the Ga/Al ratios of the rocks and minerals are typically nearly constant or show a slight increase during magmatic differentiation within single basic-acidic magmatic complexes (Nockolds and Mitchell 1948, Nockolds and Allen 1954, Borisenok and Saukov 1960, Burton and Culkin 1972). A marked enrichment of Ga is observed, however, in some extremely fractionated granitic rocks and pegmatites (Bowden 1964, Lange *et. al.* 1974, Smith 1974) as well as in granites superimposed by secondary alterations, especially albitization (Ganeev *et al.* 1961, Ganeyev and Sechina 1962, Vlasov 1968, Mishchenko *et al.* 1966, Klominsky and Absalonova 1974). In pegmatites, Ga contents up to 120 ppm

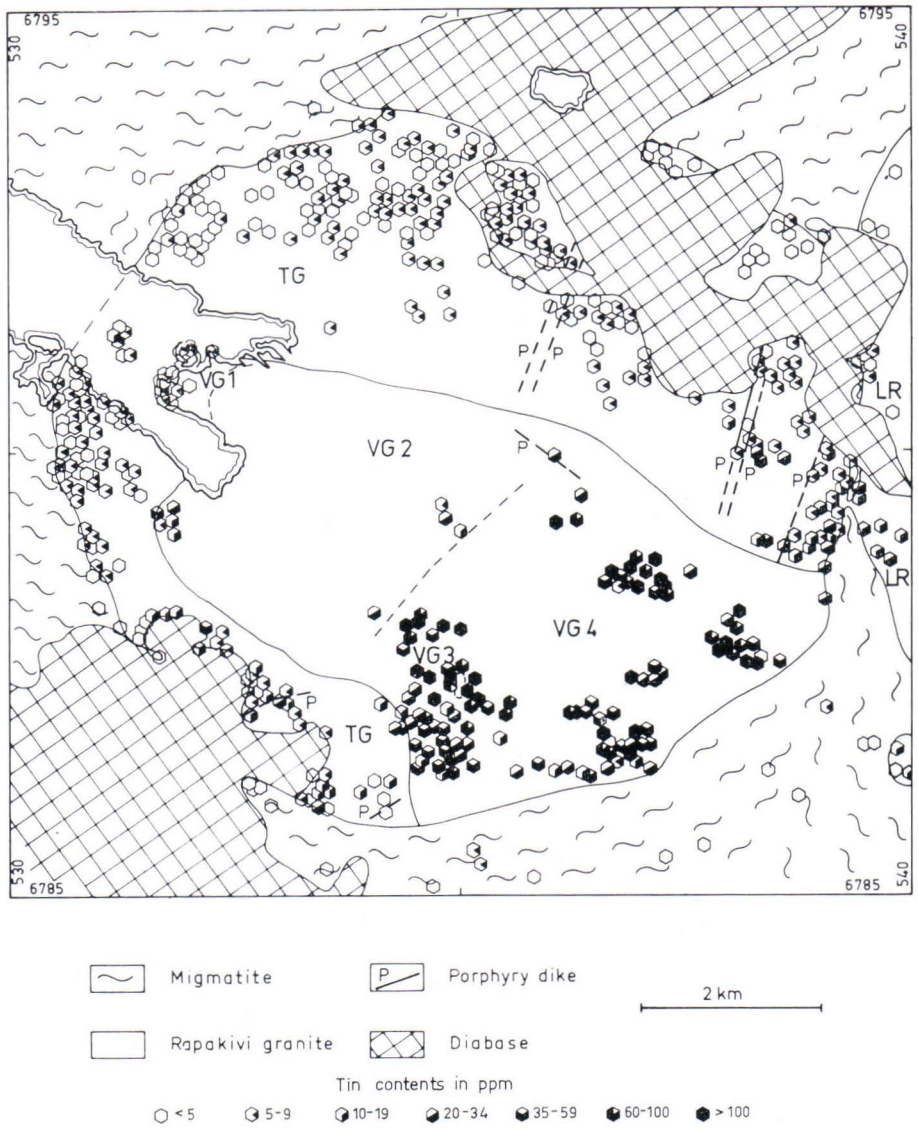

Fig. 98. Sn contents in the outcrops of the Eurajoki stock. LR, Laitila rapakivi granite; TG, Tarkki granite; VG, Väkkärä granite (VG 1, contact type; VG 2, even-grained type; VG 3, coarse-grained type; VG 4, porphyritic type).

in albite and 90 ppm in K-feldspar have been found (see Smith, *op. cit.*). In the granites (acidic members of the Ukrainan rapakivi granite series) studied by Mishchenko *et al.*, the Ga contents of the rock as a whole, the plagioclase and the microcline, were 56—65 ppm, 68—100 ppm and 50—80 ppm, respectively.

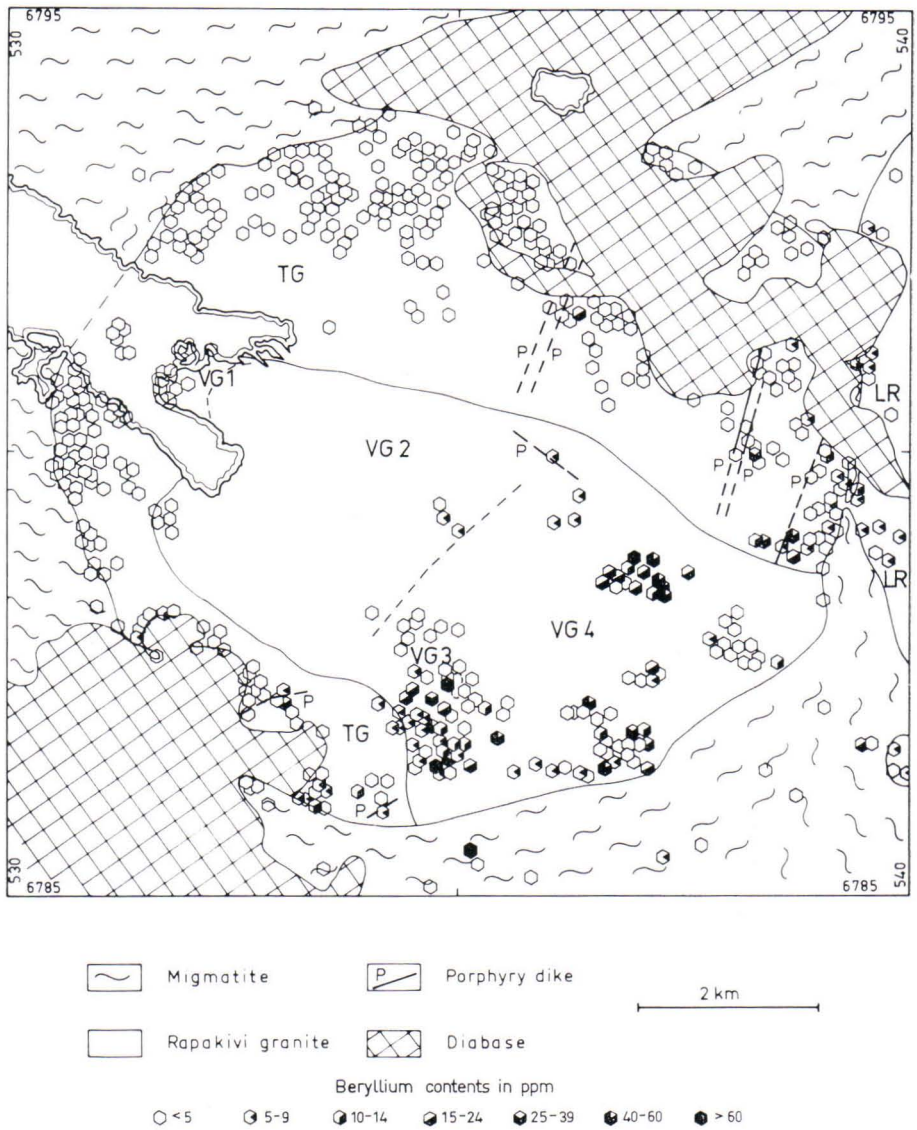

Fig. 99. Be contents in the outcrops of the Eurajoki stock. The granite symbols as in Fig. 98.

PETROLOGIC DISCUSSION

There are two contrasting main hypotheses concerning the origin of such »geochemically specialized» rare metal granites as the topaz-bearing Väkkärä granite, viz., the magmatic and the metasomatic hypothesis. The magmatic hypothesis contends that the granites are formed essentially by magmatic crystallization from extremely

Table 13

Distribution of Ga, Be and Sn between the minerals of the Tarkki and Väkkärä granites.

Mineral	Wt-% mineral	Ga (ppm)	Ga included in mineral	% total Ga in mineral	Be (ppm)	Sn (ppm)	% total Sn in biotite
Tarkki granite, sample 85/IH/67. Ga 28, Be 8, Sn < 5 ppm							
Plagioclase	19.7	n.a.			n.a.	n.a.	
K-feldspar	35.8	31	11	40	< 3	< 5	
Quartz	21.9	< 15			< 3	< 5	
Biotite	10.3	80	8	29		35	
Hornblende	4.8	60	3	10	25	19	
Porphyritic type of Väkkärä granite, sample 98/MK/67/ER. Ga 75, Be 5, Sn 36 ppm							
Albite	28.4	120	34	44	17		
K-feldspar	26.1	70	18	23	6	4	
Quartz	36.9	< 15			3	< 5	
Biotite	4.2	630	26	33	17	300	35
Topaz	2.9	< 15			3	(40)	
			78	100			
Porphyritic type of Väkkärä granite, sample 301/PL/68. Ga n.a., Be 97, Sn 68 ppm							
Albite	30.5	140	43	48	(60)	6	
K-feldspar	28.6	82	23	26	(45)	< 5	
Quartz	35.6	< 15			(20)	< 5	
Biotite	4.5	500	23	26	18	800	53
Topaz	2.8	< 15			6	< 5	
			89				
Porphyritic (fine-grained) type of Väkkärä granite, sample 10/PL/68/IH. Ga 100, Be 3, Sn 100 ppm							
Albite	27.6	150	41	41	5	18	
K-feldspar	26.7	78	21	21	< 3	11	
Quartz	32.4	< 15			< 3	4	
Biotite	3.8	520	20	20	11	600	23
Topaz	5.1	< 15			< 3	4	
			82				
Coarse-grained type of Väkkärä granite, sample 1/IH/72. Ga 82, Be 5, Sn 30 ppm							
Albite	24.0	n.a.			n.a.	n.a.	
K-feldspar	31.1	80	25	30	< 3	5	
Quartz	36.3	< 15			< 3	3	
Biotite	3.8	650	25	30	10	500	63
Topaz	0.8	n.a.			n.a.	n.a.	

n.a. not analyzed. The high contents in brackets were probably caused by impurities.

fractionated melts enriched in volatiles, especially fluorine (e.g., Rub 1972, Rub and Pavlova 1974, Tischendorf *et al.* 1969, 1972, Groves 1972, Kovalenko *et al.* 1970, Kovalenko 1974). According to the metasomatic hypothesis, the original granites were completely reworked by later fluids, thus giving them the mineralogical and geochemical characteristics of the tin-bearing and related granites, which are often called »apogranites» or »autometamorphosed granites» (e.g., Beus and Zalashkova 1962, Vlasov 1968, Fiala 1968, Štemprok 1967, 1971). Among those who accept the secondary origin, some think that the metasomatizing fluids are not in any mother-

daughter relation to the original granites but are from a deeper source (Štemprok 1967, 1971), whereas others take the view that the secondary alterations of the granites are caused by their own pore solutions. The recent findings of ongonite (topaz-bearing quartz keratofyre), a subvolcanic equivalent of lithium—fluorine granites with a rare-metal mineralization have given additional support to the possibility of a magmatic origin of lithium- and fluorine-rich granites (Kovalenko *et al.* 1971, 1974, 1975).

Application of experimental studies

The bulk compositions of specific granites are often compared, in terms of normative albite, (anorthite), orthoclase and quartz, with the results of experimental studies of the »granite system» (e.g., Tuttle and Bowen 1958, Luth *et al.* 1964, v. Platen 1965, Luth 1969, James and Hamilton 1969) to draw conclusions about the origin and development of the granites. The application of the simplified experimental studies is, however, often restricted by the complexity of the natural systems (e.g., the effects of volatiles) and by the lack of equilibrium in the rocks.

The composition of the Tarkki granite can obviously be compared best with the experimental studies of James and Hamilton (1969) of the system Ab—Or—An—Q with An 7.5 and 10 per cent and water vapor pressure 1 kb (Fig. 100). The stability fields may be changed to some degree by differences in P_{tot} and P_{H_2O} and by the fluorine content, but the composition points will evidently stay in the plagioclase field, as do the points of the tirilite of the Wiborg massif (see Vorma 1971). This is confirmed by the microscopic observation that plagioclase is normally euhedral against other major constituents of the Tarkki granite and thus has obviously crystallized earlier than these. Various textural data (the faint perthite texture and the relatively high thermal state of alkali feldspar, lack of cavities and rarity of pegmatites) suggest that the magma was not water-saturated. This is confirmed also by the occurrence of fluorine-poor biotite as anhedral flakes between feldspars and quartz (*cf.*, Maaløe and Wyllie 1975).

In Fig. 101 the compositional points of the Väkkärä granite and of the topaz-bearing quartz porphyry dike are plotted on an Ab—Or—Q diagram together with experimentally determined ternary minima and eutectics at H_2O-pressures 0.5—10 kb (Tuttle and Bowen 1958, Luth *et al.* 1964) and minima in An-bearing systems with An 5 and 3 per cent and $P_{tot} = P_{H_2O}$ 1 kb (James and Hamilton 1962). The composition points of the Väkkärä granite samples fall near the last-mentioned isobaric minima; only two of the analyzed samples of the porphyritic type scatter slightly towards the Ab corner in relation to the others. The composition point of the quartz porphyry dike is nearer the Ab corner, between the average compositions of ongonites from Mongolia (Kovalenko *et al.* 1971, 1974) and from Transbaikalia in the USSR (Kovalenko *et al.* 1975), which are also plotted in the diagram.

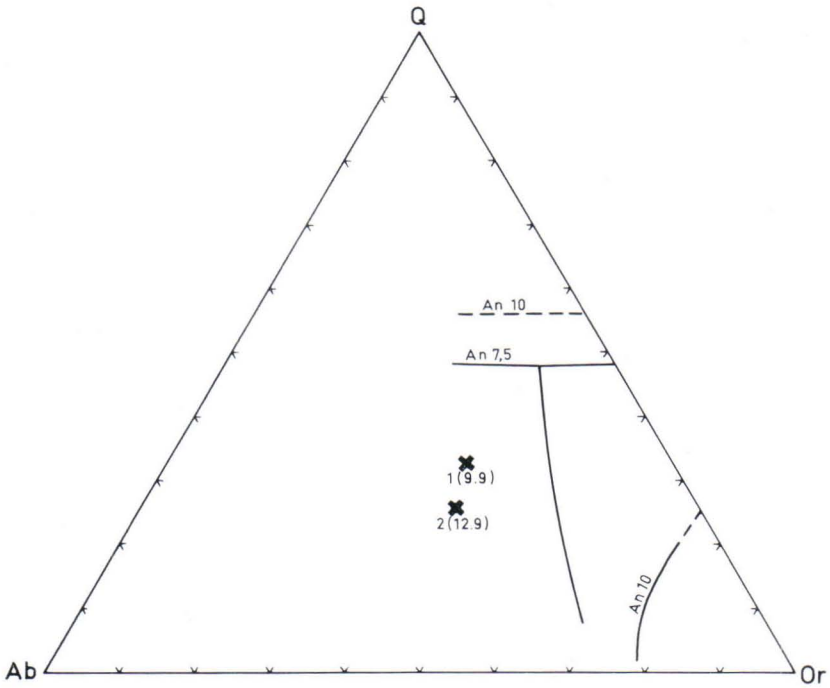

Fig. 100. Normative albite—orthoclase—quartz diagram of the Tarkki granite, compared with the experimental phase diagrams (under 1 kb water pressure) of James and Hamilton (1969). The numbers of the analytic points refer to Table 10; the numbers in brackets give the An content in the system Ab—Or—Q—An.

The abundant occurrence of miarolitic cavities in the porphyritic type of Väkkärä granite indicates the presence of a fluid (volatile) phase during late stages of crystallization (p. 40), and thus suggests that the residual magma was saturated with volatiles. According to Burnham and Jahns (1962), the solubility of water in a granitic (pegmatite) melt with 0.64—0.33 wt-% F is at 1 kb and 655°C about 4.2 wt-%.

Because the analyses of the Väkkärä granite and the quartz porphyry show unusually high contents of fluorine and microscopic observations suggest that the fluorine-bearing minerals (dark mica, topaz, fluorite) are in part primary constituents of the rock, it would be important to know and take into account the effect of fluorine upon the isobaric minima. There are several short studies on the effect of fluorine upon the crystallization of granitic magma (see Wyllie and Tuttle 1961, v. Platen 1965, Anfilogov *et al.* 1973, Kovalenko *et al.* 1974). Although the results of these studies differ notably from each other (obviously owing largely to the differences in the composition of the systems used in the experiments), they all demonstrate that a small addition of fluorine to granite—H_2O mixtures at constant pressures markedly lowers the crystallization temperature. The studies of Wyllie and Tuttle, v. Platen and Kovalenko *et al.* also show that the addition of fluorine shifts the isobaric minima

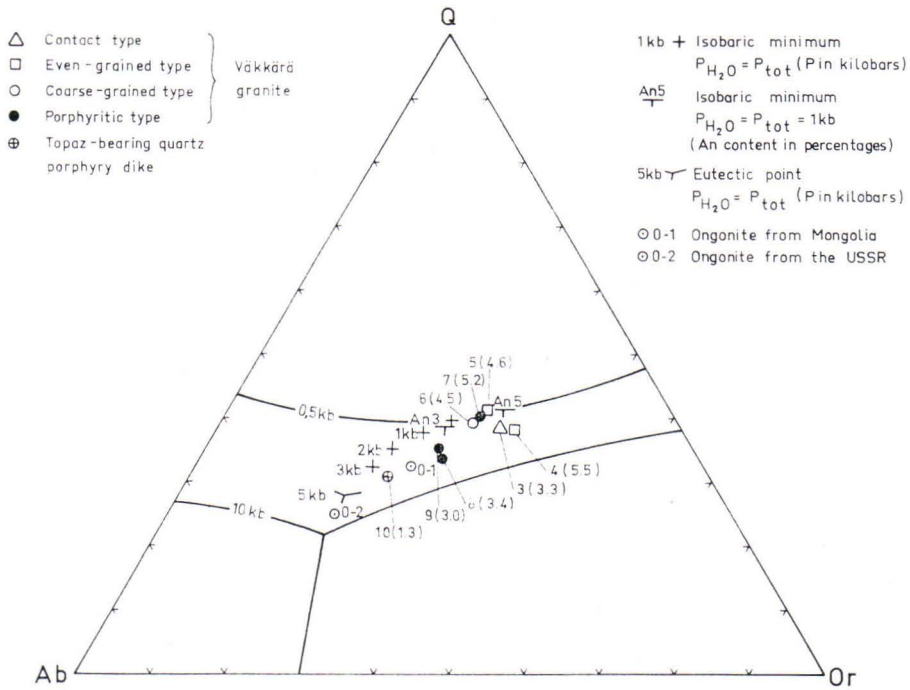

Fig. 101. Normative albite—orthoclase—quartz diagram of the different types of Väkkärä granite and of a topaz-bearing quartz porphyry dike from the Eurajoki area, compared with the experimentally determined ternary minima at water pressures of 0.5 to 10 kb (Tuttle and Bowen 1958, Luth *et al.* 1964) and minima in the An-bearing systems at 1 kb water pressure (James and Hamilton 1969). Field boundaries in the system $NaAlSi_3O_8$—$KAlSi_3O_8$—SiO_2—H_2O are shown at 0.5 and 10 kilobars. For comparison, also the average composition of ongonites from Mongolia (Kovalenko *et al.* 1971, 1974) and from Transbaikalia, USSR (Kovalenko *et al.* 1975) are marked on the diagram. The numbers of the analytic points refer to Table 10; the numbers in brackets give the An content in the system Ab—Or—Q—An.

away from the quartz corner, i.e., increases the stability field of quartz. According to v. Platen, the shift is towards the Or corner, according to Kovalenko *et al.* towards the Ab corner (the same effect as that of increasing water pressure). According to the experiments of v. Platen in the system obsidian $+H_2O$ (weight ratio obsidian: fluid 5: 1) at 2 kb pressure, the order of crystallization of the silicates was biotite—alkali feldspar—quartz—plagioclase and the crystallization ended at 675°C; the addition of 0.15 wt-% HF into the system changed the order of crystallization to quartz—plagioclase—biotite—alkali feldspar and lowered the end of crystallization to 640°C. In more acidic systems, biotite did not crystallize. The experiments of Kovalenko *et al.* (1974) show that albite, K-feldspar, quartz, topaz and mica can crystallize from an ongonite melt at fluid pressures of 0.5 and 1 kb. They suggested that . . . »the crystallization of the fluorine rich granite magma does not end at the point corresponding to the granite minimum, as in the system Ab—Or—Q—H_2O, but continues

until the residual melt acquires the composition of ongonite, that is the phase with the lowest crystallization temperature». The crystallization of a fluorine-rich ongonite melt ended at 575 $\pm$ 25° at 1 kb fluid pressure. Experiments with the microscopic heating stage showed that solidified primary melt inclusions in the topaz of the Mongolian ongonite began to melt already at 520° (Naumov *et al.* 1971). According to the petrological observations of Kovalenko (1973), the saturation concentration of fluorine depends on the composition of the magma, being inversely related to the SiO_2 content. In alaskitic magma with SiO_2 73—74 wt-%, it should not exceed 0.5 wt-%; in ongonite melts (SiO_2 about 70—72 wt-%), it may be up to 2—3.2 wt-%. The experiments of Anfilogov *et al.* (1973) with the system alaskite + NaF at P_{H_2O} 1 kb seem to show the saturation concentration of fluorine in an alaskite magma (SiO_2 76.84 wt-%) to be about 0.5 wt-%.

If the interpretations of Kovalenko (1973) and Kovalenko *et al.* (1974) are valid, then the scattering of the composition points of some of the topaz-bearing samples (samples 98/MK/67/ER and 10/PL/68/IH of the porphyritic type of Väkkärä granite, and the quartz porphyry sample) towards the Ab corner in relation to the other analyzed samples (Fig. 101) could be due to an increased fluorine content in the residual magma. Also the occurrence of quartz as euhedral megacrysts in these rocks (e.g., sample 98/MK/67/ER) could indicate an expanded stability field of quartz, and thus elevated fluorine contents, or the beginning of crystallization at considerably high water pressures. The occurrence of Li- and F-rich mica as a mineral of late crystallization in the topaz-bearing Väkkärä granite is in agreement with the assumed high fluorine content in the residual magma (see v. Platen 1965). On the other hand, the scattering of the composition points towards the Ab corner can also be explained as having been caused by increased water pressure, or by metasomatic albitization (see Štemprok 1971, Štemprok and Škvor 1974).

Application of microscopic observations

In discussions concerning the origin (magmatic or metasomatic) of the minerals and elements of granites, all conclusions should obviously be based largely on careful petrographic studies. The matter is complicated by the fact that the microscopic observations are commonly equivocal, and all replacement textures do not necessarily denote metasomatism (p. 52). However, any substantial secondary addition of an element should probably cause microscopic textures indicating the replacement of some mineral by another enriched in the element in question, or large-scale recrystallization, even if some ion-exchange reactions between fluid and crystals (isomorphic mixtures) can take place without producing such textures.

In the granites of the Eurajoki area, the replacement of biotite by chlorite and muscovite is the most common and easily observed type of alteration. Typically, the pseudomorphs so formed also contain iron oxide and anatase, which obviously are

alteration products of biotite and ilmenite. Thus the alteration of biotite does not necessarily change the Ti and Fe content of the granite. On the other hand, the chloritization of biotite denotes extraction of K from the mica structure and evidently also lowers the Sn and Li contents. These elements have been either redeposited in the same rock or transported away by the solutions that caused the alteration.

Sericitization of plagioclase increases the K contents of the aggregate, as has been verified by electron microprobe analyses utilizing a large beam diameter. The development of secondary Li-F mica in the greisenized granite also increases the contents of Li and K and other elements (Ga, Rb, Sn, etc.) concentrated in the mica. Muscovitization of biotite lowers the Li content, but the replacement of feldspar by muscovite may increase the contents of Ga, Rb, and Sn.

The secondary addition of topaz and fluorite is quite common in the late-stage types of Väkkärä granite, and the high contents of Al_2O_3 and F in these granites are partly due to these reactions.

The unusually high Na/K ratio of a couple of the porphyritic Väkkärä granite analyses (samples 98/MK/67/ER and 10/PL/68/IH) and of the topaz-bearing quartz porphyry can be due to albitization. However, in these cases, unequivocal microscopic evidence of addition of albite from the outside is lacking.

The high Fe^{3+}/Fe^{2+} ratio of the analyzed sample of coarse-grained Väkkärä granite (anal. 6, Table 10) can be correlated with the secondary development of hematite.

The topaz-bearing Väkkärä granite is characterized by unusually high contents of Ga, Rb, Sn and Li, and by low contents of Ba, Sr and Zr. The common systematic correlations between these elements suggest that their distribution may be controlled largely by a uniform process (magmatic fractional crystallization or increasing metasomatism). Ga is included essentially in the albite, microcline and mica, Rb in the microcline and mica, Sn in the Nb-rich cassiterite and mica, Li in the dark mica, Ba and Sr in the feldspars and Zr in the zircon. The high contents of Ga and Rb are due to their abundance in both the feldspars and mica. If it is assumed that the anomalous contents of, for example, Ga and Rb are related to metasomatic processes, then it must be assumed that also both the feldspars and the mica are metasomatic, or that they have re-equilibrated with each other in the presence of late- or postmagmatic Rb- and Ga-rich fluids, thus being able to increase their contents of Rb and Ga and reduce the contents of Ba and Sr. Microscopic observations show that notable recrystallization of feldspar minerals has really occurred (e.g., textures indicating deanorthitization of plagioclase, the development of intergranular albite, the patchy twinning in microcline). The fluids which »catalyzed» these recrystallization reactions also probably caused some chemical changes in the rock. But whether there had taken place a postmagmatic rearrangement of minerals of sufficient strength in such new physiochemical conditions to produce all the chemical peculiarities observed is questionable. The element correlations observed presuppose that more or less simultaneously with the assumed addition of Ga and Rb (and removal of Ba and Sr) there should have occurred also the removal of Zr and Ti and the addition of Sn. In the foregoing

(p. 97), it has been shown that at least part of the accessory cassiterite of the granite was probably formed at a higher temperature and earlier than the cassiterites of the pegmatite and greisen veins.

It is highly possible that the distribution of the elements in the Eurajoki granites is controlled more by primary magmatic evolution and the modifying action of autometasomatic reactions than by separate, essentially later postmagmatic metasomatism caused by fluids coming from some very deep source. This hypothesis is supported by the fact that the quartz porphyry dikes intersecting the Tarkki granite steadily show much the same mineralogical and geochemical peculiarities as the Väkkärä granite, deviating clearly from the Tarkki granite and from the dark porphyry dikes. The effective restriction of such reactions as the development of secondary topaz and secondary Li-F mica into the late-stage types of Väkkärä granite points to their autometasomatic origin.

SUMMARY

The mode of occurrence, the radiometric age determinations and the general petrographic character of the rocks of the composite Eurajoki stock show that it belongs to the rapakivi granite suite, although none of the rocks of the stock are characterized by the ordinary rapakivi texture. The spatial association of the different rock units (Tarkki granite, Väkkärä granite, porphyry dikes) shows features typical of the centred complexes. Greisen-type Sn, Be, W and sulphide mineralizations occur in different parts of the stock. Radiometric age determinations performed by the lead-uranium method indicate an age of about 1 570 Ma for the granites. Lead isotope ratios of galena from three greisen bodies show model ages of 1 575—1 608 Ma.

The Tarkki granite, the oldest rock of the complex, forms a horseshoe-shaped body occupying the marginal parts of the stock. This even-grained homogeneous rock represents the most basic members of the rapakivi granites and shows mineralogical and geochemical similarities to the tirilite of the Wiborg rapakivi massif. The major constituents are monoclinic, faintly perthitic alkali feldspar, quartz, partly sericitized andesine, partly chloritized biotite and hornblende. Accessories are fayalite, ilmenite, apatite, zircon, fluorite, iddingsite, grunerite, magnetite, perrierite or chevkinite, danalite and sulphides. Intergranular myrmekite, possibly formed mainly by exsolution, is commonly present, and a micrographic feldspar-quartz intergrowth is occasionally seen to occur. The two-feldspar geothermometer gives modal feldspar-equilibrium temperatures of about 750°C. Various petrographic data (lack of cavities, scantiness of pegmatites, the occurrence of interstitial fluorine-poor biotite, a very faint perthite texture and a relatively high thermal state of alkali feldspar) suggest that during the main stage of crystallization the magma was not saturated with water. However, late-stage activity of volatiles is verified by various alteration phenomena (alteration of mafic minerals, sericitization of plagioclase, greisenization). These

secondary reactions were obviously caused partly by pore fluids related to the Tarkki granite itself, partly by later fluids that emanated from the crystallizing Väkkärä granite.

The Väkkärä granite forms a younger, more acidic complex intrusive body within the stock. The contact phenomena show that the Tarkki granite was already cooled and fractured when the emplacement of the Väkkärä granite took place. The rocks of the Väkkärä granite complex are alaskitic supersolvus granites, which commonly show various mineral alterations. Marked differences in texture, mineral composition and chemical composition between the Tarkki and Väkkärä granites indicate that these rocks crystallized in different natural conditions from magmas that differed from each other in chemical composition. The textural relations and its close association with the quartz porphyry dikes suggest that the Väkkärä granite is a shallow-level (hypabyssal) intrusive complex, which completed crystallization at a lesser depth than the Tarkki granite. Petrographic and geochemical data suggest the following order of development: contact type (porphyritic fine-grained granite) → even-grained type (equigranular medium-grained granite) → coarse-grained type (nearly equigranular coarse-grained or medium-grained topaz-bearing granite) and porphyritic type (more or less porphyritic, fine-grained to medium-grained topaz-bearing granite).

The topaz-bearing types are peraluminous microcline-albite granites, in which the dark mica is lithian siderophyllite (protolithionite). The content of topaz is usually 1—3 %. Other typical accessories are fluorite, monazite, bastnaesite, xenotime, cassiterite, ilmenite, columbite and thorite. The mode of occurrence of the topaz indicates that it is in part a primary constituent, in part clearly secondary. The accessory cassiterite of the granite has higher contents of Nb, Ta, Ti and Fe than the cassiterite of the pegmatite and greisen veins, which suggests that the granite cassiterite is either a primary constituent or was formed during an early stage of autometasomatism preceding jointing and the development of pegmatite and greisen veins. The origin of other accessory minerals may be similar to that of cassiterite.

Miarolitic cavities are very common in the porphyritic type of Väkkärä granite. This indicates the presence of a fluid phase during late stages of crystallization, and thus strongly points to the possibility that the residual magma was saturated with volatiles. Evidently, the mineral crystallization took place partly from an extremely fractionated silicate melt, partly from a fluid phase.

In chemical composition, the contact type and the even-grained type of Väkkärä granite do not deviate very markedly from the composition of other acidic rapakivi granites. The topaz-bearing types are characterized by anomalously high contents of F, Li, (Be), Ga, Rb, an and Nb, and by unusually low contents of Mg, Fe, Ti, Ba, Sr and Zr, when compared with normal rapakivi granites and the average contents of granites in general.

The quartz porphyry dikes show much the same mineralogical and geochemical peculiarities as the topaz-bearing Väkkärä granite, indicating a close genetic connec-

tion (common parent magma) between these rocks. Some of the porphyry dikes are more basic, possessing the mineral composition of dacite.

Secondary reactions, caused by ascending fluids, which migrated in interstices and fractures, modified markedly the texture, mineral relations and chemical composition of the Väkkärä granite. These reactions were largely an autometamorphic adjustment of minerals to falling temperature (inversions, exsolution, recrystallization); but also chemical changes took place, as is exemplified by greisenization. The reactions started before complete solidification of the rock (late-magmatic stage) and continued after solidification and fracturing (postmagmatic stage). The fluids emanating from the consolidating Väkkärä granite escaped also into fissures and joints of the overlying and surrounding Tarkki granite, causing the development of greisen and associated quartz-beryl veins. Tin and related ore elements in the greisens originated to a large extent directly from the postmagmatic fluids, but in part they were derived from the granite minerals (especially biotite) in connection with the alteration. Fluid inclusion studies indicate a minimum temperature of 300—390°C for the tin and beryllium mineralization in these veins.

During the later geologic history of the area, the presumably most intensely greisenized and mineralized apical parts of the Väkkärä granite were removed by erosion.

ACKNOWLEDGMENTS

During the nine-year period the author has studied the petrometallogenesis of the rapakivi granites of Finland, he has been assisted, in different fields of the study, by many colleagues and co-workers from the Geological Survey of Finland. Mr. Pasi Lehmuspelto and Mr. Martti Kankkunen assisted in the field work in the Eurajoki area. The chemical analyses were performed by Mr. Pentti Ojanperä, Mr. Väinö Hoffrén, Miss Ringa Danielsson, Mrs. Anneli Forsén (née Savola), Miss Maria Hynönen, Mrs. Maija-Leena Hagel-Brunnström (née Hagel), Mr. Risto Saikkonen, Mr. Ari Puisto, Mr. Arvo Löfgren, Dr. Jaakko Siivola and Miss Tuula Paasivirta. Mr. Matti Vaasjoki and Dr. Olavi Kouvo did the radiometric age determinations. Mr. Pekka Kallio carried out the X-ray obliquity determinations of alkali feldspar. Miss Lea Aho and Miss Leena Peräkylä made most of the point-counting analyses. Mr. Erkki Halme took many of the photomicrographs. Mrs. Aino Lehti and Mrs. Marjo Kujala-Tammi drew the maps and diagrams. Dr. Atso Vorma and Dr. Kauko Laajoki read the manuscript critically, and Mr. Paul Sjöblom corrected the author's English text. The author wishes to express his deep gratitude to all these persons.

The financial support received from the Foundation of the Outokumpu Co. made it possible for the author to work during six months in 1974 in the Fluid Inclusion Laboratory of the U.S. Geological Survey, Reston, Virginia. Dr. Edwin Roedder, head of the laboratory, placed at author's disposal its equipment and offered many-sided advice, which is gratefully acknowledged.

Manuscript received September 14, 1976

REFERENCES

Anfilogov, V. N., Glyuk, D. S. and **Trufanova, L. G.** (1973) Phase relations in interection between granite and sodium fluoride at water vapor pressure of 1 000 kg/cm². Geochem. Internat. 10, 30—33.

Augustithis, S. S. (1973) Atlas of textural patterns of granites, gneisses and associated rock types. Elsevier Scientific Publ. Company, Amsterdam.

Baskin, Y. (1956) A study of authigenic feldspars. J. Geol. 64, 132—155.

Barth, T. F. W. (1959) The diffusive transformation sanidine-microcline. Estud. Geol. (Madrid) 15, 31—38. [Cited from Smith 1974, p. 384].

Bence, A. E. and **Albee, A. L.** (1968) Experimental correction factors for the electron microanalysis of silicates and oxides. J. Geol. 76, 382—403.

Beus, A. A. and **Zalashkova, N. YE.** (1962) Post-magmatic high temperature metasomatic processes in granitic rocks. Internat. Geol. Review 6 (4), 668—681.

Borisenok, L. A. and **Saukov, A. A.** (1960) Geochemical cycle of gallium. XXI Int. Geol. Congr., part 1, 96—105.

Bowden, P. (1964) Gallium in Younger Granites of Northern Nigeria. Geochim. Cosmochim. Acta 28, 1981—1988.

Buddington, A. F. (1959) Granite emplacement with special reference to North America. Bull. Geol. Soc. Am. 70, 671—747.

Burnham, C. W. and **Jahns, R. H.** (1962) A method for determining the solubility of water in silicate melts. Am. J. Sci. 260, 721—745.

Burton, J. D. and **Culkin, F.** (1972) Gallium. Sections 31 D, E and N *in* »Handbook of geochemistry II-3», edited by K. H. Wedepohl. Springer Verlag, Berlin—Heidelberg.

Borley, G. and **Frost, M. T.** (1963) Some observations on igneous ferrohastingsites. Mineral. Mag. 33, 646—662.

Czamanske, G. K. (1965) Petrologic aspects of the Finnmark igneous complex, Oslo area, Norway. J. Geol. 73, 293—322.

Deer, W. A., Howie, R. A. and **Zussman, J.** (1973) Rock-forming minerals vol. 3. Sheet silicates. Longmans, London.

Dolomanova, YE. I., Boyarskaya, R. V., Rakcheyev, A. D. and **Yakovlevskaya, T. A.** (1969) Kassiterit i yego tipomorfnyye osobennosti. [Cassiterite and its typomorphic characteristics]. P. 128—184 *in* »Tipomorphizm mineralov». Akad. Nauk SSSR. Inst. geol. rud., mestorozhd., petrogr., miner., geokhim., Moscow.

Drescher-Kaaden, F. K. (1969) Granitprobleme. Akademie-Verlag, Berlin.

Dudykina, A. S. (1959) Parageneticheskie assotsiatsii elementov-primesey v kassiteritakh razlichnykh geneticheskikh tipov olovorudnykh mestorozhdemy. [Paragenetic association of element-admixtures in cassiterites of different genetic types of tin-ore deposits]. Akad. Nauk SSSR. Inst. geol. rud., mestorozhd., petrogr., mineral., geokhim. 28, 111—121.

Elo, S. (1976) An interpretation of a recently measured gravity profile across the Jotnian sandstone formation in south-western Finland. Manuscript, Geological Survey of Finland.

Eskola, P. (1928) On rapakivi rocks from the bottom of the Gulf of Bothnia. Fennia 50 (27), 29 p.

Fiala, F. (1968) Granitoids of the Slavkovskij (Cisarskij) les Mountains. Sbor. Geol. Ved., G 14, 93—160.

Fleischer, M. (1971) Glossary of mineral species. Mineralogical Record, Inc., Maryland.

Foster, M. D. (1960) Interpretation of the composition of lithium micas. U.S. Geol. Surv. Prof. Pap. 354-E.

Ganeev, I. G., Pachadzhanov, D. N. and **Borisenok, L. A.** (1961) Geochemistry of gallium, tin and some other elements in the process of greisenization. Geochemistry 1961 (9), 822—839.

Ganeyev, I. G. and **Sechina, N. P.** (1962) Geochemical characteristics of albitized granites. Geochemistry 1962 (2), 158—166.

Gates, R. M. and **Scheerer, P. E.** (1963) The petrology of the Nonewaug granite, Connecticut. Am. Mineral. 48, 1 040—1 069.

Groves, D. I. (1972) The geochemical evolution of tin-bearing granites in the Blue Tier Batholith, Tasmania. Econ. Geol. 67, 445—457.

Haapala, I. (1973) Havaintoja rapakivigraniittien tina ja berylliumpitoisuuksista. Summary: Observations on the tin and beryllium contents of the rapakivi granites. Geologi, 25 (6), 61—67 and (7), 75. Helsinki.

—»— (1974) Some petrological and geochemical characteristics of rapakivi granite varieties associated with greisen-type Sn, Be, and W mineralization in the Eurajoki and Kymi areas, southern Finland. Pp. 159—169 *in* »Metallization associated with acid magmatism, I» edited by M. Štemprok. Ustrední ústav geologicky, Praha.

—»— (1976) Om petrologi och geokemi i finska rapakivi-varianter associerade med Sn, Be, W och sulfidmineralisationer. Abstracts, XII Nordiska Geologvintermötet 1976, 21. Chalmers tekniska högskola and Göteborgs universitetet, Göteborg.

Haapala, I. and **Laajoki, K.** (1969) A study of isotropic-pseudoanisotropic zoning in sphalerite. Bull. Geol. Soc. Finland 41, 93—98.

Haapala, I. and **Ojanperä, P.** (1969) Triplite and wolframite from a greisen-bordered veinlet in Eurajoki, SW Finland. Bull. Geol. Soc. Finland 41, 99—105.

Haapala, I. and **Ojanperä, P.** (1972) Genthelvite-bearing greisens in southern Finland. Geol. Surv. Finland, Bull. 259, 22 p.

Hall, A. (1967) The variation of some trace elements in the Rosses granite complex, Donegal. Geol. Mag. 104 (2), 99—109.

Härme, M. (1958) General geological map of Finland. Pre-Quarternary rocks. Turku (Sheet B1). Geological Survey of Finland.

Heinrich, E. Wm. and **Moore, D. G.** (1970) Metasomatic potash feldspar rocks associated with igneous alkalic complexes. Canadian Mineral. 10, 571—584.

James, R. S. and **Hamilton, D. L.** (1969) Phase relations in the system $NaAlSi_3O_8$ — $KAlSi_3O_8$ — $CaAl_2Si_2O_8$ — SiO_2 at 1 kilobar water vapor pressure. Contr. Mineral. Petrol. 21, 111—141.

Kahma, A. (1951) On contact phenomena of the Satakunta diabase. Bull. Comm. géol. Finlande 152, 84 p.

Kaitaro, S. (1956) On central complexes with radial lamprophyric dikes. Bull. Comm. géol. Finlande 172, 55—65.

Kelly, W. C. and **Turneaure, F. S.** (1970) Mineralogy, paragenesis and geochemistry of the tin and tungsten deposits of the Eastern Andes, Bolivia. Econ. Geol. 65, 609—680.

Khazov, R. A. (1973) Geologicheskie osobennosti olovyannogo orudeneniya Severnogo Priladozh'ya. [Peculiarities of tin ore formation in the northern part of the Ladoga region]. Akad. Nauk SSSR, Karel'skiy filial, Inst. geol. Trudy 15.

Klominsky, J. and **Absalonova, E.** (1974) Geochemistry of the Karlovy Vary granite massif (Czechoslovakia). Pp. 189—196 *in* »Metallization associated with acid magmatism, I» edited by M. Štemprok. Ústrední ústav geologicky, Praha.

Köhler, A. and **Raaz, F.** (1951) Über eine neue Berechnung und graphische Darstellung von Gesteinsanalysen. Neues Jb. Mineral. Monatsh., 1951 (11), 247—263.

Kovalenko, V. I. (1973) Distribution of fluorine in a topaz-bearing quartz keratofyre (ongonite) and solubility of fluorine in granitic melts. Geochem. Internat. 10, 41—49.

—»— (1974) On the genesis of rare-metal granites and their mineralization. Pp. 197—200 *in* »Metallization associated with acid magmatism, I», edited by M. Štemprok. Ústrední ústav geologicky, Praha.

Kovalenko, V. I., Grebennikov, A. M. and **Antipin, V. S.** (1975) Ongonite of the Arybulak stock, Transbaikal: The first find of a subvolcanic analog of rare metal-bearing lithium-fluorine granite (»apogranite») in the USSR. Akad. Nauk SSSR, Earth Sci. Sect. 220, 158—160.

Kovalenko, V. I., Kuzmin, M. I., Antipin, V. S. and **Petrov, L. L.** (1971) Topaz-bearing quartz keratofyre (ongonite), a new variety of subvolcanic igneous dike rocks. Dokl. Akad. Nauk SSSR, Earth Sci. Sect. 199, 132—135.

Kovalenko, V. I., Kuzmin, M. I. and **Letnikov, F. A.** (1970) Magmatic origin of lithium and fluorine-bearing rare-metal granite. Dokl. Akad. Nauk SSSR, Earth Sci. Sect. 190, 189—192.

Kühne, R., Wasternack, J. and **Schulze, H.** (1972) Fortschritte der Metallogenie im Erzgebirge. C. Postmagmatische Metasomatose im Endo-Exocontact der jüngeren postkinematischen Granite des Erzgebirges. Geologie 21, 494—520.

Laitakari, A. (1925) Über das jotnische Gebiet von Satakunta. Bull. Comm. géol. Finlande 73, 43 p

—»— (1928) Palingenese am Kontakt des postjotnischen Olivindiabases. Fennia 50 (35), 25 p.

Lange, H., Tischendorf, G., Pälchen, W., Klemm, I. and **Ossenkoph, W.** (1972) Fortschritte der Metallogenie im Erzgebirge. B. Zur Petrographie und Geochemie der Granite des Erzgebirges. Geologie 21, 457—492.

Lehijärvi, M. and **Lonka, A.** (1964) The hornblende rapakivi dike of Jaala—Iitti. Bull. Comm. géol. Finlande 215, 127—141.

Lemberg, J. (1868) Die Gebirgsarten der Insel Hochland, chemischgeognostisch Untersucht. Archiv f. Naturkunde. Liv-, Est- und Kurland. I Ser. Bd IV, 337—392.

Luth, W. C. (1969) The systems $NaAlSi_3O_8$ — SiO_2 and $KAlSi_3O_8$ — SiO_2 to 20 kb and the relationship between H_2O content, PH_2O and Ptotal in granitic magmas. Am. J. Sci., Schairer Vol. 267-A, 325—341.

Luth, W. C., Jahns, R. H. and **Tuttle, O. F.** (1964) The granite system at pressures of 4 to 10 kilobars. J. Geophys. Research 69 (4), 759—773.

Lundqvist, T. (1973) Potash feldspar megacrysts of a granite at Skagsudde, Central Sweden. Sveriges Geol. Unders. Ser. C 687, 32 p.

Maaløe, S. and **Wyllie, P. J.** (1975) Water content of a granite magma deduced from the sequence of crystallization determined experimentally with water-undersaturated conditions. Contrib. Mineral. Petrol. 52, 175—191.

Madel, J. (1975) Geochemical structures in a multiple intrusion granite massif. N. Jb. Miner. Abh. 124, 103—127.

Martin, R. F. (1974) Controls of ordering and subsolidus phase relations in the alkali feldspars. Pp. 313—336 in "The feldspars", edited by W. S. MacKenzie and J. Zussman. Manchester University Press, New York.

Mishchenko, V. S., Kuts, V. P. and **Orlova, L. A.** (1966) The geochemistry of gallium in high-temperature postmagmatic processes. Geochem. Internat. 3, 330—340.

Naumov, V. B., Kovalenko, V. I., Kuz'min, M. I., Vlacykin, N. V. and **Ivanov, G. V.** (1971) Thermometric study of inclusions of melt in topaz from the topaz-bearing quartz keratophyre (ongonite). Dokl. Akad. Nauk SSSR, Earth Sci. Sect. 199, 104—106.

Noble, D. C., Korronga, M. K., Hedge, C. E. and **Riddle, G. O.** (1972) Highly differentiated subalkaline rhyolite glass from Glass Mountain, Mono County, California. Bull. Geol. Soc. Am. 83, 1 179—1 184.

Nockolds, S. R. (1947) The relation between chemical composition and paragenesis in the biotite mica of igneous rocks. Am. J. Sci. 245, 401—420.

Nockolds, S. R. and **Mitchell, R. L.** (1948) The geochemistry of some Caledonian plutonic rocks. Trans. Roy. Soc. Edinburgh 61, 533—575.

Nockolds, S. R. and **Allen, R.** (1953) The geochemistry of some igneous rock series. Geochim. Cosmochim. Acta 4, 105—142.

Phillips, E. R. (1974) Myrmekite — one hundred years later. Lithos 7, 181—194.

Pitcher, W. S. and **Berger, A. R.** (1972) The geology of Donegal. A study of granite emplacement and unroofing. John Wiley and Sons, Inc., New York.

v. Platen, H. (1965) Kristallisation granitischer Schmelzen. Beitr. Mineral. Petrogr. 11, 334—381.

Puranen, M. (1963) A geophysical investigation of the Satakunta sandstone area in south-western Finland. Geoexploration I, 6—15.

Ragland, P. C. (1969) Composition and structural state of the potassic phase in perthites as related to petrogenesis of a granitic pluton. Lithos 3, 167—189.

Ramberg, H. (1962) Intergranular precipitation of albite formed by unmixing of alkali feldspar. N. Jb. Miner. Abh. 98, 14—34.

Rieder, M. (1970) Chemical composition and physical properties of lithium-iron micas from the Krusné hory Mts. (Erzgebirge) Part A; Chemical composition. Contr. Mineral. Petrol. 27, 131—158.

Roedder, E. (1962) Studies of fluid inclusions I: Low-temperature application of a dual-purpose freezing and heating stage. Econ. Geol. 57, 1 045—1 061.

—»— (1971) Fluid inclusion studies of the porphyry-type ore deposits at Bingham, Utah, Butte, Montana and Climax, Colorado. Econ. Geol. 66, 98—120.

Roedder, E. and **Coombs, D. S.** (1967) Immiscibility in granite melts, indicated by fluid inclusions in ejected granite blocks from Ascension Island. J. Petrol. 8, 417—451.

Rub, M. G. (1972) The role of gaseous phase during the formation of ore-bearing magmatic complexes. Chem. Geol. 10. 89—98.

Rub, M. G., Asihmina, N. A., Khasov, R. A. and **Khasova, V. I.** (1974) To the petrochemistry of the Precambrian tin-bearing granites from the North Cis-Ladoga region. Izv. Akad. Nauk SSSR., Ser. geol. 1974 (4), 42—59. (In Russian).

Rub, M. G. and **Pavlov, V. A.** (1974) Geochemical and petrographical features of granitoids accompanied by stanniferous, rare-earth and tungsten mineralization. Pp. 210—214 *in* »Metallization associated with acid magmatism, I» edited by M. Štemprok. Ústrední ústav geologicky, Praha.

Saavedra, J. (1976) Geochemical and petrological characteristics of mineralized granit of the West centre of Spain. Manuscript. MAWAM working group meeting 1976 in Salamanca, Spain.

Sahama, Th. G. (1945) On the geochemistry of the east Fennoscandian rapakivi granites. Bull. Comm. Géol. Finlande 136, 15—67.

Sainsbury, C. L. (1969) Geology and ore deposits of the central York Mountain, eastern Seward Peninsula, Alaska. U.S. Geol. Surv. Bull. 1 287, 101 p.

Sainsbury, C. L., Mulligan, R. R. and **Smith, W. C.** (1969) The Circum-Pacific »tin belt» in North America. Pp. 123—148 *in* »A second technical conference on tin, I», edited by W. Fox. Internat. Tin Council, London.

Sattran, V. and **Klominsky, J.** (1970) Petrometallogenic series of igneous rocks and endogenous ore deposits in the Czechoslovakian part of the Bohemian Massif. Sbor. geol. Ved. LG 12, 65—154.

Savolahti, A. (1956) The Ahvenisto massif in Finland. Bull. Comm. géol. Finlande 174, 96 p.

—»— (1962) The rapakivi problem and the rules of idiomorphism in minerals. Bull. Comm. géol. Finlande 204, 33—111.

Sederholm, J. J. (1911) Beskrifning till bergartskartan B 2, Tammerfors. Résumé en francais. General geological map of Finland 1: 400 000, Geological Survey of Finland, 121 p.

Singh, D. S. and **Bean, J. H.** (1968) Some general aspects of tin minerals in Malaysia. Pp. 457—478 *in* »A technical conference on tin, II». International Tin Council, London.

Simonen, A. (1960) Pre-Quartenary rocks in Finland. Bull. Comm. géol. Finland 191, 49 p.

Simonen, A. and **Vorma, A.** (1969) Amphibole and biotite from rapakivi. Bull. Comm. géol. Finlande 238, 28 p.

Skinner, B. J. (1966) Thermal expansion. Pp. 75—96 in »Handbook of physical constants», edited by S.P. Clark, Jr. Geol. Soc. Am., Mem. 97.

Smith, J. V. (1974) Feldspar minerals 2, Chemical and textural properties. Springer Verlag, Berlin—Heidelberg.

Stacey, J. S. and **Kramers, J. D.** (1975) Approximation of terrestrial lead isotope evolution by a two-stage model. Earth Planet. Sci. Lett. 26, 207—221.

Štemprok, M. (1967) Genetische Probleme der Zinn-Wolfram Vererzung im Erzgebirge. Mineral. Deposita 2, 102—118.

—»— (1971) Petrochemical features of tin-bearing granites in the Krusné hory Mts. Czechoslovakia. Soc. Mining Geol. Japan, Spec. Issue 4, 112—118 (Proc. IMA-IAGOD Meetings »70». Joint Symp. Col.)

Štemprok, M. and **Škvor, V.** (1974) Composition of tin-bearing granites from the Krusné hory metallogenic province of Czechoslovakia. Sbor. geol. Ved., LGM 16, 7—79.

Stewart, D. B. and **Roseboom, E. H., Jr.** (1962) Lower temperature terminations of the three-phase region plagioclase-alkali feldspar-liquid. J. Petrol. 3, 280—315.

Stormer, J. C., Jr. (1975) A practical two-feldspar geothermometer Am. Mineral. 60, 667—674.

Streckeisen, A. L. (1967) Classification and nomenclature of igneous rocks. N. Jb. Mineral. Abh. 107, 144—240.

Strunz, H. (1970) Mineralogische Tabellen, 5. Auflage. Akad. Verlagsgesellschaft. Geest & Portig K.-G., Leipzig.

Tauson, L. V. and **Kozlov, V. D.** (1973) Distribution functions and ratios of trace-element concentrations as estimators of the ore-bearing potential of granites. Pp. 37—44 *in* »Geochem. Exploration 1972», edited by M. J. Jones. Inst. Min. Metall., London.

Taylor, S. R. (1965) The application of trace element data to problems in petrology. Pp. 133—213 *in* »Physics and chemistry of the earth 6» edited by L. H. Ahrens *et. al.*

Thornton, C. P. and **Tuttle, O. F.** (1960) Chemistry of igneous rocks, I. Differentiation index. Am. J. Sci. 258, 664—684.

Tischendorf, G. (1970) Zur geochemischen Spezialisierung der granite des westerzgebirgischen Teilplutons. Geologie 19, 25—40.

Tischendorf, G., Freise, G. and **Schindler, R.** (1969) Die Dunkelglimmer der westerzgebirgischen Granite und ihre Bedeutung als petrogenetische und metallogenetische Kriterien. Geologie 18, 384—399 and 1 024—1 044.

Tischendorf, G., Lächelt, S., Lange, H., Pälchen, W. and **Meinel, G.** (1972) Geochemical specialization of granitoids in the territory of German Democratic Republic. 24 th Internat. geol. congress, Canada, Section 4, 266—275.

Toulmin, P., III (1964) Bedrock geology of the Salem, quadrangle and vicinity, Massachusetts. U.S. Geol. Surv., Bull. 1163-A.

Trüstedt, O. (1907) Die Erzlagerstätten von Pitkäranta am Ladoga-See. Bull. Comm. géol. Finlande 19, 333 p.

Turekian, K. K. and **Wedepohl, K. H.** (1961) Distribution of elements is some major units of the Earth's crust. Geol. Soc. Am. Bull. 72, 175—192.

Tuttle, O. F. and **Bowen, N. L.** (1958) Origin of granite in the light of experimental studies in the system $NaAlSi_3O_8$—$KAlSi_3O_8$—SiO_2—H_2O. Geol. Soc. Am. Mem. 74.

Vaasjoki, O. (1956) A comparison of the minor base metal contents of some Finnish galenas. Bull. Comm. géol. Finlande 172, 47—53.

Vernon, R. H. (1975) Deformation and recrystallization of a plagioclase grain. Am. Mineral. 60, 884—888.

Vinogradov, A. P. (1962) The average contents of elements in main igneous rocks of the earth's crust. Geochemistry, 1962 (7), 641—664.

Vlasov, K. A., editor (1964) Geochemistry and mineralogy of rare elements and genetic types of their deposits. III. Genetic types of rare-element deposits. Acad. Sci. USSR. Ministr. Geol. USSR. Israel Program for Scientific Translations, Jerusalem 1968.

Vogel, T. A., Smith, B. L., and **Goodspeed, R. M.** (1968) The origin of antiperthites from some charnockitic rocks in the New Jersey Precambrian. Am. Mineral. 53, 1 696—1 708.

Vorma, A. (1971) Alkali feldspar of the Wiborg rapakivi massif in southeastern Finland. Bull. Comm. géol. Finlande 246, 72 p.

Wahl, W. (1947) A composite lava flow from Lounatkorkia, Hogland. Bull. comm. géol. Finlande 140, 287—302.

Wasserburg, G. J. (1963) Diffusion processes in lead-uranium systems. J. Geophys. Res. 68 (16), 4 823—4 846.

Wyllie, P. J. and **Tuttle, O. F.** (1961) Experimental investigation of silicate systems containing two volatile components. Part II. The effects of NH_3 and HF, in addition to H_2O on the melting temperatures of albite and granite. Am. J. Sci. 259, 128—143.

GEOLOGIC MAP OF THE EURAJOKI AREA

BY ILMARI HAAPALA

0 1 2 km

Scale 1:30 000

Migmatitic schists and gneisses

Normal Laitila rapakivi granite

Fine-grained Laitila rapakivi granite

Tarkki granite

Väkkärä granite:

- Contact type
- Even-grained type
- Coarse-grained type
- Porphyritic type

Quartz porphyry dike

Dark porphyry dike

Greisen

Diabase

Breccia

Contact showing dip

Schistosity

Schistosity with lineation

Outcrop

Drill hole

Sn Cassiterite

W Wolframite

Be Beryl

BeB Bertrandite

BeG Genthelvite

16108—76/100g

ISBN 951-690-068-2